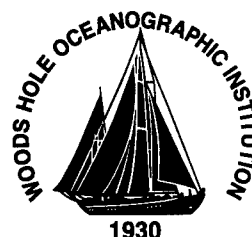


MIT/WHOI 2002-04

**Massachusetts Institute of Technology
Woods Hole Oceanographic Institution**



**Joint Program
in Oceanography/
Applied Ocean
Science
and Engineering**



DOCTORAL DISSERTATION

*The Role of Denitrification in the Nitrogen Cycle of New
England Salt Marshes*

by

Michael Robert Hamersley

February 2002

DISTRIBUTION STATEMENT A
Approved for Public Release
Distribution Unlimited

20020924 013

MIT/WHOI

2002-04

The Role of Denitrification in the Nitrogen Cycle of New England Salt Marshes

by

Michael Robert Hamersley

Massachusetts Institute of Technology
Cambridge, Massachusetts 02139

and

Woods Hole Oceanographic Institution
Woods Hole, Massachusetts 02543

February 2002

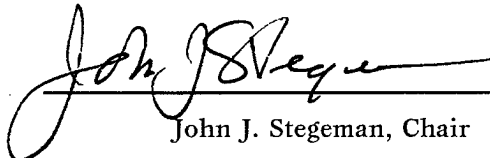
DOCTORAL DISSERTATION


Financial support came through the generosity of the Education Department at the Woods Hole Oceanographic Institution, the Coastal Systems Group at the School for Marine Science and Technology, University of Massachusetts, the Reinhart Coastal Research Center, and the Biology Department at WHOI.


Reproduction in whole or in part is permitted for any purpose of the United States Government. This thesis should be cited as: Michael Robert Hamersley, 2002. The Role of Denitrification in the Nitrogen Cycle of New England Salt Marshes. Ph.D. Thesis. MIT/WHOI, 2002-04.

Approved for publication; distribution unlimited.

Approved for Distribution:


John J. Stegeman, Chair
Department of Biology


Paola Malanotte-Rizzoli
MIT Director of Joint Program


John W. Farrington
WHOI Dean of Graduate Studies

**THE ROLE OF DENITRIFICATION IN THE NITROGEN CYCLE
OF NEW ENGLAND SALT MARSHES**

By

Michael Robert Hamersley

B.Sc., University of Victoria, 1991
M. E. Des., University of Calgary, 1996

Submitted in partial fulfillment of the requirements for the degree of

Doctor of Philosophy

at the

MASSACHUSETTS INSTITUTE OF TECHNOLOGY

and the

WOODS HOLE OCEANOGRAPHIC INSTITUTION

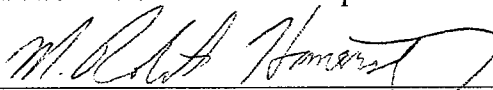
December, 2001

© 2001 M. Robert Hamersley

All rights reserved.

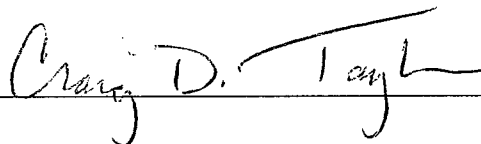
The author hereby grants to MIT and WHOI permission to reproduce paper and electronic copies of this thesis in whole or in part and to distribute them publicly.

Signature of Author



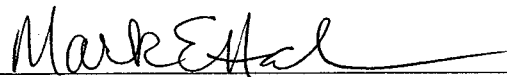
Joint Program in Oceanography
Massachusetts Institute of Technology
and Woods Hole Oceanographic Institution
December 2001

Certified by



Craig Taylor
Thesis Supervisor

Accepted by



Mark Hahn
Chair, Joint Committee for Biology
Woods Hole Oceanographic Institution

ACKNOWLEDGEMENTS

All that we know of Man, Nature, God, is just that which they
are not; it is that which they throw off as repugnant.

Aliester Crowley, "The Book
of Lies", 1913.

Many thanks are due to my two major advisors, Brian Howes and Craig Taylor. Brian Howes took me into his lab originally as a guest student, encouraged me to apply to the Joint Program, and was my principal WHOI advisor during my first two years as a student, and continued to be my main source of direction and research funding throughout my time in the Joint Program. Brian is a wizard, a continual reminder of what I have to shoot for in scientific thinking. Craig Taylor gave help, advice, and office space from the beginning, and later took on the task of principal WHOI advisor. His laid-back attitude and humor helped me keep my cool on many an occasion. The other members of my committee have also been very supportive and encouraging. Thanks to John Waterbury, and to Jon King for reaching across the gulf from MIT. Lauren Mullineaux gave encouragement and graciously agreed to serve as the Chair for my Thesis Defense. I am grateful to Mark Hahn for his official and personal support. A special thanks goes to Julia Westwater in the Education office for her help. I also owe thanks to Richard Harbison for Chairing my Thesis Proposal Defense.

I had many collaborators in data collection, analysis, and interpretation. Brian's work in salt marsh biogeochemistry for the last 20 years formed the foundation of this research. Many members of his laboratory made important contributions. David White

deserves special mention for his mentoring during my first years at WHOI. His work with ^{15}N isotopes was the antecessor of my work in Chapter 4. Kirsten Smith and I collaborated on research in Mashapaquit Marsh, and she contributed her sediment carbon data. Her work is published in a thesis: Salt marsh uptake of watershed nitrate (Smith, 1999). George Hampson identified the benthic macrofauna and provided field support on the coldest day, the single January sampling (Figure 3.3). Paul Henderson analyzed the nitrate samples and contributed in many other ways. Other members of the lab that played an influential role were Dale Goehringer and David Schlezinger. Susan Brown-Leger and Marie Evans gave valuable technical and analytical support. Many volunteers and interns helped me in the field and laboratory. Michael DeLeo, in particular, volunteered months of his time processing the ^{15}N samples and in dedicated and effective field and laboratory support. Other volunteers that helped me in the field and the lab are my good friends: Rebecca Green, Matthew Jull, Lisbeth Kimbell, Jennifer Loose and Patrick Miller, my father, Michael Hamersley, and two of my brothers, Shannon and Tristan Hamersley, intern Staci Jasin, and numerous other volunteers and interns. My thanks to Jennifer Loose for the loan of the computer which enabled me to write at home. I am grateful to my mother, Denise Forest, for many different kinds of help and support.

Financial support came through the generosity of the Education Department at WHOI, the Coastal Systems Group at the School for Marine Science and Technology, University of Massachusetts, the Reinhart Coastal Research Center, and the Biology Department at WHOI. I owe them some good science in return, I guess! More than anything, this work was inspired by the insight and support of Brian Howes and his passion for salt marsh biogeochemistry. My thanks.

BIOGRAPHY

M. Robert Hamersley

EDUCATION

- Dec. 2001 Doctor of Philosophy - Biological Oceanography. Massachusetts Institute of Technology / Woods Hole Oceanographic Institution, Massachusetts, USA
Dissertation: The role of denitrification in the nitrogen cycle of New England salt marshes.
Advisors: Dr. Craig T. Taylor, Dr. Brian L. Howes
- 1996 Master of Environmental Design - Environmental Science. University of Calgary, Alberta, Canada
Thesis: A biogeochemical evaluation of ecotechnology for nitrogen removal from concentrated wastewater.
Advisors: Dr. Richard Revel, Dr. Brian L. Howes
- 1991 Bachelor of Science – Biology. University of Victoria, British Columbia, Canada
Thesis: Isozyme electrophoresis of an amphidiploid *Aster* and its progenitors.
Advisor: Dr. Geraldine A. Allen

EXPERIENCE

- 1998 – present Guest Investigator, School for Marine Science and Technology, University of Massachusetts, New Bedford, Massachusetts, USA
Supervisor: Dr. Brian L. Howes
- 1994 - 1996 Guest Student, Woods Hole Oceanographic Institution, Woods Hole, Massachusetts, USA
Supervisor: Dr. Brian L. Howes
- 1993 Research Assistant, Department of Biology, University of Calgary, Alberta, Canada
Supervisor: Dr. Robert Barclay
- 1990 - 1991 Research Assistant, Department of Biology, University of Victoria, British Columbia, Canada
Supervisor: Yussef Ibrahim

PUBLICATIONS

Hamersley, M.R., Howes, B.L., White, D.S., Johnke, S., Young, D., Peterson, S.B. and J.M. Teal. 2001. Nitrogen balance and cycling in an ecologically engineered septage treatment system. *Ecological Engineering*. 18:61-75.

PUBLICATIONS IN SUBMISSION

- Hamersley, M.R. and B.L. Howes. Particulate organic carbon availability controls denitrification in a septage-treating artificial wetland. *Water Research* (in submission).
- Hamersley, M.R., Howes, B.L., and D.S. White. The contribution of floating plants to ammonium and nitrogen removal via nitrification/denitrification in a septage-treating artificial wetland. *Journal of Environmental Quality* (in submission).

PUBLICATIONS IN PREPARATION

- Hamersley, M.R. and B.L. Howes. Contribution of denitrification to C, N, and O cycling in sediments of a New England salt marsh. (in preparation for submission to Marine Ecological Progress Series).
- Hamersley, M.R. and B.L. Howes. Evaluation of the N_2 flux approach for measuring sediment denitrification. (in preparation for submission to Applied Environmental Microbiology).
- Hamersley, M.R. and B.L. Howes. Coupled nitrification-denitrification in vegetated salt marsh sediments measured *in situ* using a $^{15}NH_4^+$ tracer. (in preparation for submission to Limnology and Oceanography).
- Hamersley, M.R. and B.L. Howes. Competition between plant uptake and coupled nitrification-denitrification for NH_4^+ measured *in situ* in salt marsh sediments. (in preparation for submission to Limnology and Oceanography).

CONFERENCES AND PRESENTATIONS

- Estuarine Research Federation International Conference, Providence, Rhode Island. October 15, 1997. The Role of Floating Plants in Nitrification and Nitrogen Removal in an Aerated Septage Treatment System.
- Ecological Society of America 80th Annual Meeting, Snowbird, Utah. August 3, 1995. Nitrogen Removal in an Ecologically Engineered Septage Treatment System.
- Woods Hole Oceanographic Institution Summer Lecture Series, Woods Hole, MA. July 27, 1995. Nitrogen Cycling in an Artificial Wetland Designed for Septage Treatment.

AWARDS, GRANTS, AND HONORS

- | | |
|-------------|---|
| 1997 - 2001 | Fellowship (stipend and tuition), Education Department, Woods Hole Oceanographic Institution |
| 2000 | Research grant (\$4000), Reinhart Coastal Research Center, Woods Hole Oceanographic Institution |
| 1997 | Honorable Mention – Conference Presentation, Estuarine Research Federation International Conference |
| 1992 - 1994 | Scholarship (stipend and tuition), Natural Sciences and Engineering Research Council (Canada) |
| 1991 | Graduated (B.Sc.) with 1 st Class Honors, University of Victoria |

ABSTRACT

I used direct measurements of nitrogen gas (N_2) fluxes and a ^{15}N stable isotope tracer to determine the contribution of denitrification to salt marsh sediment N cycling. Denitrification in salt marsh tidal creekbeds is a major sink for groundwater nitrate of terrestrial origin. I studied creekbed denitrification by direct measurements of N_2 fluxes in closed chambers against a low- N_2 background. I undertook experiments and simulation modeling of sediment N_2 fluxes in closed chambers to optimize the key experimental parameters of this approach. Denitrification in these sediments was driven by the degradation of labile organic matter pools which are depleted during long incubations. Sediment thickness was the most important parameter controlling the required incubation time. Errors of up to 13% with gas headspaces and 80% with water headspaces resulted from headspace N_2 accumulation and the resulting collapse of the sediment-water diffusion gradient. These errors could be eliminated by using headspaces of sufficient thickness. Headspace flushing to reduce ammonium accumulation did not affect denitrification rates, but caused transient disturbance of N_2 flux rates. Direct measurements of O_2 , CO_2 , N_2 , and inorganic N fluxes from the sediments of a salt marsh tidal creek were made in order to examine the interaction of denitrification with the carbon, oxygen, and N cycles. Organic carbon concentration and lability were the primary controls on metabolic rates. CO_2/N flux ratios averaged 6.1, indicating respiration driven by algal biomass. Allochthonous denitrification accounted for 39% of total sediment denitrification ($2.7 \text{ mol N m}^{-2} \text{ yr}^{-1}$). 46% of remineralized ammonium was denitrified, while the contribution of autochthonous denitrification to O_2 and CO_2 fluxes was 18% and 10%, respectively. A ^{15}N -ammonium tracer was used to study competition between plants and nitrifying bacteria for remineralized ammonium. In undisturbed sediments of *Spartina alterniflora*, plant uptake out-competed nitrification-denitrification, with plant uptake accounting for 66% of remineralized ammonium during the growing season. Under N fertilization ($15.5 \text{ mol m}^{-2} \text{ yr}^{-1}$), both plant N uptake and denitrification increased, but denitrification dominated, accounting for 72% of the available N. When plant uptake was hydrologically suppressed, nitrification-denitrification was stimulated by the excess N, shifting the competitive balance toward denitrification.

TABLE OF CONTENTS

Title Page.....	1
Acknowledgements	3
Biography	5
Abstract	7
Table of Contents	8
List of Tables.....	10
List of Figures	11
Chapter 1: Introduction	14
Chapter 2: Evaluation of the N ₂ flux approach for measuring sediment denitrification	24
Abstract	25
Introduction	26
Methods.....	32
Results	40
Discussion	44
Chapter 3: Contribution to denitrification to C, O, and N cycling in sediments of a New England salt marsh.....	67
Abstract	68
Introduction	69
Methods.....	71

Results	77
Discussion	96
Chapter 4: Competition Between Plant Uptake and Coupled Nitrification-Denitrification for NH_4^+ Measured <i>in situ</i> in Salt Marsh Sediments.....	104
Abstract.....	105
Introduction.....	105
Methods	110
Results.....	119
Discussion.....	135
Chapter 5: Conclusions	143
References	153
Appendix 1: Algorithm for modeling of N_2 flux.....	162

LIST OF TABLES

Table 2.1	Experimental procedures for N_2 gas flux measurements of denitrification	28
Table 2.2	N_2 flux calculations and symbols	37
Table 2.3	Effects of two experimental manipulations of headspace NH_4^+ concentrations on sediment metabolism	45
Table 3.1	Metabolic fluxes in Mashapaquit Marsh creek sediments	80
Table 3.2	Characteristics of sandy and muddy creek sediments from Mashapaquit Marsh	81
Table 4.1	Characteristics of unfertilized and XF fertilized vegetated salt marsh plots	111
Table 4.2	T_0 recovery of injected ^{15}N tracer in vegetated salt marsh sediment cores	114
Table 4.3	Loss and retention of $^{15}NH_4^+$ tracer from unfertilized and XF fertilized vegetated salt marsh plots	121

LIST OF FIGURES

Figure 2.1	Diagram of sediment flux chamber	34
Figure 2.2	Calibration of N ₂ flux model and paired aerobic/anaerobic flux chambers	41
Figure 2.3	Change in metabolic rates of salt marsh creek sediments through time.....	43
Figure 2.4	Modeled sediment porewater N ₂ off-gassing from a single aerobic flux chamber.....	49
Figure 2.5	Modeled effect of sediment thickness on denitrification N ₂ fluxes calculated with paired aerobic/anaerobic flux chambers	51
Figure 2.6	Modeled underestimation of sediment denitrification with flux chamber headspaces of various thicknesses.....	53
Figure 2.7	Modeled sediment N ₂ flux into a water headspace as a result of the collapse of sediment-water concentration gradients	55
Figure 2.8	Modeled effect of headspace flushing during incubation on sediment N ₂ fluxes.....	58
Figure 2.9	Modeled macrofaunal irrigation effects on denitrification N ₂ fluxes calculated with paired aerobic/anaerobic flux chambers	62
Figure 3.1	Location of the Mashapaquit Marsh with in the sandy outwash aquifer of Cape Cod, Massachusetts, USA	72
Figure 3.2	Gas fluxes from sediment cores during incubation in flux chambers	78

Figure 3.3	Seasonal cycles of sediment-watercolumn fluxes measured in sandy and muddy salt marsh creek sediments	84
Figure 3.4	Relationship between field temperature and salt marsh creek sediment metabolic rates	86
Figure 3.5	Relationship between sediment organic carbon content and metabolic rates in salt marsh creek sediments	87
Figure 3.6	Carbon-specific sediment C, O, and N fluxes at 4 sites along the salinity gradient of a salt marsh tidal creek.....	88
Figure 3.7	Watercolumn NO_3^- -driven denitrification in aerobic salt marsh creek sediment microcosms	90
Figure 3.8	Inhibition of sediment NO_3^- uptake by presence of O_2 decreases with increasing sediment O_2 consumption.	92
Figure 3.9	Elemental ratios of C, N, and O_2 fluxes across the sediment-water interface in salt marsh creek sediment microcosms	93
Figure 3.10	Contribution of autochthonous denitrification to C, O, and N fluxes in salt marsh creek sediments.....	95
Figure 4.1	Example of $^{15}\text{NH}_4^+$ tracer recovery from undisturbed vegetated salt marsh sediments	120
Figure 4.2	Seasonal denitrification rates in <i>S. alterniflora</i> salt marsh sediments.....	123
Figure 4.3	Uptake of $^{15}\text{NH}_4^+$ tracer by <i>S. alterniflora</i>	125
Figure 4.4	Porewater S^{2-} and <i>S. alterniflora</i> biomass in hydrologically-controlled laboratory lysimeters and reference field site	128

Figure 4.5	Relationship of porewater S^{2-} to aboveground <i>S. alterniflora</i> biomass in hydrologically-controlled lysimeters and reference field site.....	130
Figure 4.6	NH_4^+ and biomass in hydrologically-controlled lysimeters	131
Figure 4.7	Short-term fate of ^{15}N for top 15 cm of sediment in hydrologically- controlled lysimeters	134
Figure 4.8	Loss of ^{15}N tracer by coupled nitrification-denitrification in hydrologically-controlled lysimeters	136
Figure 4.9	Peak aboveground biomass and denitrification in fertilized and unfertilized vegetated salt marsh plots	138

CHAPTER 1

Introduction

Nitrogen (N) limits productivity in coastal waters and excessive N inputs can lead to eutrophication, causing watercolumn anoxia, loss of submerged aquatic vegetation, and damage to coastal fisheries (Ryther and Officer, 1981; Kautsky *et al.*, 1986).

Denitrification, the microbial loss of N through conversion to N_2 gas, plays an important role in controlling N availability to support coastal production & eutrophication.

Estuarine denitrification removes as much as 40 – 50% of terrestrial N before it reaches shelf and oceanic waters (Seitzinger, 1988). On the Atlantic coast of the U.S., salt marshes also play an important role in intercepting N as it flows from terrestrial to aquatic environments (Harvey and Odum, 1990; Howes *et al.*, 1996).

Nitrogen enters salt marshes primarily via groundwater, freshwater streams and tidal water (Valiela and Teal, 1979; Wolaver *et al.*, 1983). In glacial outwash soils such as those of Cape Cod, Massachusetts, groundwater nitrate (NO_3^-) from fertilizers and soil-based sewage disposal techniques is the primary source of N to salt marshes (Valiela *et al.*, 1990; Howes *et al.* 1996). Groundwater flows also contribute a substantial portion of the anthropogenic N load to coastal embayments (19% in Buzzards Bay, Massachusetts; Howes and Goehring, 1996). However, up to 80% of the influent groundwater NO_3^- may be removed during transit through a salt marsh (Howes *et al.*, 1996). The disappearance of groundwater NO_3^- results from microbial denitrification, the anaerobic heterotrophic respiratory pathway in which NO_3^- is converted to biologically less available N_2 gas. Salt marshes and estuaries therefore may act as buffers against the transport of potentially eutrophicating groundwater N into coastal waters.

Although the term denitrification had already been coined to describe the loss of NO_3^- to gaseous products, in a landmark 1886 study, Gayon and Dupetit (reviewed in Zumft, 1992) identified the intermediate species nitric oxide and nitrous oxide in studies of pure bacterial cultures. Denitrification received early attention because it was responsible for the loss of fertilizer N applied in agriculture. By the mid-twentieth century, experiments in natural soils had demonstrated high losses of N in aerated systems due to coupled nitrification-denitrification (Chapman *et al.*, 1949; Wijler and Delwiche, 1954). Direct evidence of denitrification in marine sediments came in 1971 (Goering and Pamatmat, 1971), and the highest marine denitrification rates have been reported from eutrophic estuarine and coastal sediments (reviewed in: Seitzinger, 1988). At present, the global oceanic N cycle appears to be unbalanced, with denitrification losses exceeding gains by 60 – 90% (Christensen *et al.*, 1987).

The NO_3^- substrate for denitrification is produced in nature from ammonium (NH_4^+) by nitrifying bacteria. The obligately aerobic chemoautotrophic oxidation of NH_4^+ first produces nitrite (NO_2^-) via an unstable hydroxylamine intermediate. Further chemoautotrophic oxidation converts NO_2^- to NO_3^- . Bacterial genera known to nitrify include *Nitrospira*, *Nitrospina*, *Nitrobacter*, *Nitrosovibrio*, *Nitrosoloba*, *Nitrosomonas*, *Nitrosococcus*, and *Nitrococcus* (McCaig *et al.*, 1994; Teske *et al.*, 1994; Stephen *et al.*, 1996). The abundance of nitrifying bacteria in natural waters and sediments is usually determined by culturing on specialized media and MPN methods (Matulewich and Finstein, 1978; Schmidt and Belser, 1982). Densities of nitrifying bacteria determined in this manner are <3 times lower than total bacterial densities, a figure which appears too

low to account for the contribution of nitrification to sediment O₂ and N cycling (18% and 46%, respectively: Chapter 3) (Chèneby *et al.*, 2000). Since these methods only register obligate NH₄⁺ oxidizers, it is probable that much of the nitrification taking place in natural environments is mediated by facultative nitrifiers. The advent of 16S rDNA probes for key genes involved in nitrification has demonstrated the large diversity of nitrifying bacteria. Nitrification has been found in four Proteobacterial subdivisions (α through δ) and one new bacterial phylum (*Nitrospira*) has been created based on 16S rRNA sequences (Teste *et al.*, 1994). Analyses of samples from diverse environments are continually increasing the known diversity of nitrifying bacteria (McCaig *et al.*, 1994; Teske *et al.*, 1994; Stephen *et al.*, 1996).

Denitrification itself is not really a single metabolic process, but a series of reductions, each coupled to oxidative phosphorylation in heterotrophic bacteria. The complete denitrification of NO₃⁻ requires four steps (NO₃⁻ → NO₂⁻ → NO → N₂O → N₂), each of which may be active to a greater or lesser degree in different bacterial strains. In nature, however, the intermediate products tend not to accumulate (reviewed in: Ferguson, 1994), and the bulk process may be described as the conversion of NO₃⁻ to N₂ gas. In natural environments, the production of N₂ from NO₃⁻ likely results from the action of consortia of denitrifying bacteria capable of carrying out one or more of these steps. Denitrification is inhibited by oxygen, although the precise mechanism of this inhibition is not well characterized. Oxygen only appears to inhibit cellular NO₃⁻ uptake and transport and the reduction of NO₂⁻ to NO (Ferguson, 1994). However, with only disputable exceptions, all denitrifying bacteria are facultative anaerobes, also capable of

aerobic heterotrophy. Denitrifiers are found in nearly all environments, from aquatic water columns to sediments, terrestrial soils, polluted environments, and within plants and animals. Although most denitrifiers are mesophilic, two psychrophilic and two moderately thermophilic strains are known. Although many denitrifiers are halotolerant, halophiles are found only among the denitrifying Archaeobacteria. Denitrifying bacteria are even more diverse than nitrifying bacteria, and though represented largely by the eubacteria, also include members of the Archaea (reviewed in Zumft, 1992). A recent review notes 130 species distributed over 50 genera (Zumft, 1992). Among the Proteobacteria, the α , β , and γ subclasses are represented, as are Gram-positive bacteria of the genera *Bacillus* and *Streptomyces* (Zumft, 1992; Chénby, 2000). Denitrification is also known from one species of fungi (although the reactions are not coupled to ATP production) (Ferguson, 1994). A variety of novel metabolic pathways of N transformation have recently been investigated in pure culture. Briefly, these include anaerobic NH_4^+ oxidation, aerobic denitrification, and nitrifier denitrification, the production of N_2 from NH_4^+ and NO_3^- (reviewed in Jetten *et al.*, 1997). However, the ecological and geochemical significance of these pathways is still unknown.

Nitrification and denitrification, though they are adjacent stages in the N cycle, spatially may occur proximately or separately. Nitrification takes place in aerobic surface layers of sediments where NH_4^+ released by mineralization or diffusing from deeper in the sediments is available (Patrick and Reddy, 1976). Anaerobic conditions within sediments and soils also make them ideal environments to support denitrification. Although denitrification is inhibited by O_2 , it can occur in anaerobic microniches in

otherwise aerobic soils and sediments, allowing close association with nitrifying bacteria (Jørgensen, 1978; Jenkins and Kemp, 1984; Bonin *et al.*, 1986). Similarly, O_2 released by the roots of aquatic macrophytes supports coupled nitrification-denitrification in deeper layers of the sediment (Reddy *et al.*, 1989). Such spatially coupled nitrification-denitrification is termed autochthonous denitrification. Based on the diffusion rate of NO_3^- , Jenkins and Kemp (1984) calculated a distance between nitrifiers and denitrifiers averaging 80 mm, indicating very tightly associated consortia operating in fine scale concentration gradients, most likely within labile organic particles (Jørgensen, 1977). Denitrification which is dependent on NO_3^- produced elsewhere (by watercolumn nitrification, advected fertilizer NO_3^- , nitrified wastewater, or other sources) is termed allochthonous denitrification.

Both allochthonous and autochthonous denitrification are controlled by complex feedbacks between the availability of substrate (organic carbon) supporting denitrification and the diffusion of O_2 , NH_4^+ , and NO_3^- (reviewed in: Meyer-Reil, 1994; Paerl and Pinckney, 1996). Thus denitrification is highly dependent on the physical structure of the sediments, and on the proximity of aerobic and anaerobic environments to each other (limiting diffusion rates). Although physical factors play a dominant role, community-specific bacterial physiology may also be important, as the metabolic capabilities of bacterial consortia may differ from site to site (Cavigelli and Robertson, 2000; Braker *et al.*, 2001).

The gaseous loss of N_2 is one of the most difficult N fluxes to measure, and in constructing N budgets for natural environments, denitrification has often been calculated

by difference between other, more easily measurable terms (reviewed in Seitzinger, 1988). The summing of multiple terms leaves large uncertainties in denitrification rates calculated in this way. A variety of techniques for measuring or estimating *in situ* denitrification rates have been developed over the last 25 years, but of most note are techniques which can be used *in situ* or in intact sediments (reviewed in: Seitzinger, 1988; Cornwell *et al.*, 1999).

Measuring denitrification in salt marsh sediments requires consideration of the unique features of these sediments. The regularly flooded marsh includes two divergent environments: the vegetated marsh, usually covered with salt-tolerant grasses like *Spartina spp.*, and muddy or sandy creekbottoms: narrow channels through the vegetated marsh which merge to create wider channels and shallow embayments. Denitrification in unvegetated salt marsh tidal creek sediments is supported by both autochthonous and allochthonous NO_3^- . The lack of vegetation permits direct measurement of N_2 fluxes from sediments in enclosed flux chambers. N_2 flux measurements of denitrification have been applied in a variety of freshwater and marine sediments (see citations in Chapter 3). However, because of the high concentration of N_2 in the atmosphere, the small fluxes due to denitrification are difficult to measure (Seitzinger *et al.*, 1980; Lamontagne and Valiela, 1995). N_2 fluxes can be measured in closed chambers with a low- N_2 headspace, but initially, diffusive fluxes from porewater N_2 pools in equilibrium with atmospheric N_2 dominate over denitrification fluxes. Thus long incubations are required for sediment “off-gassing” before denitrification can be measured (Seitzinger *et al.*, 1980; Nowicki, 1994).

In some sediments, the depletion of labile organic matter may cause metabolic rates to slow during long incubations. Another potential limitation of N_2 flux measurements in closed incubation chambers is disturbance of sediment-water diffusion gradients by changes in the gas headspace N_2 concentration (Jury *et al.*, 1982; Devol, 1987). Changes in the concentration of headspace N_2 primarily result from accumulation of N_2 during incubation and from mid-incubation flushing of the headspace, undertaken to reduce headspace water NH_4^+ accumulation. In order to optimize protocols for measuring denitrification N_2 flux, I combined experimental observations of N_2 flux with a simulation model of N_2 diffusion in order to minimize incubation times and disturbances of diffusion gradients. Sensitivity analysis revealed the key parameters affecting the accuracy of denitrification measurements made by the N_2 flux approach, and using the model, a general approach to optimizing the protocol for different sediments was developed (Chapter 2).

Although the importance of denitrification to the salt marsh N cycle is well established (Valiela and Teal, 1979; White and Howes, 1994a), denitrification also affects the cycling of C and O_2 . Sediment nitrification is dependent on NH_4^+ regenerated through the heterotrophic degradation of organic matter and on the diffusion rate of O_2 into the sediments. Denitrification requires labile organic matter for its own heterotrophic requirements; in addition, the anaerobic niches required to support denitrification are created through heterotrophic O_2 consumption. I investigated the links between the C, O, and N cycles in an unvegetated salt marsh tidal creek by simultaneously measuring fluxes of O_2 , CO_2 , and inorganic N species across the sediment

water interface in closed flux chambers over seasonal cycles. I studied the influence of sediment organic matter content and composition on metabolic rates in two sediment types, and determined the contribution of denitrification to the overall cycling of C, O, and N, in these salt marsh creek sediments (Chapter 3).

Nitrogen cycling in the vegetated marsh is structured by plant-sediment interactions, and large fluxes of nitrogen are internally recycled (White and Howes 1994a). NH_4^+ is released in the sediments by biomass degradation, making it available for re-uptake by plants. However, coupled nitrification-denitrification competes with plants for available NH_4^+ . The partitioning of NH_4^+ between plants and nitrifying bacteria is controlled by complex feedbacks involving the oxidation state of the sediment and NH_4^+ availability.

Much of the productivity of the marshes along the Atlantic coast of North America is due to *Spartina alterniflora* Loisel, but the growth of this grass is limited by N availability (Turner, 1976; Sullivan and Daiber, 1974; Valiela and Teal, 1974). In the low marsh, short-form *Spartina* rarely grows above 10 – 30 cm, but near the creekbanks, the tall form grows to 1 – 3 m (Howes *et al.*, 1986). In the short-form *Spartina* swards away from the creekbanks, poor drainage of tidal water results in more reducing sediment conditions and the accumulation of S^{-2} , which limits plant N uptake rates (Morris and Dacey, 1984). Along creekbanks, porewater drainage is improved, resulting in air entry into the sediments. The flux of air in and out of the sediments leads to more oxidizing conditions, low sulfide (S^{-2}) levels, and increased ability of plants to incorporate N (Howes *et al.*, 1986; Howes and Goehringer, 1994). The limitation of *Spartina* growth

by N availability can be overcome by fertilization. Increased plant growth increases evapotranspiration, which results in air entry into the sediments, increased sediment oxidation, and further increases in plant growth in a positive feedback cycle.

The dependence of N cycling in vegetated salt marsh sediments on tidal cycles and plant/sediment interactions makes it desirable to study these processes *in situ*. ^{15}N tracers have previously been used to study the remineralization of NH_4^+ from plant biomass and the long-term retention of ^{15}N in salt marsh sediments (White and Howes, 1994a, 1994b). In this study, I developed techniques using *in situ* injections of $^{15}\text{NH}_4^+$ to examine short-term competition between plant N incorporation and nitrification-denitrification for remineralized NH_4^+ . The partitioning of NH_4^+ between plants and nitrifiers was studied under conditions where plant N uptake was stimulated by N fertilization, and inhibited by reducing conditions in the sediment created by experimental flooding of hydrologically-controlled lysimeters (Chapter 4).

Linkages between denitrification and other salt marsh biogeochemical processes can be studied by adaptations of methods used to study denitrification in aquatic sediments. Denitrification in the salt marsh takes place within the context of linked biogeochemical fluxes of C, O, and N, and is structured by physical processes and the N metabolism of salt marsh primary producers. Knowledge of the interaction of denitrification with other salt marsh processes will increase our understanding of the unique role of salt marshes as intermediaries in the flux of nutrients from terrestrial to coastal environments.

CHAPTER 2

Evaluation of the N₂ Flux Approach for Measuring Sediment Denitrification

Abstract

N_2 production in aquatic ecosystems has been used as a direct measure of denitrification which avoids many of the artifacts and complexities associated with indirect approaches and tracer techniques. A variety of approaches for measuring sediment denitrification by N_2 gas flux are currently being applied. However, measurement protocols are typically determined based upon initial results or previous studies. I present a process level study and general model for evaluating and optimizing N_2 gas flux approaches in closed chamber incubations. Experimental manipulations of artificial and natural sediments were used to conduct a sensitivity analysis of key design parameters in N_2 flux measurements. Results indicated that the lowering of N_2 concentrations within the headspace overlying sediments to increase measurement sensitivity requires incubations of several days to weeks for diffusive off-gassing of porewater N_2 pools before the denitrification supported N_2 flux can be measured. However long incubations can result in underestimates of denitrification in some systems, due to a depletion of labile organic matter. Sediment thickness was found to be the primary determinant of off-gassing time. Attempts to increase measurement sensitivity and shorten incubation times by reducing the headspace thickness to 1 - 2 cm were found to result in underestimates of denitrification by 3 – 13% for gas headspaces to nearly 80% for water headspaces, but errors were negligible with thicknesses above 10 cm (gas) or 15 cm (water). Accumulation of dissolved inorganic N in the overlying water during incubation was not sufficiently reduced by periodic flushing to affect denitrification rates, but caused transient sharp fluctuations in N_2 flux. Parallel incubations of cores with

aerobic and anaerobic headspaces have also been attempted to reduce incubation time. However, faster off-gassing rates in aerobic chambers with active macrofaunal irrigation made anaerobic chambers poor controls for diffusive fluxes. The best approach found to minimize incubation time and reduce errors was to select the minimum sediment thickness necessary to include the entire depth distribution of nitrification-denitrification for a particular sediment system. Disturbance of sediment gas profiles by headspace flushing should be avoided where possible. Gas headspaces should be close to 10 cm thick, particularly when incubating thick sediment cores. Anaerobic cores to control for diffusive N_2 fluxes shorten incubation time, but should not be used in sediments with macrofaunal irrigation extending below 6 cm.

Introduction

Denitrification, the microbial reduction of nitrite (NO_2^-) and nitrate (NO_3^-) to N_2 gas, plays an important role in the N cycle as it removes N from pools available to plant uptake. Accurate measurement of denitrification rates plays an important role in the construction of N budgets for natural environments, and is essential to understanding the ecological effects of anthropogenic N enrichment (Valiela and Teal, 1979; Smith, 1999). Aquatic sediments have emerged as major sites of denitrification activity, accounting for up to 85% of total global denitrification (Christensen *et al.*, 1987; Schlesinger, 1991; Middelburg *et al.*, 1996). However, measuring denitrification presents special problems, since substrates for denitrification are produced and consumed by a variety of microbial

processes, and N_2 production rates are small relative to background N_2 concentrations (Wijler and Delwiche, 1954; Blackburn, 1979; Seitzinger, 1988).

Denitrification in marine sediments has been inferred from porewater NO_3^- profiles (Vanderborght and Billen, 1975) and deviations from expected stoichiometries of N and P regeneration (Nixon *et al.*, 1975). However, broad application of denitrification measurements in ecological and biogeochemical studies of aquatic sediments did not take place until the adaptation of ^{15}N tracer methods and acetylene block techniques developed in the soil sciences (Yoshinari and Knowles, 1976; van Kessel, 1977; Sørensen, 1978). Early work with these techniques was often restricted to the measurement of sediment denitrification of watercolumn NO_3^- (allochthonous denitrification), while studies of denitrification of NO_3^- produced *in situ* by nitrification of regenerated NH_4^+ (autochthonous denitrification) were under-represented (Jenkins and Kemp, 1984).

While refinements of the ^{15}N isotope techniques continue to be developed (Nielsen, 1992), it was the development of techniques for measurement of sediment N_2 production that enabled simple and direct measurements of autochthonous denitrification in intact sediments with inexpensive equipment (Seitzinger *et al.*, 1980; for reviews see Seitzinger *et al.*, 1993; van Luijn, 1996). Sediment N_2 flux measurements are typically made in intact sediment cores incubated in closed chambers with a low- N_2 headspace, allowing the relatively small denitrification fluxes to be measured against a low- N_2 background. In the past decade, N_2 flux approaches have been broadly applied (see Table 2.1 for references). Autochthonous denitrification is measured with low NO_3^- headspace

Table 2.1. Experimental procedures for determining sediment denitrification rates by measurement of N₂ gas fluxes.

Method	Core		Sediment		Headspace thickness		Off-gassing		Measurement		Reference
	dia.	depth	cm	cm	Air	Water	incubation ^a	incubation ^a	incubation	chamber closure	
	cm	cm	cm	cm	cm	cm	days	days	time (total) ^b	time ^c	
Aerobic flux chambers ^d	8.0	18-20	5-7	0	0	0	0	4 hr	4 hr	4 hr	Kaplan <i>et al.</i> , 1979
	7.8	4	1.3	3.2	13	13	13	30	1-2	1-2	Seitzinger <i>et al.</i> , 1980
	7.8	5	1.3	6.4	11	11	11	5-15	1-3	1-3	Seitzinger <i>et al.</i> , 1984
	7.8	7	1.5	6.4	10	10	10	14	1	1	Seitzinger and Nixon, 1985
	6.8	5-6	6.5	5.1	28	28	28	28-56	3-7	3-7	Gardner <i>et al.</i> , 1987
	6.8	7	2.0	8.5	10	10	10	4-8	1-2	1-2	Seitzinger, 1987
	7.2	7	1.4	4.1	9-12	9-12	9-12	4-15	1-3	1-3	Yoon and Brenner, 1992
	6.8	6	2.0	21.3	10	10	10	4-8	1	1	Seitzinger <i>et al.</i> , 1993
	6.8	6	2.0	17.0	10	10	10	4-8	1	1	Seitzinger, 1994
	6.8	7	1.8	4.1	9	9	9	10-15	2-3	2-3	Zimmerman and Benner, 1994
Paired aerobic/anaerobic flux chambers ^d	5.6	2-4	4.1	4-6	10	10	10	20	1	1	van Luijn <i>et al.</i> , 1996
	5.6	2-4	4.1	4-6	10	10	10	30	1	1	van Luijn <i>et al.</i> , 1999
	8.0	5	1.4	15.9	2	2	2	5	3-5	3-5	Nowicki, 1994
	8.0	20	1.4	15.9	2	2	2	4-5	4-5	4-5	Nowicki <i>et al.</i> , 1999
Ambient dissolved N ₂ headspace ^e	8.8	8-12	6.6-10	6.6-10	3	3	3	4	7	7	This study
	23 ^f	-	0.0	4-8	0	0	0	0.2-1.5	0.2-1.5	0.2-1.5	Devol, 1987; 1991; Devol and Christensen, 1993
	15.6	30	0.0	15.9	0	0	0	0.17-0.5	0.17-0.5	0.17-0.5	Lamontagne and Valiela, 1995
	56.0	9	0.0	1.0	0	0	0	2+	1	1	Nowicki <i>et al.</i> , 1999

^a In some cases, the precise off-gassing incubation and incubation times were not explicit. Times were then estimated using all the information given.

^b Total measurement incubation time after off-gassing incubation.

^c Duration of flux chamber closure between headspace flushes.

^d laboratory flux chambers except Kaplan *et al.*

^e field flux chambers except Lamontagne and Valiela.

^f Square dimensions.

water, while total denitrification (autochthonous + allochthonous) can be measured by using headspace water containing NO_3^- near *in situ* levels. In addition, this method allows denitrification to be measured simultaneously with other sediment-water fluxes such as O_2 , CO_2 , ammonium (NH_4^+), and NO_3^- for integrated investigations of sediment C, O and N cycling (e.g. Zimmerman and Benner, 1994; Chapter 3). However, the limitations of the N_2 flux method must be understood in order for it to be applied correctly.

The measurement of N_2 fluxes from flooded sediments presents a number of problems, including: separation of the initial diffusive flux of porewater N_2 into a low- N_2 headspace from denitrification-derived N_2 production, departures of the closed chamber environment from *in situ* conditions during incubation, and the inhibition of sediment N_2 flux rates by the decline in the concentration gradient across the sediment-water interface due to headspace N_2 accumulation.

Since sediment porewater N_2 pools are in near equilibrium with atmospheric N_2 concentrations, sediments incubated with a low- N_2 headspace support an initially large diffusive N_2 efflux from the sediments. This porewater “off-gassing” continues until initial porewater N_2 pools are depleted, whereupon the underlying denitrification fluxes can be measured (Seitzinger *et al.*, 1980). The period required for sufficient N_2 off-gassing to occur and N_2 flux to reflect N_2 production by denitrification can vary from 9 – 28 days (Table 2.1), raising the possibility of temporal changes in sediment conditions, macrofaunal irrigation, or the labile organic matter pool. Although in some coastal sediments, long core holding times do not appear to result in changes in metabolic rates

(Nowicki, 1994), in sediments dependent on continuous inputs of fresh algal biomass nutrient cycling may decline over the course of long incubations. Also, during long incubations, headspace water NH_4^+ and NO_3^- may rise to well above *in situ* levels. Potential stimulation of natural rates of nitrification and/or denitrification by elevated headspace water NO_3^- concentrations can be diminished by frequent replacement of headspace water. However, this approach also affects the accumulation of N_2 required for measurement of denitrification, and introduces the potential for N_2 contamination and disturbance of sediment N_2 profiles. The problems of long incubation times have recently been addressed by a modification of the N_2 flux approach using parallel incubation of pairs of cores, one with an aerobic and one with an anaerobic headspace. This approach attempts to provide a control for diffusive porewater N_2 off-gassing through anaerobic suppression of coupled nitrification-denitrification, and significantly reduces the incubation time required to obtain accurate denitrification rates (Nowicki, 1994). However, potential alteration of macrofaunal irrigation, hence rates of N_2 off-gassing, is of concern.

Simulation models can be used to understand the dynamics of diffusive N_2 flux in closed flux chambers in order to optimize protocols for denitrification rate determinations. Models of diffusion and denitrification in sediments held in closed flux chambers differ in important respects from the diagenetic models developed by Berner (1980) and applied to porewater NH_4^+ and NO_3^- profiles in marine sediments (Vanderborght and Billen, 1975; Soetaert *et al.*, 1996). Unlike the steady state, open systems modeled in the diagenetic equations, N_2 concentration profiles in sediment

systems in closed flux chambers are not in equilibrium. Organic particle fluxes to the sediments from the water column may also be ignored. Therefore, in flux chamber incubation of sediments, a sufficient understanding of N_2 fluxes need consider the production and diffusion of N_2 alone. Some workers have modeled diffusive N_2 fluxes in closed chambers in order to put constraints on sediment off-gassing times for specific systems (Nowicki, 1994; van Luijn, 1996), but a general treatment of the problem as it relates to shortening incubation times and reducing errors has not been attempted.

Flux models have been developed for field chamber measurements of N_2O fluxes out of soils (Matthias, *et al.*, 1978; Jury *et al.*, 1982). These models investigated the inhibition of N_2O sediment fluxes by headspace N_2O accumulation during incubation, resulting from the decline in the concentration gradient which drives the N_2O emission. Various mathematical methods were proposed to correct for this underestimation. However, these models are not directly applicable to closed chamber methods for measuring denitrification, since field chambers used for N_2O flux measurements have no bottom boundary and no off-gassing flux. In addition, these models used two-dimensional diffusion equations to describe the diffusion of gas from below the field chamber, and equations describing diffusional fluxes in unsaturated soils, which differ from those in submerged sediments.

In the present study, I tested a general model of N_2 diffusion and production in closed chambers with low N_2 -headspaces in order to optimize the key parameters of N_2 flux measurement protocols and potentially expand the utility of this method,. I also experimentally investigated the effects of long incubation times on measured

denitrification rates. In my analysis, the importance of minimizing incubation time by optimizing sediment depth and flux chamber dimensions is emphasized, and the effectiveness of various methods of determining denitrification N_2 fluxes is evaluated.

Methods

Experimental

Experiments were conducted to examine the effects on measured denitrification rates a) of long incubation times resulting in either lower rates due to depletion of labile organic matter pools or stimulation due to accumulation of NH_4^+ in overlying water and b) measurement protocols relating to selection of headspace volume or matrix (water and/or gas) or thickness of sediment cores. Denitrification was measured using N_2 flux in closed chambers ($N = 2$) containing intact sediment cores and using parallel incubations with aerobic and anaerobic headspaces (Nowicki, 1994). The anaerobic cores acted as control for diffusive N_2 off-gassing as well as potential N_2 contamination. Sandy (density 1.22 g cm^{-3} , C content $0.55 \text{ mol C cm}^{-3}$) and muddy (density 0.39 g cm^{-3} , C content $1.2 \text{ mol C cm}^{-3}$) sediments were collected from the unvegetated tidal creek at Mashapaquit Marsh, Cape Cod, Massachusetts, USA (see Figure 3.1) as described in Chapter 3.

In order to determine the effect of NH_4^+ accumulation on sediment metabolism during incubations, sediments from sandy and muddy sites were subjected to treatments designed to lower NH_4^+ accumulation. In one experiment in muddy sediments, headspace water was replaced daily with fresh half-strength seawater and the

denitrification rate determined from the difference between initial N_2 concentration (after gas and water headspace flushing and core closure) and final concentration (just before the next headspace flush). Controls received the same treatment except that after flushing, the original headspace water was replaced. All water was removed and replaced under an Ar atmosphere. A second experiment was conducted where NH_4^+ concentrations were reduced, but without introducing the potential for N_2 contamination or disturbance of sediments. Mesh bags of zeolite pellets (6 mesh) were suspended in the headspace water of flux chambers to adsorb dissolved NH_4^+ , while control chambers contained bags of polyethylene disks. Headspace water was not flushed for either treatment. NH_4^+ concentration in the headspace water was determined on samples collected through the valved port and analyzed immediately for NH_4^+ by a colorimetric indophenol method (Scheiner, 1976).

In order to evaluate the distribution of denitrification with depth in the sediment, denitrification rates were measured using cores of four thicknesses (0 – 2, 0 – 4, 0 – 6, 0 – 10 cm. Sediments were collected from the sandy site, with 4 chambers established for each sediment thickness (2 aerobic and 2 anaerobic, as above).

For all experiments, sediments (8 - 12 cm thick) were collected in glass cylinders (8.8 cm dia. x 25 cm). Overlying water was replaced with 7 – 10 cm of half-strength filtered (0.45 μm) seawater, leaving a 7 – 10 cm gas headspace. A magnetic stir bar in a cage (60 rpm) was fitted into the cylinder at the gas-water interface. The top and bottom

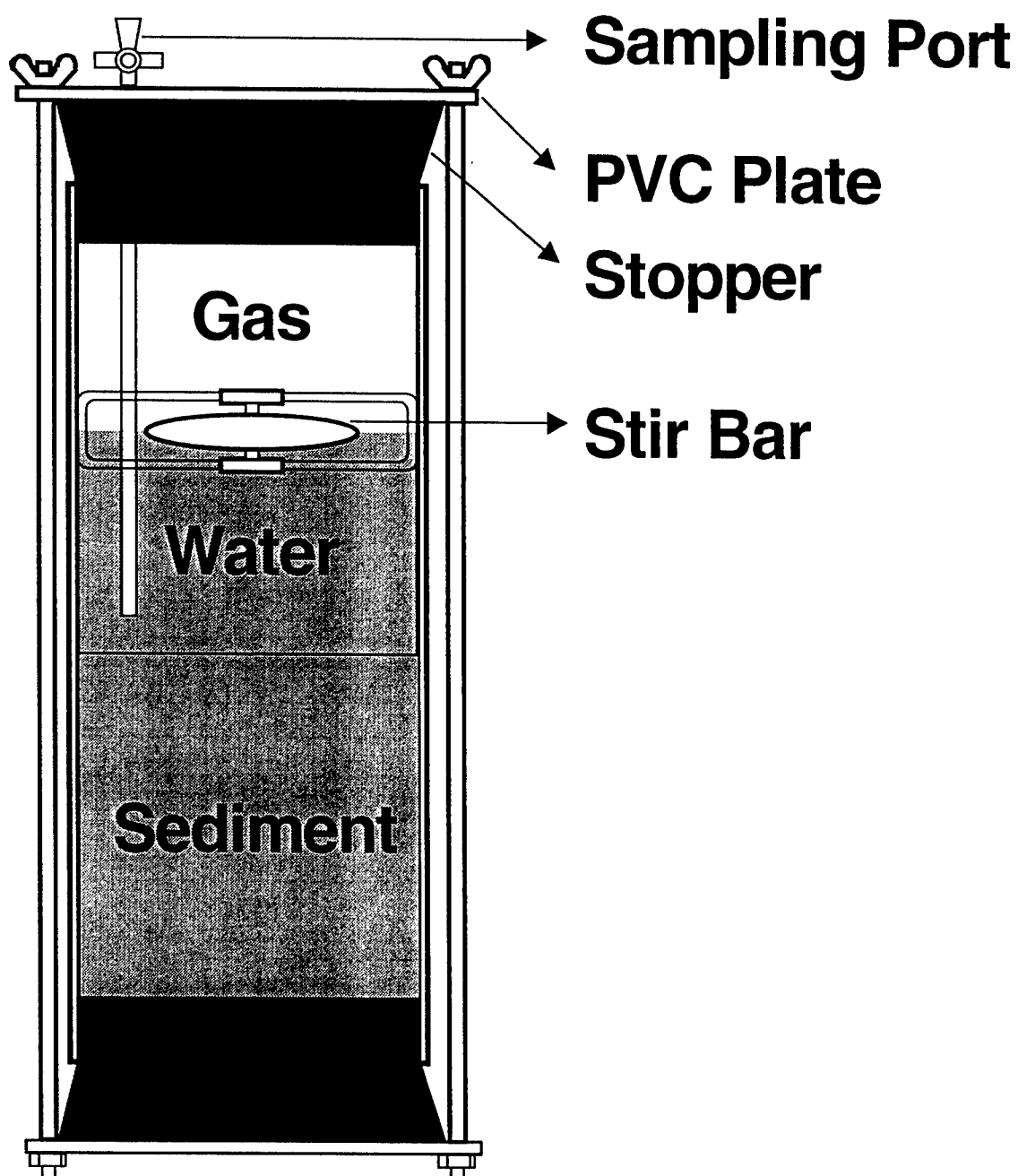


Figure 2.1 Diagram of chamber for measuring N_2 flux from sediments. Sediments are collected and incubated in a glass core tube (8.8 cm) with a headspace consisting equally of gas and water phases. Gas samples are withdrawn through the top butyl stopper and water samples through the valved sampling port.

of the flux chamber were sealed with two butyl stoppers compressed onto the chamber by a press (Figure 2.1). The top stopper was fitted with a valved port for sampling headspace water. Each flux chamber was held completely immersed in a water bath (at field temperatures) to minimize diffusion of atmospheric gas into the chamber. The valved port and tubing were kept filled with headspace water to further minimize contamination by atmospheric gas.

Four replicate chambers were established for each sediment site, with 2 each incubated with an aerobic or anaerobic headspace. The gas phase of the flux chamber was flushed for 30 minutes at 1 L min^{-1} with either a mixture of 80% He/20% O_2 (aerobic) or 100% He (anaerobic). The flush gas was introduced through the valved port and bubbled through the headspace water, then vented through a flowmeter and water trap. After 30 min, each cylinder was pressurized to 1.3 atm using a low-pressure regulator attached to the gas cylinder. This overpressure allowed gas samples to be withdrawn and compensated for pressure losses from O_2 consumption and DIC production.

Before each headspace gas measurement the pressure of each chamber's headspace was measured with a electronic pressure gauge (Cole-Parmer). Gas samples (5 mL) were then withdrawn using a He flushed gas-tight locking syringe with a non-coring septum needle. Gas samples were analyzed for N_2 using a Shimadzu GC-14A gas chromatograph equipped with a thermal conductivity detector and calibrated with a certified N_2 standard (3%) (O_2 was measured similarly). Measurements were made daily

for the first week; and less frequently during the second week. At the end of the experiment the volume of the gas and water headspaces were measured.

Calculations

Sediment denitrification rates were calculated using Equations 2.1 – 2.6 (Table 2.2). Sediment N_2 flux was calculated from the change in total headspace mass over time (Equation 2.1). Gas concentration measurements (C_i as % gas composition by volume) were converted to masses using the ideal gas law, and the measured pressure (P_i), temperature (T) and volume (V) of the gas headspace. The cumulative headspace N_2 mass produced was calculated using Equation 2.2, by summing the N_2 mass present in the headspace at timepoint i , the cumulative mass withdrawn for sampling up to the last sampling period (W_{i-1}), and the cumulative mass lost via leaks to the atmosphere (L_i). Since the headspace water and gas phases were well mixed, they were assumed to be in equilibrium, and since dissolved N_2 accounted for <1% of total N_2 , only the gas portion was considered. W_i was calculated using Equation 2.3, and L_i was calculated by Equation 2.4 using the difference between the expected headspace pressure and P_i . During incubation of aerobic cores, significant O_2 uptake occurs due to aerobic respiration and oxidation of reduced end products of metabolism. Although equivalent amounts of CO_2 are released from the sediments, much of the CO_2 remains dissolved in the headspace water, resulting in a net drop in headspace gas pressure. The expected pressure is calculated by Equation 2.5 from the net changes in the partial pressures of O_2 and CO_2 . Flux rates across the sediment/water interface were calculated from regressions of the linear parts of the curve of mass over time, using 3-5 timepoints and expressed as

Table 2.2. N₂ flux calculations and symbols

Equations:

$$F = A^{-1} \frac{\delta N}{\delta t} \quad (2.1)$$

$$N_i = \frac{P_i V C_i}{RT} + W_{i-1} + L_i \quad (2.2)$$

$$W_i = \sum_{t=0}^i \frac{S_i P_i C_i}{RT} \quad (2.3)$$

$$L_i = \sum_{t=0}^i (P_{(e)i} - P_i) \frac{V(C_i + C_{i-1})}{2RT} \quad (2.4)$$

$$P_{(e)i} = P_0 - \frac{\sum_{t=0}^i S_i P_i}{V} - (P_{(O_2)0} - P_{(O_2)i}) - (P_{(CO_2)0} - P_{(CO_2)i}) \quad (2.5)$$

$$F_d = F_o - F_a \quad (2.6)$$

Symbols:

Symbol	Description	Units
A	area of core	m ²
C	concentration of N ₂ in headspace	mL mL ⁻¹
F_d	denitrification N ₂ flux from sediments	mmol N m ⁻² d ⁻¹
F_a	N ₂ flux (anaerobic)	mmol N m ⁻² d ⁻¹
F_o	N ₂ flux (aerobic)	mmol N m ⁻² d ⁻¹
i	timepoint (numbered sequentially from 0)	
L	cumulative N ₂ lost through leaks	mmol N
N	N ₂ mass in headspace	mmol N
P	pressure of headspace	atm
$P_{(e)}$	expected pressure calculated from known losses	atm
$P_{(CO_2)}$	partial pressure of CO ₂ in headspace	atm
$P_{(O_2)}$	partial pressure of O ₂ in headspace	atm
R	gas constant	atm cm ³ mmol ⁻¹ °K ⁻¹
S	total volume of gas withdrawn for assay	cm ³
T	temperature	°K
t	time	d
V	total volume of gas phase of headspace	cm ³
W	cumulative N ₂ mass withdrawn in gas sampling	mmol N

mmol m⁻² d⁻¹ (Nowicki, 1994). Corrections for the diffusion of porewater N₂ into the low-N₂ headspace were made by subtraction of the N₂ fluxes in chambers where coupled nitrification-denitrification was anaerobically inhibited (Equation 2.6).

Modeling Diffusion-Driven N₂ Fluxes

A model was developed to allow optimization of experimental protocols to minimize the incubation time needed to accommodate sediment off-gassing and minimize declines in sediment N₂ efflux resulting from N₂ accumulation in the chamber headspace during incubation. The model is based on a simplified version of the general diagenetic equation (Berner, 1980), considering only the diffusion and reaction terms in one dimension:

$$\frac{\partial C}{\partial t} = D_a \frac{\partial^2 C}{\partial z^2} + R \quad (2.7)$$

where C is the concentration of N₂, t is time, D_a is the apparent diffusion coefficient (see below), z is the depth in the sediment, and R is the N₂ production term.

The sediment was divided into 1 cm layers with an overlying headspace layer and $\partial C/\partial t$ for the bottom and top boundaries boundary was set to 0. Sensitivity analysis showed that finer division of the sediment column had no effect on modeled rates. Based on experimental evidence, N₂ production from denitrification was assigned to the top 2 cm of sediment alone (see below). No denitrification was ascribed to the filter-sterilized (0.22 µm) headspace water. Since the stirred headspace water and gas phases were in equilibrium, and the mass of dissolved gas in the headspace water phase was very small

(<1%) relative to the gas phase, the model functions as if the gas phase is directly over the sediments, with N₂ diffusing across the sediment-gas interface according the concentration gradient calculated from the Bunsen coefficient (Weiss, 1970).

The model was calibrated with data from experimental measurements of diffusive N₂ flux from anaerobic sediments and combusted mineral sand. All terms were explicit (temperature, salinity, porosity, and thickness of sediment and headspace gas). The initial concentration of N₂ in the porewater was determined from the equilibrium concentration of N₂ in the headspace gas of anaerobic (no denitrification) chambers, divided by the water content of the sediment (porosity). The model was coded for numerical simulation of the timecourse of incubation (Appendix 1), with a time step of one minute (chosen after sensitivity analysis). The apparent diffusion coefficient (D_a) was then adjusted to fit the observations of N₂ flux. D_a was considered to be a composite of a number of terms, including diffusion, porosity, tortuosity, and advection by headspace water flow.

After calibration, the model was run under conditions of varying sediment thickness and porosity, and gas headspace thicknesses. Since the results of the model are independent of the area of the sediments incubated, the term “headspace thickness” is used to describe the one-dimensional component of headspace volume independent of the core area. Although the specific results of these runs are dependent on the value of D_a used, the experimentally determined value (0.00012 cm s⁻¹) was used for all model runs. The results were weakly dependent on temperature and salinity, since these parameters only apply to calculation of the Bunsen coefficient, and therefore the initial concentration

of porewater N_2 . Temperature was held at 20°C, and salinity at 32 ppt for all model runs. For all simulations, the model was first allowed to come to steady state with an infinite headspace at atmospheric N_2 concentrations to calculate the initial sediment N_2 concentration. Since most investigators replace the headspace gas and water after the initial off-gassing incubation, and in order to separate off-gassing effects on measured rates from subsequent effects, model runs examining measurement incubations on previously off-gassed sediments were started with sediment N_2 pools set at equilibrium with a 0.01 atm N_2 headspace.

Results

In sediments without denitrification (anaerobic), N_2 efflux into a low- N_2 headspace was initially high, as a result of the large N_2 concentration gradient between sediment and headspace (Figure 2.2a). As the sediment N_2 pool is depleted, diffusion slows until equilibrium is attained. In sediments with denitrification (aerobic), after the initial period of rapid N_2 off-gassing, the continuous input of N_2 from denitrification maintains a flux out of the sediment (Figure 2.2a). Accurate denitrification rates could be calculated after a 3 day incubation by subtracting the N_2 off-gassing flux in anaerobic chambers from the N_2 fluxes in aerobic chambers (Figure 2.2b).

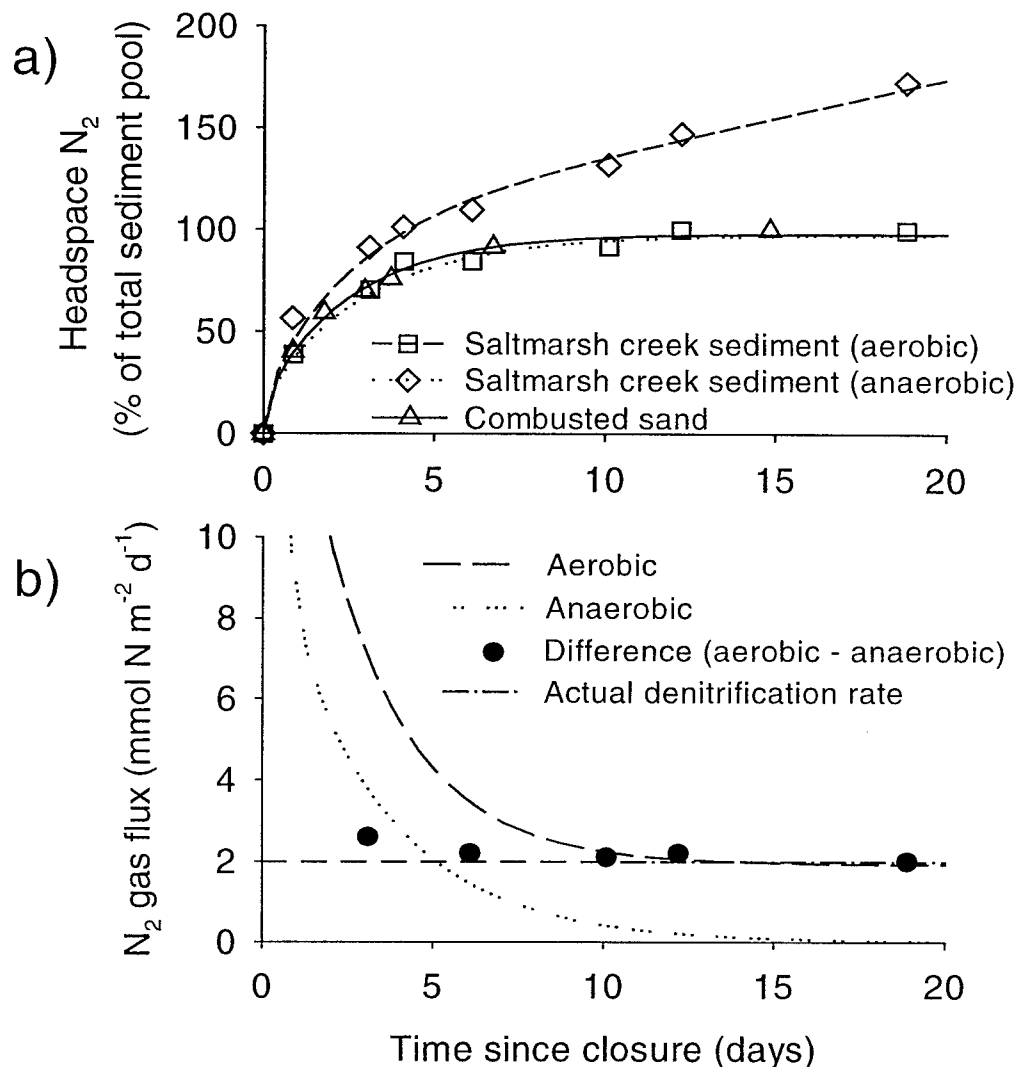


Figure 2.2 N_2 fluxes from sediments incubated in flux chambers (leak-corrected) and verification of N_2 flux model and paired aerobic/anaerobic chamber calculations of denitrification rates. **a)** N_2 flux into low- N_2 headspace from combusted (carbon-free) mineral sand, and saltmarsh creek sediment incubated aerobically and anaerobically (points). Model results are plotted as lines. All inputs to model are measured parameters except the diffusion coefficient, which was selected to fit curve to points. N_2 effluxes from anaerobic sediment and combusted sand are due to diffusion from sediment pools alone, excess ($> 100\%$) evolution of N_2 from aerobic sediment is due to denitrification of nitrate generated *in situ* by nitrification of mineralized N. **b)** Calculation of denitrification as the difference between N_2 fluxes in aerobic versus anaerobic incubations. Modeled N_2 flux plotted as lines; points represent flux calculated from experimental data.

Effect of Incubation Time

Rates of O₂ consumption and denitrification in the salt marsh creek sediments of this study in most cases declined during incubation times of 2 weeks (Figure 2.3). In metabolically active sediments with high O₂ consumption rates (mean 58 mmol m⁻² d⁻¹), the O₂ consumption rate in the second week of incubation changed by +24% to -60% from the rate observed during the first week after collection (Figure 2.3a). On average, O₂ consumption fell by 19% from week 1 to week 2 (t-test, N = 39; p < 0.001). The relationship between changes in O₂ consumption and the initial rate was most pronounced for sandy sediments (r = -0.82, N = 21; p < 0.001) versus muddy sediments (r = -0.43, N = 18; p = 0.075). Similarly, denitrification rates also tended to decline from week 1 to week 2 of incubation in sandy and muddy sediments with high denitrification rates, although the response was highly variable (Figure 2.3b). Denitrification in muddy sediments fell by an average of 14%, although the change was not significant (t-test, N = 16; p = 0.09). In sandy sediments, denitrification fell by up to 88% when denitrification rates were high (r = -0.82, N = 13; p < 0.001), but appeared to increase in sediments with low initial denitrification rates.

Sediment Thickness and Ammonium Accumulation

No significant relationship was found between incubated sediment thickness (2, 4, 6, or 10 cm) and sediment carbon-adjusted O₂ consumption (linear regression, r² = 0.004, N = 8). Likewise denitrification was poorly correlated with sediment thickness (linear regression, r² = 0.28, N = 8), indicating that both O₂ consumption and denitrification in these sandy sediments were active predominately in the top 2 cm of the sediment.

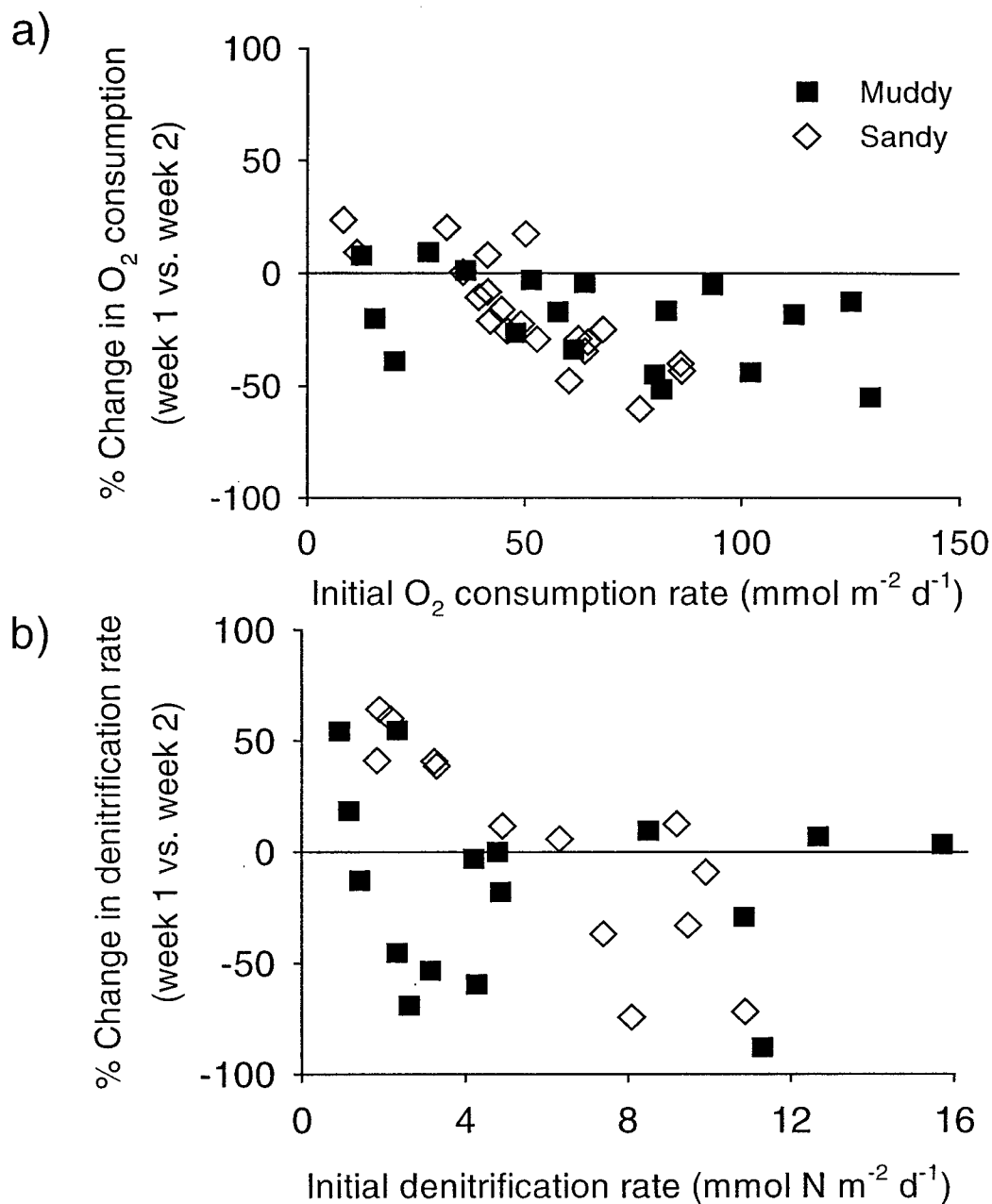


Figure 2.3 Change in metabolic rates of salt marsh creek sediments from the first to second weeks of incubation. In general rates tended to decline at higher levels of **a)** oxygen uptake and **b)** denitrification. The declines were greater in low organic (sandy) versus high organic (muddy) sediments, presumably due to depletion of labile organic matter.

Reducing NH_4^+ accumulation by either daily changes of headspace water or adsorption with zeolite had no discernable effect on rates of denitrification or O_2 consumption. Daily flushing reduced NH_4^+ concentrations nearly 5-fold, from a mean of 260 to 58 μM , compared to the *in situ* porewater concentration of 6 μM (Table 2.3). However, denitrification and O_2 consumption rates did not significantly differ between the treatments (2-tailed t test, $p > 0.18$). Similarly, the zeolite treatment reduced NH_4^+ concentrations by 3-fold, from 440 μM to 140-170 μM , but again there was no significant difference in either O_2 consumption or denitrification rates (2-tailed t test, $p > 0.18$).

Discussion

Placing a low N_2 atmosphere over sediments to increase the detection of N_2 efflux for determination of denitrification rates necessitates long incubation times to allow off-gassing of the sediment N_2 pool. However, a simple model can be used to adjust measurement protocols to optimize the key parameters of sediment thickness and headspace gas thickness.

Model Verification

The simulation model was successfully used to model diffusive fluxes in estuarine sediments and combusted sand (Figure 2.2a). The model accurately represented the high initial N_2 efflux in both aerobic and anaerobic chambers based upon a slowing of diffusion due to the declining concentration gradient within the sediment as the porewater N_2 pool off-gasses. The apparent diffusion coefficient (D_a) was calculated by a fit of the

Table 2.3. Effects of two experimental manipulations of headspace NH_4^+ concentrations on sediment metabolism. Values are mean \pm SE (N = 2).

Experiment A Headspace water change	NH_4^+ (μM)	Denitrification ^a ($\text{mmol m}^{-2} \text{d}^{-1}$)	O_2 consumption ^a ($\text{mmol m}^{-2} \text{d}^{-1}$)
Control (unchanged)	260 (41)	3.4 (1.5)	69 (4)
Flushed daily	58 (7)	3.8 (1.9)	70 (7)
Ratio	4.5	0.9	1.0
Experiment B Zeolite adsorption of NH_4^+			
Control - muddy	440 (10)	2.2 (0.4)	81 (16)
Zeolite - muddy	140 (40)	2.5 (0.1)	84 (4)
Ratio	3.1	0.9	1.0
Control - sandy	440 (70)	1.7 (0.5)	106 (2)
Zeolite - sandy	170 (30)	1.3 (0.8)	100 (36)
Ratio	2.6	1.3	1.1

^a No significant differences between treatments (2-tailed t test; $p > 0.18$)

model to the data. Although the relative importance of the factors which contribute to D_a (porosity, tortuosity, macrofaunal irrigation) were not determined, for the purposes of this study, it was only necessary to determine their composite effect on diffusion, and that this composite D_a could be applied consistently to all of the sediment systems in question. D_a was found to be $0.00012 \text{ cm}^2 \text{ s}^{-1}$ for both sandy and muddy sediments ($N = 8$), and $0.00017 \text{ cm}^2 \text{ s}^{-1}$ for combusted sand ($N = 4$). The apparent diffusion coefficients were about 5 times the molecular diffusion coefficient (Broeker and Peng, 1982). Similar differences between D_a and molecular diffusion coefficients have been observed by other researchers in both artificial and marine sediments, and the difference may be due to advection of headspace water through the sediments by stirring, irregular surface characteristics, and variations in effective sediment porosity (Boynnton, 1981; Güss, 1998). The higher D_a in the artificial sediment may be due to the absence of the layer of fine organic material at the sediment surface found in sandy and muddy sediments which would have facilitated advection of headspace water through the sediments.

N_2 fluxes in both the aerobic and anaerobic cores could be modeled using the same D_a , indicating a minor role for macrofaunal irrigation in these aerobic sediments. Macrofauna in these sediments were primarily amphipods known to irrigate only the top 1 cm of sediment (George Hampson, pers. comm.). The visual redox discontinuity (depth of light-colored, oxidized sediment) was $\sim 0.5 \text{ cm}$, with oxidized macrofaunal burrows and tubes extending below this zone were rare (pers. obs.)

Off-gassing Incubation Times

The long incubations needed to accommodate sediment off-gassing were found to affect metabolic rates in some sediments, although the effect was variable and depended on the overall metabolic activity of the sediment at the onset of measurement (Figure 2.3). Although Nowicki (1994) found no change in denitrification rates from days 3-5 to days 7-11 in shallow bay sediments, Gardner *et al.* (1987) observed a decline in N₂ flux rates well into the 4th week of incubation in lake sediments. Changes in metabolic rates of sediments over time could result from the depletion of labile algal organic carbon pools, which are important contributors to sediments which lie within the euphotic zone or below unstratified waters. In such sediments, labile organic carbon pools within sediments held *in vitro* may become depleted, leaving more recalcitrant carbon pools with lower metabolic rates. In the present study, the decline in metabolic rates associated with the higher activity sediments is consistent with this process (Figure 2.3). Higher initial metabolic rates were also associated with spring and summer incubations (Chapter 3) when labile carbon may play a more important role in sediment metabolism. Thus, particularly in sediments where algal carbon plays a significant role in sediment metabolism, minimizing core holding and incubation times may be important in obtaining accurate denitrification measurements.

Clearly, procedures which reduce the incubation time of metabolic measurements will help to avoid artifacts and improve accuracy. The N₂ efflux simulation model provides an approach for optimizing protocols specific to a sediment system aimed at reducing incubation time. The primary factors controlling off-gassing, hence the time

required before denitrification rates can be obtained, are sediment thickness and porosity. The time required for porewater N_2 off-gassing is primarily dependent on the size of the sediment N_2 pool. Thin sediment cores off-gas quickly both because of their low N_2 mass and because the diffusion path is shorter. Porosity (ϕ) also affects the time required for sediment off-gassing since high porosity sediments contain more water and more N_2 and therefore take longer to off-gas (Figures 2.4a and 2.4b). For purposes of denitrification measurement, it is sufficient that the sediment should off-gas to the point where the diffusive flux is an acceptable percentage of the denitrification flux. For illustrative purposes, an error in the denitrification rate of $\pm 5\%$ was chosen. In general, longer off-gassing incubations are required for accurate measurement of small denitrification fluxes because the diffusive flux must be allowed to attenuate to a lower level (Figures 2.4c and 2.4d). A check on the applicability of the model can be made by comparing modeled off-gassing times with those reported in the literature (see references in Table 2.1). A typical 5 – 7 cm thick sediment requires a 10 day off-gassing incubation, similar to the modeled off-gassing times in Figure 2.4.

The paired aerobic/anaerobic flux chamber approach (Nowicki, 1994) was designed to shorten incubation times by using an anaerobic chamber as a control for diffusion-driven N_2 fluxes. Figure 2.2b illustrates the application of the paired cores to determining denitrification rates. The “aerobic” and “anaerobic” curves are the first derivatives (slopes) of the model curves in Figure 2.2a. N_2 fluxes calculated by difference (aerobic flux – anaerobic flux) approach the actual denitrification rate ($2.0 \text{ mmol N m}^{-1} \text{ d}^{-1}$) faster than the N_2 flux out of the aerobic core alone. In this instance,

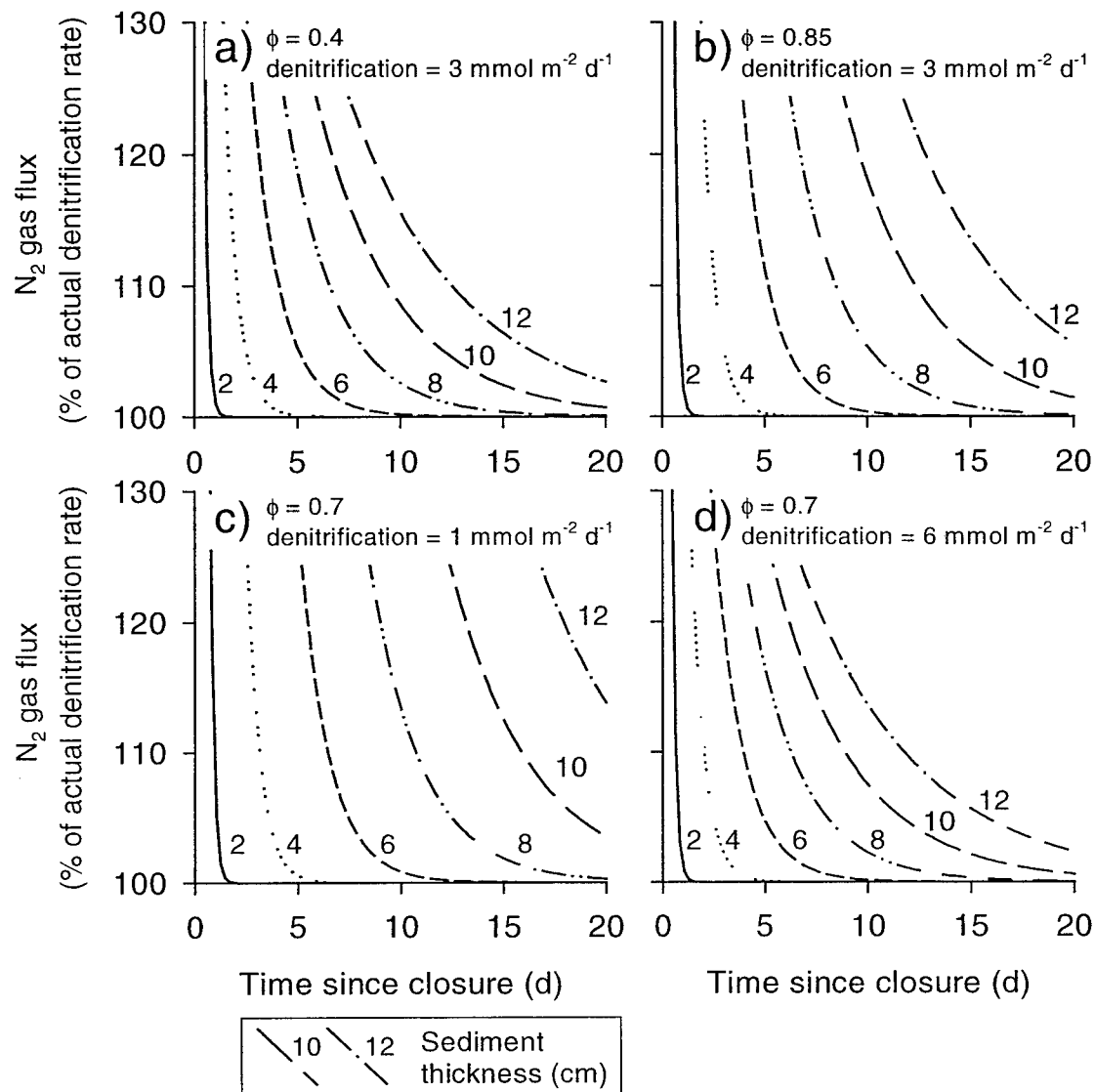


Figure 2.4 Modeled porewater N_2 off-gassing from sediments in aerobic flux chambers. **a) & b)** N_2 flux from sediments of different thicknesses as % of actual denitrification rate for two different sediment porosities representing typical sandy ($\phi = 0.4$) and muddy ($\phi = 0.85$) sediments. Higher porosity sediments take longer to de-gas because of higher water, and therefore porewater N_2 content. **c) & d)** N_2 flux from sediments of different thicknesses as % of actual denitrification rate for two different denitrification rates. Flux decreases over time as a result of depletion of sediment N_2 pools. Thicker sediments take longer to de-gas. N_2 fluxes in sediment with higher denitrification rate come to within 5% of actual rate faster since diffusive N_2 fluxes are a smaller proportion of denitrification rate. Headspace gas continually flushed with 0.01 atm N_2 .

paired aerobic/anaerobic cores allowed the calculation of the denitrification rate ~ 5 days earlier than a single aerobic flux chamber would have allowed.

However, this technique is not free from diffusion-induced errors. Porewater N_2 concentrations in denitrifying sediments in the field are out of equilibrium with the atmosphere due to the excess N_2 production of denitrification. At steady state, and with no consumption of N_2 within the sediments, porewater in the entire sediment column will be enriched in N_2 above atmospheric equilibrium levels. With paired flux chambers, although coupled nitrification-denitrification is stopped in the anaerobic core, this excess N_2 is still present, so that when the aerobic and the anaerobic cores are overlain with a low- N_2 headspace, the N_2 flux out of the sediments is initially the same for both cores. As both sediments off-gas, the N_2 flux rates diverge, until the difference between them approximates the denitrification N_2 flux (Figures 2.2 and 2.5). Denitrification N_2 fluxes calculated by difference (aerobic – anaerobic) approach the actual denitrification rate more rapidly the thinner the sediment core that can be used.

Inhibition of N_2 Efflux by Headspace Accumulation

Another approach to reducing incubation time has been to use very small headspaces overlying the sediments in order to more rapidly accumulate N_2 , reducing the interval required to obtain measurable changes. However, if too small a headspace is employed, the N_2 concentration gradient driving N_2 emission is reduced and an artificially low denitrification rate is measured. This underestimation is a function of the

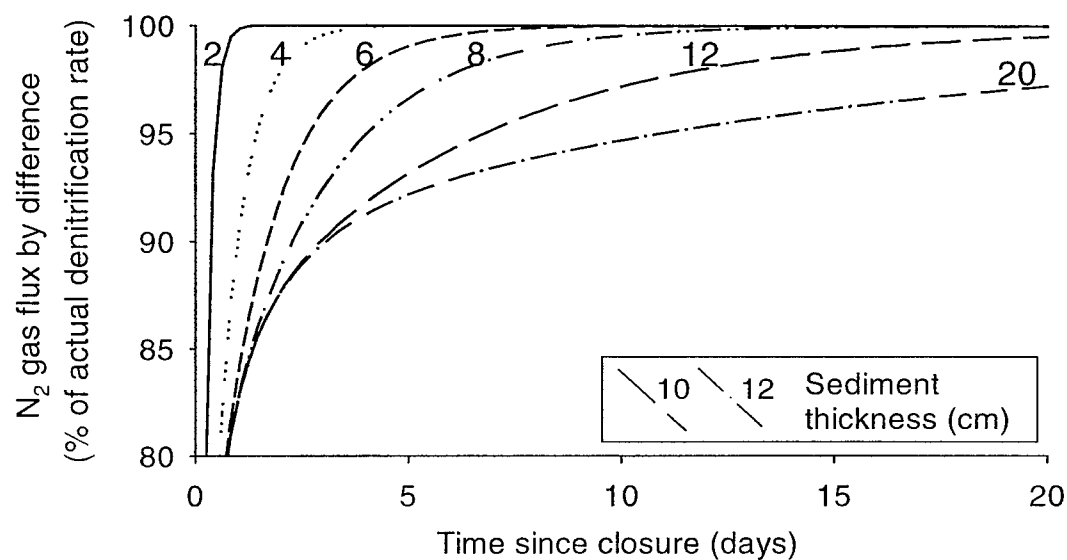


Figure 2.5 Modeled time required for the differential N_2 efflux (aerobic – anaerobic chambers) to equal the actual denitrification rate in sediments of different thicknesses (2 – 20 cm). Fluxes from thicker sediments are more depressed because of greater storage of denitrified N_2 in sediment porewaters. Porosity has no effect because the paired core acts as a control for all sediment parameters, likewise figure is normalized for all denitrification rates.

ratio of the headspace volume to the gas storage capacity of the sediments (porosity \times sediment volume) (Figure 2.6).

In typical protocols, after sediment off-gassing, the flux chamber is flushed and sealed and denitrification can be determined from the accumulation of N_2 in the headspace. As N_2 accumulates, and the concentration gradient across the sediment surface decreases, the excess denitrification N_2 which does not escape to the headspace is stored in the sediment. Underestimation of denitrification is greatest with small headspaces, since N_2 accumulates faster, causing the concentration gradient across the sediment surface to collapse faster (Figure 2.6). This process is only of concern at very small headspaces thickness (1 or 2 cm - Table 2.1), while increasing headspace thickness over 10 cm has no discernable benefit. Because the N_2 storage capacity of thin sediments is low, the underestimation is lowest for thin sediments. In thicker sediments, denitrification N_2 continues to diffuse into deeper layers of the sediment as headspace N_2 concentrations increase, further reducing the concentration gradient across the sediment surface and reducing the N_2 flux rate. Higher water content (porosity) of sediments has the same effect as greater sediment thickness due to greater storage capacity (examples in Figures 2.6a and 2.6b are for $\phi = 0.85$, illustrating a near maximum underestimation of denitrification).

Underestimation of denitrification due to artificial lowering of N_2 efflux by headspace N_2 accumulation can also occur with the paired aerobic/anaerobic flux chamber protocol (Figure 2.6b), even though it might be thought that the anaerobic core flux would control for this effect. However, because N_2 production by denitrification in

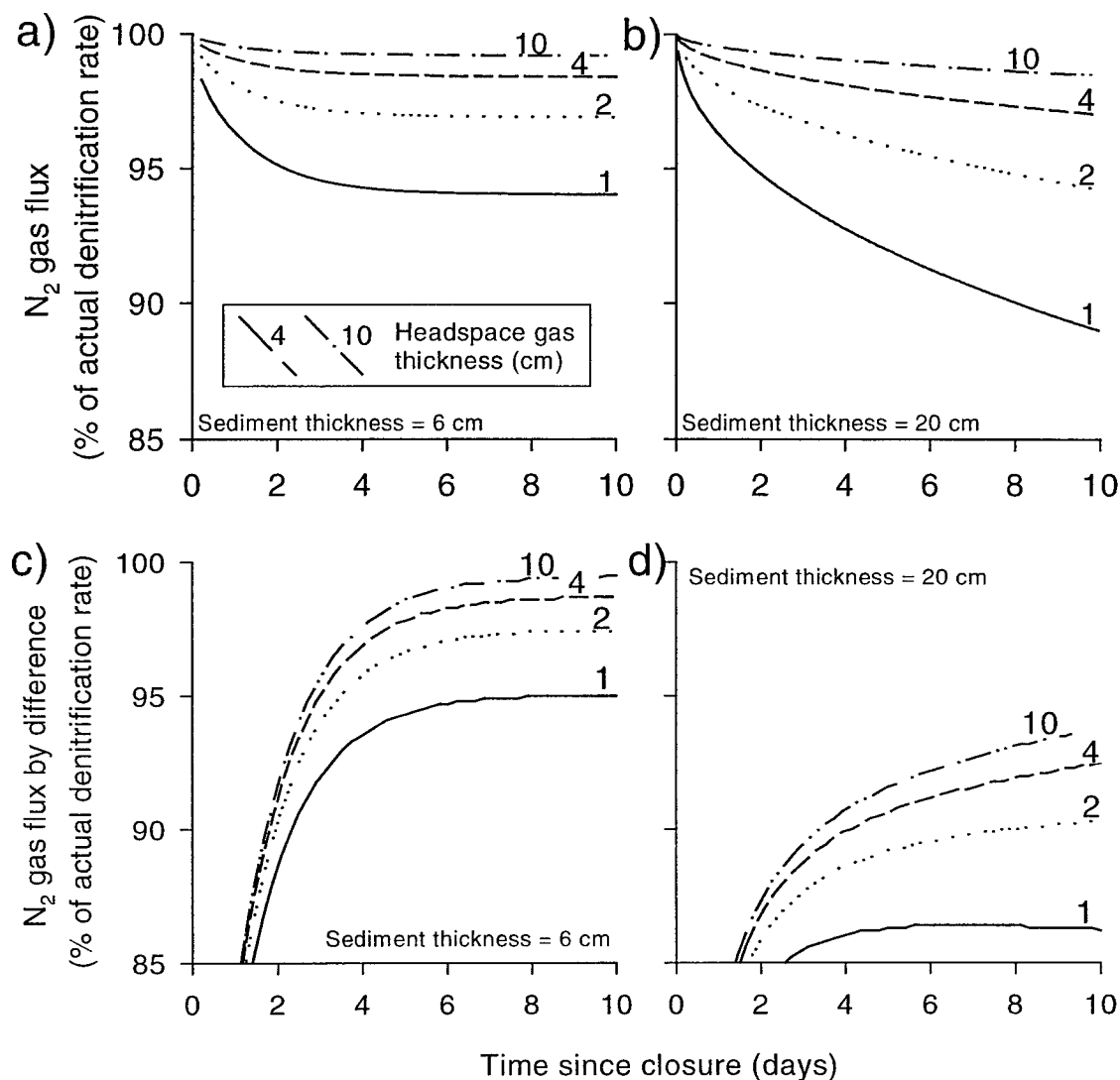


Figure 2.6 Underestimation of denitrification rates in N_2 flux measurements from previously off-gassed sediments. Underestimation results from collapse of N_2 concentration gradient as N_2 builds up in headspace – effect is largest for small headspaces. The effect increases with increasing sediment thickness and porosity ($\phi = 0.85$ shown) because of greater N_2 storage capacity. Denitrification rate does not affect accuracy of measurements since the inhibition of N_2 flux is proportional to the N_2 production rate. **a) & b)** Underestimation of denitrification in an aerobic chamber with 6 cm (a) and 20 cm (b) sediment thicknesses. **c) & d)** Underestimation of denitrification in parallel incubations of aerobic and anaerobic chambers with 6 cm (c) and 20 cm (d) sediment thicknesses. Underestimations are independent of porosity and denitrification rate.

the aerobic core causes aerobic headspace N_2 concentrations to rise faster than anaerobic headspace N_2 concentrations, inhibition of the aerobic flux relative to the anaerobic flux can occur. As with aerobic chamber fluxes the effect is controlled by the headspace gas thickness. Thick sediments and thin headspaces lead to the largest underestimations of denitrification rates (up to 13%) (Figure 2.6d).

Advances in gas chromatographic techniques have permitted some workers to measure N_2 gas fluxes against an ambient N_2 background (Devol, 1991; Devol and Christensen, 1993; Lamontagne and Valiela, 1995; Nowicki, 1999; see Table 2.1). In order to be able to make these measurements, a water-only headspace is used, so that small denitrification fluxes measurably affect headspace N_2 concentrations. Measuring N_2 fluxes against an ambient N_2 background has the advantage of avoiding the necessity for sediment off-gassing, and can be employed in the field for *in situ* measurements. However, a number of problems have been noted by workers, including large measurement errors (Lamontagne and Valiela, 1995) and headspace O_2 depletion before significant N_2 accumulation occurs (Devol, 1991; Lamontagne and Valiela, 1995; Nowicki, 1999). In addition, the use of a water-only headspace results in underestimations of denitrification much more severe than that noted for gas headspaces (as discussed by Devol and Christensen [1993]) because of the very small capacity for N_2 storage in the headspace compared with a gas headspace.

The simulation model can be used to examine the measurement of denitrification against ambient N_2 concentrations in water-only headspaces (Figure 2.7). As with the gas + water phase incubations, denitrification underestimation is minimized with thick

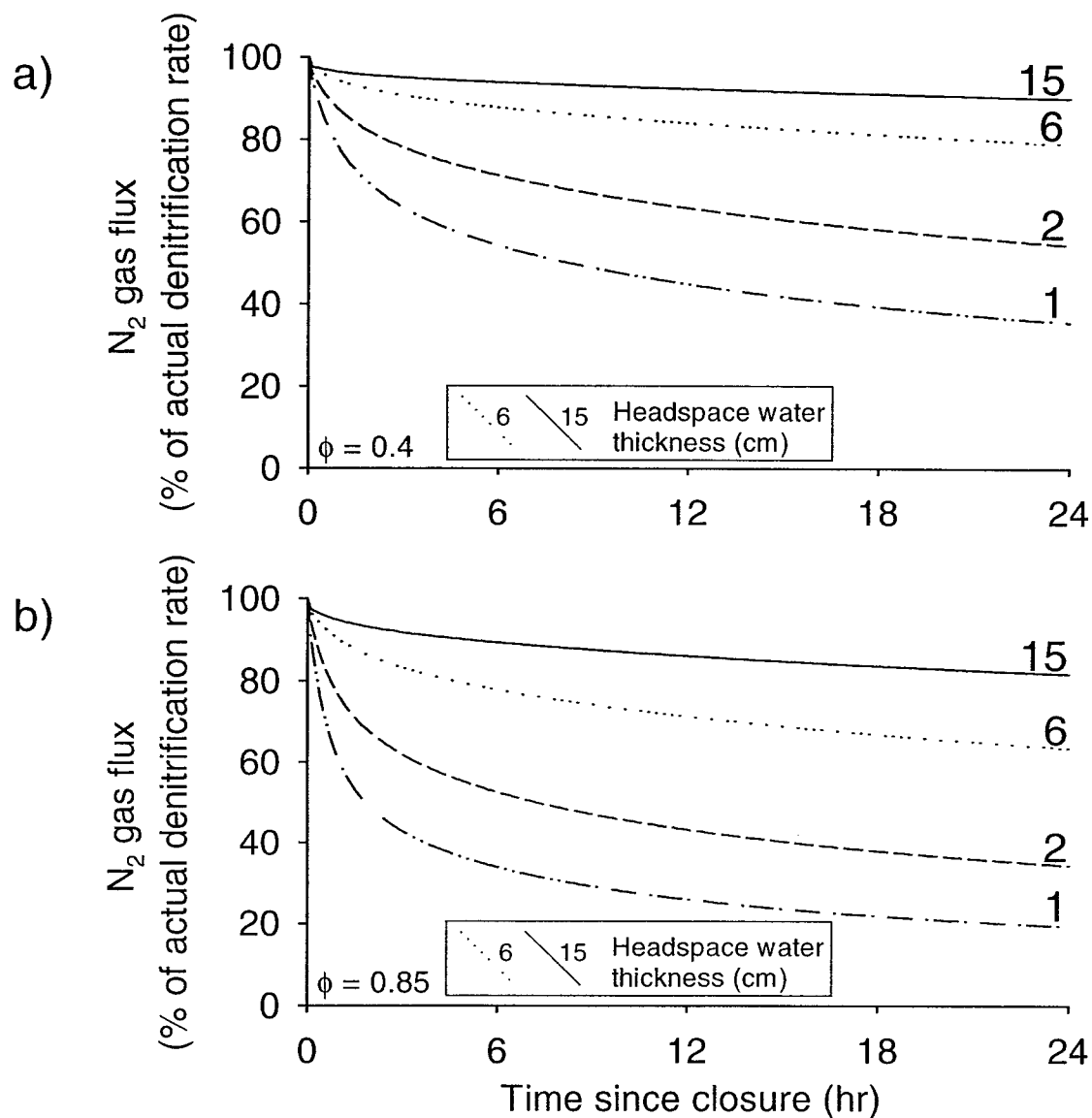


Figure 2.7 Underestimation of denitrification in chambers with water-filled headspaces of different thicknesses from a sandy ($\phi = 0.4$) and a muddy ($\phi = 0.85$) sediment. Sediment thickness has no effect since efflux is against ambient N₂ background, the reduction in N₂ efflux results from the accumulation of N₂ and the collapse of the diffusion gradient. Curves are valid for any denitrification rate. Greater depression of rates at higher sediment porosities results from lower denitrification N₂ concentration (due to higher sediment water content) and therefore a lower concentration gradient across the sediment-water interface.

headspaces, as is the possibility of O₂ depletion during the course of the incubation. However, a larger headspace means that denitrification N₂ fluxes are more diluted and difficult to measure. Porosity also affects the degree of N₂ flux inhibition, as noted for incubations with gas + water headspaces in Figure 2.6, with high porosity sediments suffering the largest underestimations (up to 80%).

Devol and Christensen (1993) were among the first to recognize this potential problem and corrected for it by only using the first 3 timepoints – taken over ~4 hours – in their N₂ flux measurements. It appears that they greatly reduced their underestimation (compared to 24 hr) with this approach, but in muddy sediments with a 4 - 8 cm headspace (Table 2.1), a 10 - 25% underestimate may still have occurred (Figure 2.7). The use of a 15 cm headspace results in a 8 – 18% underestimation of denitrification after 24 hours (Lamontagne and Valiela, 1995). Nowicki (1994) noted that measurements made with *in situ* water-filled benthic flux chambers at ambient N₂ levels were less than half of parallel measurements made with the paired aerobic/anaerobic flux chambers. This is consistent with my prediction from the simulation model for a 1 cm water-filled chamber of an underestimate of 32 – 40% (averaged over 24 hr) (Figure 2.7).

Disturbances of N₂ Flux by Headspace Flushing

Most coastal and shelf sediments have positive NH₄⁺ fluxes (Middelburg *et al.*, 1996), which result in headspace NH₄⁺ accumulation during chamber incubations, and potentially stimulate nitrification and denitrification rates (Seitzinger *et al.*, 1993). Therefore, most investigators flush the headspace water and gas every 1 – 2 days to restore the water phase to *in situ* conditions (Chamber closure time, Table 2.1).

Typically, this process must be repeated 4 or more times for an accurate estimate of flux rates. Although frequent flushing of water and gas headspaces restores surface conditions to near *in situ* levels, up to twice as many gas concentration measurements must be made than if chambers are kept closed because an extra initial measurement must be made in between each flush. However, in the sediments used in the present study, neither daily headspace flushes nor zeolite reduced NH_4^+ concentrations to *in situ* levels and neither treatment affected sediment metabolism (Table 2.3).

Further, flushing introduces perturbations in the N_2 flux rate (Figure 2.8) and the possibility of contamination of headspace gas by dissolved N_2 introduced in the new headspace water (Nowicki, 1994; van Luijn, 1996). In an example modeled after the protocols of Seitzinger (1980) and others (Table 2.1), an aerobic core is flushed every two days (Figure 2.8a). After two days of closed incubation, N_2 gas fluxes remain close to true denitrification fluxes. During this time, N_2 accumulates in the headspace and in the sediments. When the headspace is flushed, a new low- N_2 gas phase is established. The concentration gradient is now increased, and a sharp spike of off-gassing occurs, followed by a gradual return to pre-flush conditions. As expected, the fluctuation is greatest in flux chambers with small headspaces, because the accumulation of N_2 in the headspace, and the associated sediment storage, is also greater. Headspace flushing has the same effect on paired aerobic/anaerobic chamber flux measurements (Figure 2.8b and 2.8c). The spike of sediment off-gassing probably accounts for some of the flux increase noted by Nowicki (1994) and attributed to atmospheric N_2 introduced during headspace flushing.

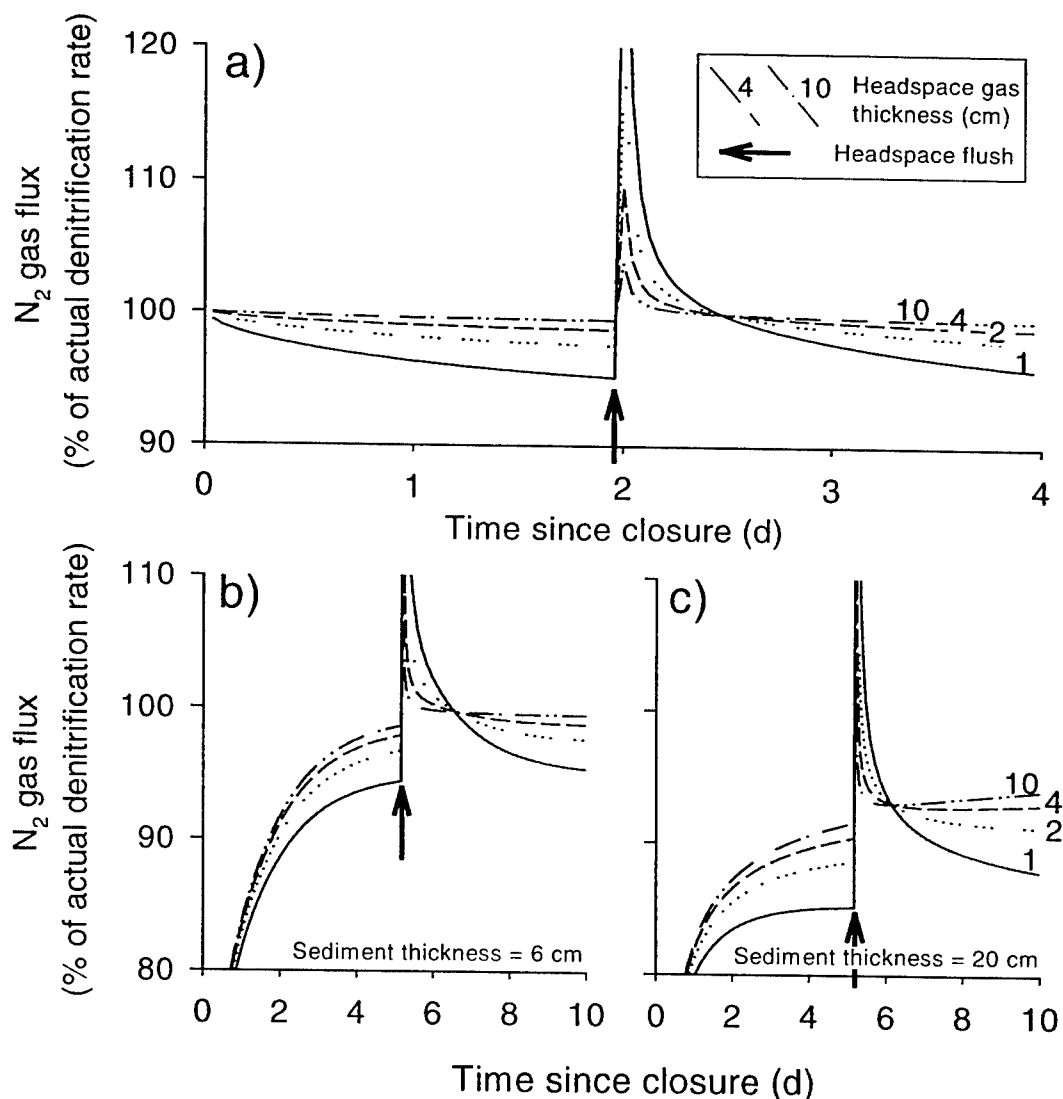


Figure 2.8 Modeled gas fluxes during incubation with headspace flush (low N_2 gas - arrows). N_2 flux spikes result from build-up of N_2 in sediment porewaters as a result of inhibition of N_2 flux (due to headspace N_2 accumulation) prior to flushing **a)** Aerobic flux chamber. After off-gassing incubation, core is closed from day 0 – 2, headspace is flushed, and chamber is closed again from day 2 – 4 (as in Seitzinger, 1987 and others). Fluctuations are larger for small headspaces. Sediment storage during closed period is released after headspace flushing because concentration gradient increases when headspace gas is replaced by low- N_2 headspace gas. Sediment thickness = 6cm. Compare to Figure 2.6a. **b) & c)** Denitrification calculated with paired aerobic/anaerobic flux chambers. Chambers are closed from day 0 – 5, headspace is flushed, and chambers are closed again from day 5 – 10 (as in Nowicki, 1994). Two sediment thicknesses are shown. Compare to Figures 2.4b & 2.4c.

During periods of chamber closure, O₂ concentrations decline, and with long closures or small headspaces, metabolic rates may be affected if hypoxic conditions develop in the chamber. Hypoxia is frequently cited as a problem in incubations with water-filled headspaces (Devol and Christensen, 1993; Lamontagne and Valiela, 1995; Nowicki *et al.*, 1999), but can be avoided with large headspaces and/or shorter incubation times. Pressure changes resulting from O₂ consumption also can significantly affect the measurement of denitrification fluxes (Equation 2.2). During incubations, O₂ consumption is accompanied by CO₂ production, but 80% or more of the total CO₂ pool may remain in dissolved forms, and headspace pressure falls due to molar gas reduction. During incubations of salt marsh sediment cores (this study), molar gas reduction ranged to 0.03 atm d⁻¹, which without correction, results in an overestimation of the denitrification flux of up to 15% over the course of a 5 day incubation. Since leaks and sample withdrawals can also change the chamber headspace pressure, accurate measurements of gas flux necessitate regular measurements of the headspace pressure.

Headspace flushing may not reduce headspace NH₄⁺ concentrations sufficiently to affect coupled nitrification-denitrification, but instead may introduce artifacts as a result of the disturbance of sediment N₂ profiles. On the other hand, long periods of chamber closure raise the possibility of inhibition of N₂ flux by headspace accumulation, depletion of headspace O₂, and pressure changes as a result of molar gas reduction. However, these problems can be overcome by good experimental design, including sufficiently large headspaces and pressure measurements, and the problems introduced by flushing the headspace provide little significant benefit to N₂ flux protocols.

Sediment Thickness and Depth Distribution of Denitrification

Whether aerobic flux chambers or paired aerobic/anaerobic chambers are used to determine denitrification N_2 fluxes, the incubated sediment thickness is the key experimental parameter that has the greatest effect on off-gassing incubation times and along with headspace thickness, the inhibition in N_2 efflux due to N_2 accumulation in the headspace. Sediment thicknesses should therefore be minimized, but the chosen sediment thicknesses must reflect the depth distribution of denitrification. Sediment thicknesses of 2-20 cm have been used by various researchers (Table 2.2), but the depth distribution of denitrification depends on the penetration of O_2 (redox structure of sediment column) and the availability of organic C. In most sediments, from the deep sea to the continental shelves, total organic carbon content decreases through the top 10-15 cm of the sediments before becoming constant (Soetaert *et al.*, 1996). Since little further carbon respiration is taking place, denitrification is typically not significant below this depth. In estuarine and salt marsh sediments, most C respiration takes place in the upper 2 cm (Jørgensen, 1982; Howes *et al.*, 1985). Thus it is again unlikely that significant denitrification takes place below 10-15 cm. In many cases, most of the denitrification appears to be taking place in the top 2-4 cm, where O_2 penetration supports nitrification and beyond which little NO_3^- is found (Henriksen and Kemp, 1988).

In the present study, denitrification and O_2 consumption rates in 2 cm cores were not significantly different from those of thicker cores. Similarly, a model study was done in which total denitrification was distributed across the top 1 – 8 cm of sediment, increasing by 1 cm at a time. The best fit was obtained with denitrification distributed

within the top 2 cm of sediment (Figure 2.2). Although the minimum thickness of sediment required for an accurate denitrification measurement likely varies among sediment systems, in general, the thicknesses typically used (2-7 cm; Table 2.1) may depth-integrate sediment processes while shortening off-gassing incubation times.

Macrofaunal Irrigation of the Sediments

Calculation of denitrification with parallel incubations of aerobic and anaerobic chambers assumes that the only difference between N_2 flux out of anaerobic and aerobic cores results from N_2 inputs from denitrification. However, in sediments with high macrofaunal densities, irrigation of the sediments by macrofaunal activity tends to increase the flux of porewater N_2 in aerobic cores above the diffusional flux observed in anaerobic cores, where macrofauna are killed or inactivated by anoxia. Since the resulting anaerobic off-gassing correction would then be too small, denitrification rates so determined would be too large. The result is that incubation times would need to be increased to allow diffusive fluxes in aerobic and anaerobic chambers to come into equilibrium. The effects of macrofaunal irrigation can be modeled by increasing the apparent diffusion coefficient for the aerobic core. A simplified example is shown in Figure 2.9a, where D_a for the aerobic core has been increased by a factor of 1.5. Figure 2.9a should be compared to Figure 2.5, where D_a is the same for both the aerobic and the anaerobic core. In Figure 2.9a, the initial calculated N_2 flux (by difference) exceeds the denitrification rate as predicted. In contrast, in Figure 2.5, the calculated flux begins lower than the denitrification flux. In thin sediments, the larger D_a means that the initial porewater N_2 is quickly exhausted, causing N_2 flux rates to rapidly drop below those of

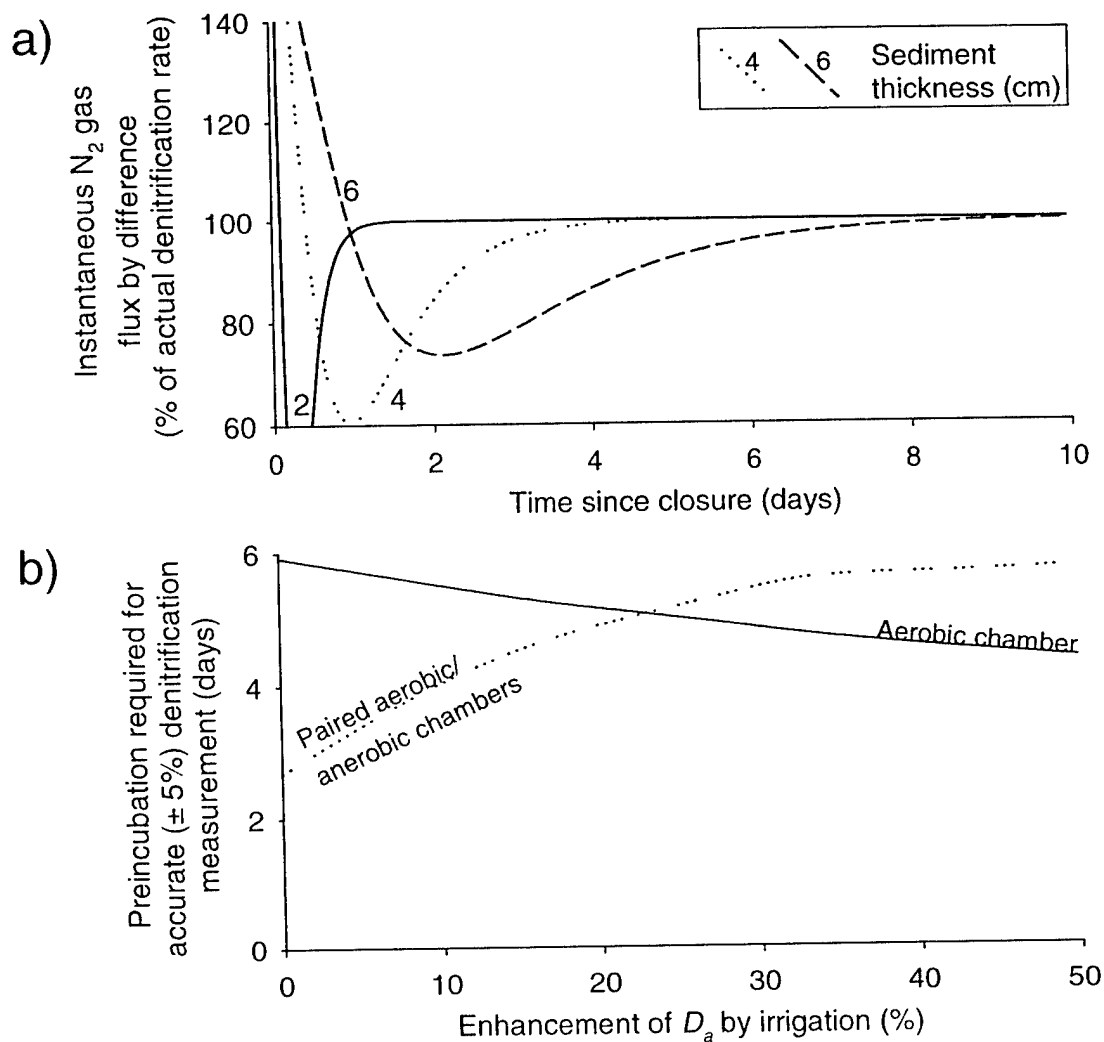


Figure 2.9 Modeled macrofaunal irrigation effects on denitrification fluxes calculated with paired aerobic/anaerobic flux chambers. **a)** N_2 flux as a % of denitrification rate after chamber closure for a variety of sediment thicknesses. Irrigation enhancement of porewater N_2 flux in aerobic chamber is 1.5 times the anaerobic D_a . Compare to Figure 2.5a but note difference in scale. **b)** Effect of irrigation-enhanced D_a on the preincubation time required for accurate ($\pm 5\%$) denitrification measurements. Off-gassing incubation times with paired flux chambers can quickly exceed those required for aerobic flux chambers. This figure serves as an example only, since the shape of such a figure is highly depended on factors like porosity, denitrification rate, and diffusion coefficient.

the anaerobic core, where diffusion of porewater N_2 pools is still taking place. This effect is transient, and eventually N_2 pools in the anaerobic core are exhausted as well, and the calculated flux returns toward the actual denitrification value. In thicker sediments with deep macrofaunal irrigation, porewater N_2 pools are not quickly exhausted, even with the higher D_a . The calculated flux remains elevated above the actual level for many days, and may extend the off-gassing incubation time beyond that required for aerobic flux chambers (Figure 2.9b). The effect of macrofaunal enhancement of D_a varies with the degree of enhancement (Figure 2.9b). Since the enhancement of D_a is not likely to be known, denitrification fluxes calculated with paired aerobic/anaerobic flux chambers on sediments with deep irrigation (such as by the presence of large numbers of polychaetes) may not have any advantage in incubation time over single aerobic chambers.

Optimization of N_2 Flux Protocols

N_2 gas flux measurement of denitrification offer a simple yet accurate way to directly measure denitrification fluxes of N_2 from flooded sediments. Artifacts and errors can be avoided with proper preparation. Although some of the potential errors are small, the sum of multiple sources of error could become significant. Sediments for N_2 flux measurements should be collected to depths which include all macrofaunal and respiratory activity. Initially, the extent of macrofaunal irrigation should be investigated. Cores of representative sediments should be collected in clear-sided core tubes and the presence of macrofaunal burrows and the depth of the redox discontinuity (visually the beginning of dark reduced sediment) should be noted. If possible, macrofaunal densities

and identification of species can help evaluate the depth and extent of irrigation. The need to capture all sediment metabolic activity must be balanced against lengthening incubation times and potential depletion of labile organic matter. The minimum sediment thickness required to capture all of the denitrification or O_2 consumption may be determined experimentally with incubations of sediments of different thicknesses. Sediments should be collected in the same chambers they are to be incubated in if the original porewater and labile C profiles are to be retained.

If macrofaunal activity is determined to be significant at deep levels, aerobic flux chambers should be used. Measurements can be made until rates are linear, but by then labile organic pools may have been depleted. Paired aerobic/anaerobic chambers are preferable if macrofaunal activity is restricted or absent. The chamber design should have space for adequate headspace thicknesses. A thick water layer prevents NH_4^+ or other metabolites from accumulating to high concentrations, and does not interfere with the gas measurements if adequately stirred. Headspace gas thicknesses should be ~ 10 cm to prevent accumulation of N_2 and inhibition of flux rates, and to provide an adequate supply of oxygen.

Incubations against ambient N_2 concentrations require no off-gassing incubation but require the greatest measurement sensitivity, whereas incubations against an N_2 -free headspace require the longest off-gassing incubation and the least measurement sensitivity. It is possible to incubate sediments with lowered headspace N_2 concentrations, decreasing the off-gassing incubation time, but still retaining adequate sensitivity.

I found that the entire incubation could be done without flushing the headspace. In my protocol, freshly collected cores are sealed in the chambers with the low-N₂ headspace, and no measurements made until day 4. By this time, the N₂ efflux rates from both the aerobic and anaerobic sediments could be fit well by a linear regression (Figure 2.2a). However, investigators may want to determine the sensitivity of their systems to NH₄⁺ accumulation and design appropriate flushing procedures. While most errors can be reduced by following the above guidelines, finer optimization of particular sediment systems can be accomplished by modeling (Methods, Appendix 1). Modeling might be especially important with thick sediments, or sediments with very low rates of N₂ flux, where it may be desirable to reduce the headspace thickness from 10 cm to increase measurement sensitivity.

The use of paired aerobic/anaerobic flux chambers can significantly shorten off-gassing incubation times, and therefore reduce the risk of depletion of labile organic material, and associated changes in metabolic rates. However, the inhibition of macrofaunal irrigation in anaerobic control cores can contribute an unknown amount of error to denitrification measurements. The off-gassing incubation time required for determination of accurate N₂ fluxes with either aerobic flux chambers or paired aerobic/anaerobic chambers is highly dependent on the sediment thickness used, since thicker sediments require longer to off-gas. Most of the metabolic activity of sediments may be taking place in the upper 2 - 4 cm, so minimizing sediment thickness can shorten off-gassing incubation time. Inhibition of N₂ fluxes by headspace N₂ accumulation occurs at small headspace gas thicknesses with either method., but significant

underestimations of denitrification ($> 3\%$) only occur at headspace thicknesses of <2 cm, and with long chamber closure times. N_2 flux protocols using water only headspaces at ambient N_2 concentrations are particularly susceptible to underestimation of denitrification, which may reach 80% in 24 hr with headspaces under 2 cm, but can be avoided by the use of a 15 cm headspace. Although the results of this study are generalizable to many sediment types, model studies of particular sediment systems are required in order to determine the appropriate off-gassing incubations and understand potential errors.

CHAPTER 3

Contribution of denitrification to N, C, and O cycling in sediments of a New England Salt Marsh

Abstract

The metabolism of sediments from a small Cape Cod, USA salt marsh receiving high nitrate (NO_3^-) loads in groundwater ($32 \text{ mmol N m}^{-2} \text{ d}^{-1}$) was studied in laboratory microcosms. Simultaneous measurements of the fluxes of O_2 , CO_2 , N_2 , and dissolved inorganic N from both sandy and muddy sediments were made over annual cycles. Sediment organic C content and quality were the primary controls on metabolic rates, followed by seasonal effects, including temperature. Although the C content of muddy sediments was twice that of sandy sediments, the sandy sediment C was twice as labile, and mean metabolic rates did not differ from muddy sediments (mean O_2 consumption = $60 \text{ mmol m}^{-2} \text{ d}^{-1}$, CO_2 production = $52 \text{ mmol m}^{-2} \text{ d}^{-1}$, and autochthonous denitrification = $5.2 \text{ mmol m}^{-2} \text{ d}^{-1}$). The average CO_2/N flux ratio (6.1), and sediment $\delta^{13}\text{C}$ (-19.4) at both sites, similar to algal biomass, support a sediment metabolism based primarily on algal biomass. 46% of the NH_4^+ remineralized within the sediments was lost to N_2 by coupled nitrification-denitrification. Autochthonous denitrification accounted for 61% of the total annual denitrification ($2.7 \text{ mol m}^{-2} \text{ y}^{-1}$); the balance was denitrification of watercolumn NO_3^- . However, the only significant source of N to benthic alga in the saltmarsh creekbottom was groundwater NO_3^- . Total denitrification, therefore gives the true size of the allochthonous, groundwater NO_3^- - driven denitrification flux.

Introduction

Salt marsh primary productivity is limited by the availability of nitrogen (N) (Sullivan and Daiber, 1974; Valiela and Teal, 1974). N sources to the salt marsh include tidal water, rain, N fixation, and riverine and groundwater terrestrial inputs (Valiela and Teal, 1979; Capone and Bautista, 1985). However, in populated areas, terrestrial N inputs, primarily nitrate (NO_3^-), dominate salt marsh N budgets as a result of sewage disposal and agricultural runoff (Sewell, 1982; Valiela *et al.*, 1990; Smith, 1999). Salt marshes have the capacity to intercept terrestrial N, thereby limiting its availability to support primary productivity and eutrophication in coastal aquatic environments (Fujita *et al.*, 1989; Harvey and Odum, 1990; Howes *et al.*, 1996).

A New England, USA salt marsh environment typically consists of intermittently-flooded vegetated peats of halophilic macrophytes such as *Spartina spp.* and the usually-flooded unvegetated sediments of the creeks which drain the marsh and comprise about one third of its total area (Valiela and Teal, 1979; Howes *et al.*, 1996). Creekbottom sediments are the primary site of contact with terrestrial nutrient inputs through riverine and groundwater flows (Weiskel *et al.*, 1996; Howes *et al.* 1996). Allochthonous NO_3^- entering a salt marsh is subject to loss or retention by competing processes. It may be retained by algal uptake or it can be lost through direct denitrification or export. If it retained in biomass, then it is subject to losses through burial or export or remineralization of NH_4^+ . Remineralized NH_4^+ can be retained by algal uptake or lost through nitrification-denitrification to N_2 .

The high productivity of salt marsh creekbottoms, further supported by high N inputs, results in the accumulation of organic material, most of which forms the basis for detrital food chains (Teal, 1962; Vince *et al.*, 1981). Anaerobic metabolism (especially sulfate reduction) plays a dominant role in subtidal sediments (Jørgensen, 1982), although denitrification is also significant.

I studied the contribution of denitrification to fluxes of N, C, and O in the sediments of Mashapaquit Marsh, located in West Falmouth, Cape Cod, Massachusetts, USA, a small (5.7 ha) salt marsh which was the subject of an earlier study using mass balance and hydrological methods to determine the fate of groundwater NO_3^- inputs (Figure 3.1; Smith, 1999). Two thirds of the marsh's area consists of vegetated peats of *S. patens* and *S. alterniflora*. The remaining third is occupied by the usually-flooded sediments of the salt marsh creek. Mashapaquit Marsh receives freshwater flows (via Mashapaquit Creek and groundwater seepage faces) from a 284 ha watershed of highly permeable glacial outwash deposits (Smith, 1999). Watershed flows ($2.21 \times 10^6 \text{ m}^3 \text{ y}^{-1}$) are predominantly as groundwater, with $0.21 \times 10^6 \text{ m}^3 \text{ y}^{-1}$ resulting from land disposal of treated wastewater from a regional wastewater treatment facility. Total N fluxes into the salt marsh are $32 \text{ mmol N m}^{-2} \text{ d}^{-1}$, of which 87% derives from wastewater disposal (64% from the wastewater treatment facility and 23% from septic wastewater disposal). Smith (1999) showed that 40 - 50% of the influent N was removed before being exported via tidal flows, and that creekbottom denitrification of watercolumn NO_3^- accounted for 70% of this N loss.

The purpose of the present study was to determine the contribution of denitrification to the overall fate of N, C, and O₂, within the salt marsh sediments. Simultaneous measurements were made of the fluxes of O₂, CO₂, N₂, and dissolved inorganic N species across the sediment-water interface of salt marsh creek sediments over spatial gradients and seasonal cycles. The source of the organic N supporting autochthonous denitrification was determined through the analysis of biogeochemical flux ratios and the isotopic signatures and characteristics of sediments.

Methods

Study Site

Mashapaquit Marsh is a 5.7 ha marsh with tidal exchanges with West Falmouth Harbor, a shallow embayment of Buzzards Bay, on the west side of Cape Cod, Massachusetts, USA (Figure 3.1). This creek is flushed by semi-diurnal tides with a mean range of 1.2 m, with nearly complete drainage during spring tides. Work was focused on a sandy and a muddy site (sites S & M) at the upper end of the marsh, areas receiving groundwater N fluxes (Smith, 1999). Two more sites (sites 3 & 4) were sampled on two summer dates for comparison.

Sediment Mapping

The characteristics of creekbottom sediments were determined on samples (top 2 cm) collected every 5 m along 8 transects across the marsh creek. Known volumes of sediment were weighed wet, then dried to constant weight at 60 °C to determine porosity

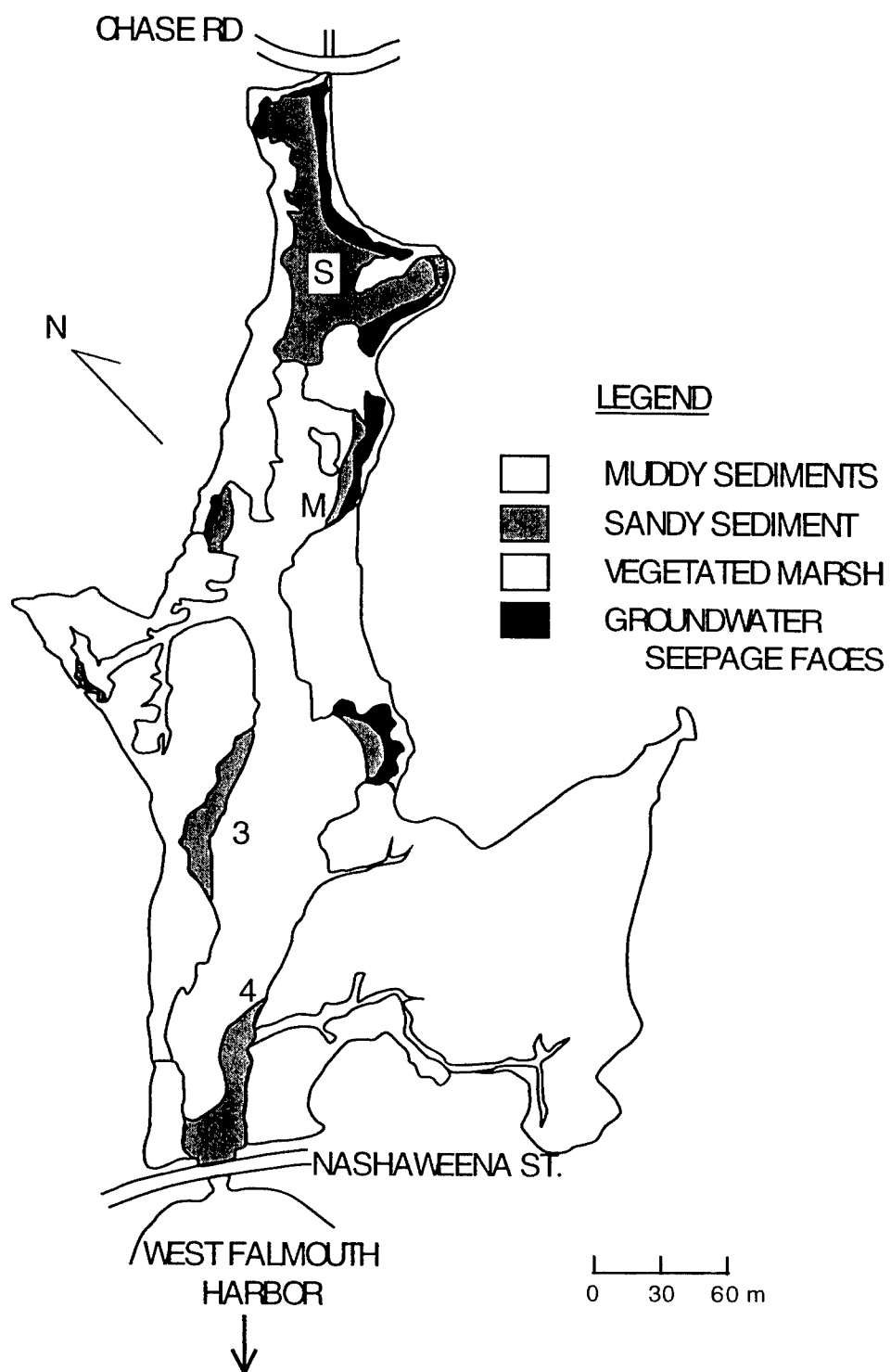


Figure 3.1 Location of the study site within the sandy outwash aquifer of Cape Cod, Massachusetts, USA. S, M, 3, and 4 indicate the sampling sites. Sediment composition as determined by sampling and visual observation are indicated.

and density. Dried samples were ground, and analyzed for particulate organic C and N on a Perkin-Elmer 2400 elemental analyzer. Sediment carbonate content analysis (see below) showed that carbonate accounted for < 0.01% of total sediment C.

Sediment Core Collection

Sediment cores were collected to 8-12 cm deep at low tide in glass core tubes (8.8 cm dia.) in shallow water (30 cm) at low tide. The sediments were handled carefully to avoid disturbance of sediment structure or porewater substrate profiles. Samples were immediately transported at *in situ* temperatures and with headspace water aeration to the laboratory (1 hr).

At time of core collection, surface water and sediment temperature were measured. Surface water and sediment porewater (at 2 and 10 cm depth) was collected and filtered (0.45 μm Millipore) in the field. 15 cc of surface sediment (2 cm depth) were collected in a dark container for sediment pigment (chl α and pheophytin) determination. All samples were placed on ice for immediate transport to the laboratory.

Sediment Incubations

Denitrification was measured on intact sediments in closed chambers using an N_2 gas flux approach modified from Nowicki (1994) (described in detail in Chapter 2). Chambers were incubated with N_2 -free headspace gas to increase sensitivity. Parallel incubations of anaerobic microcosms (no nitrification) were made to control for diffusion-driven N_2 gas fluxes out of the sediments and introduction of atmospheric N_2 into the chambers. Fluxes of O_2 , CO_2 , NH_4^+ , and NO_x^- were measured simultaneously with N_2

flux. Each measurement was made with 2 aerobic and 2 anaerobic microcosms. The sediments were overlaid with 8 cm of filtered (0.22 μm Millipore) half-strength seawater (mean salinity of Mashapaquit Marsh water). The use of filtered, low-nitrate ($< 2 \mu\text{M}$) headspace water allowed the separation of watercolumn from benthic processes. An externally-driven (60 rpm) magnetic stirbar in a cage was placed at the water-gas interface. Over the headspace water was a gas headspace of ~ 10 cm, of either 80% He /20% O_2 (aerobic microcosms) or 100% He (anaerobic microcosms) initially at 1.3 atm to prevent mass fluxes of atmospheric N_2 into the microcosms. The whole apparatus was sealed top and bottom with rubber stoppers held together in a press (Figure 2.1).

On each sampling date, a 5 mL gas sample was withdrawn through the top stopper with a gas-tight valved syringe. The gas sample was analyzed for O_2 , CO_2 , and N_2 with a Shimadzu GC-14A gas chromatograph. A water sample was withdrawn from the valved port through a 0.22 mm syringe filter (Dynatech). Water samples were analyzed for ammonium (NH_4^+), nitrite and nitrate (NO_x^-), and dissolved CO_2 (see below). An equal volume of He-sparged half-strength filtered seawater was reintroduced through the valved port to restore headspace water volume. The first sample date was on day four of microcosm closure, to allow initial rapid off-gassing of porewater dissolved gas pools (Chapter 2). Samples were typically taken for four consecutive days (days 4 – 7), followed by a fifth sample on day 10. Dissolved CO_2 pools were typically only measured on days 4, 6, and 10. After the incubation, sediments were sectioned (0 – 2 cm, 2 – 4 cm, and remainder) for porosity, density, and sediment organic C and N determination.

Measured headspace gas concentrations were converted to masses using the measured headspace volume and pressure, and corrected for losses due to gas withdrawals and leaks of atmospheric N_2 into the chambers (calculations in Table 2.2). Leaks were determined from the difference between the measured headspace pressure and the pressure expected after gas sample withdrawals and molar gas reduction (Loss of O_2 and accumulation of dissolved CO_2).

O_2 , NH_4^+ , and NO_x^- flux were calculated by a linear regression of their concentrations over days 4 – 7. CO_2 flux was calculated by a linear regression over the three points for which both gas and dissolved concentrations were measured. Denitrification N_2 flux was calculated as the difference between linear regressions of N_2 flux in the two aerobic cores and in the two anaerobic cores, which controlled for sediment porewater off-gassing or diffusion of atmospheric N_2 into the microcosms. All other flux measurements were the mean of measurements made on two aerobic cores.

Nitrate uptake: In order to determine the sediment NO_3^- uptake constants and to compare autochthonous with allochthonous denitrification, cores collected from each of sites S and M were subjected to two treatments. Half of the cores from each site were incubated as usual with NO_x^- -free headspace water, while in the other half a solution of KNO_3 was added to bring the headspace water NO_3^- concentration in both aerobic and anaerobic microcosms up to $\sim 600 \mu M$. N_2 flux from denitrification of headspace water NO_3^- was calculated by subtracting the denitrification N_2 flux in the microcosms receiving ambient headspace water from the total N_2 flux in the aerobic microcosms

receiving NO_3^- -enriched headspace water. NO_3^- uptake coefficients were calculated using the first order rate constant at *in situ* bottomwater NO_3^- concentrations.

Bottomwater nitrate timecourse: NO_3^- uptake coefficients calculated from the above experiments were used to determine the *in situ* NO_3^- uptake rate using the mean *in situ* concentrations of NO_x^- . Since bottom water in the salt marsh creek shifts from fresh to saline every tidal cycle, a time course of bottomwater NO_3^- was taken to determine the average NO_3^- concentration in January (the time of lowest sediment metabolism) and again in August (maximum sediment metabolism) over a complete tidal cycle.

Beginning two hours before low tide, a water sample was collected from 4 cm above the surface of the sediment. Sampling was repeated every two hours through high tide and until 2 hours after the next low tide. All samples were filtered upon collection (0.45 μm Millipore) and transported on ice to the laboratory where they were analyzed for NO_x^- and salinity.

Analytical

Gas chromatography: Gas samples were analyzed on a Shimadzu GC-14A gas chromatograph fitted with a thermal conductivity detector. Samples were injected off-column into a 1.5 mL sample loop, to avoid uncertainties resulting from gas volume, temperature and pressure variations. Calibration was with a certified gas mixture (Scott Specialty Gasses), of 2% CO_2 , 15% O_2 , and 3% N_2 .

Sediment and water chemistry: NH_4^+ was analyzed immediately (to prevent ammonia volatilization) by a colorimetric indophenol method (Scheiner, 1976). NO_x^-

was analyzed with azo dye after cadmium reduction on a Lachat Automated Ion Analyzer (Wood *et al.*, 1967). Dissolved CO₂ in water samples and sediment carbonate concentrations were determined by headspace equilibration after acidification, followed by infrared analysis (Beckman Model 15A). Salinity was measured with a YSI conductivity meter. Known volumes of sediment were weighed, dried to constant weight at 60 °C to determine porosity and density. Dried and ground samples were analyzed for particulate organic C and N on a Perkin-Elmer 2400 elemental analyzer. 15 cc sediment samples were mixed with 30 mL chilled 1 mg MgCO₃ L⁻¹ acetone, and analyzed for chl α and pheophytin content on a 10-AU Turner fluorometer. Isotopic composition of sediments (¹³C & ¹⁵N) was determined on a Europa Scientific Integra mass spectrometer (Stable Isotope Facility, University of California, Davis).

Results

N₂ concentrations in the headspace of anaerobic (He headspace) salt marsh creek sediment microcosms rose rapidly after initial closure, due to diffusion driven by the large concentration gradient of N₂ across the sediment-water interface (Figure 3.2a). After four days, diffusion rates slowed as a result of the depletion of sediment N₂ pools, and sediment N₂ flux became constant. This remaining flux consisted of residual diffusion of porewater N₂ and diffusion of atmospheric N₂ into the microcosm's headspace. In the absence of headspace NO_x⁻, and with nitrification inhibited by anaerobic conditions, no denitrification N₂ flux occurred in these cores (Nowicki, 1994). In aerobic cores (He/O₂ headspace) the same pattern was observed, although N₂ flux rates

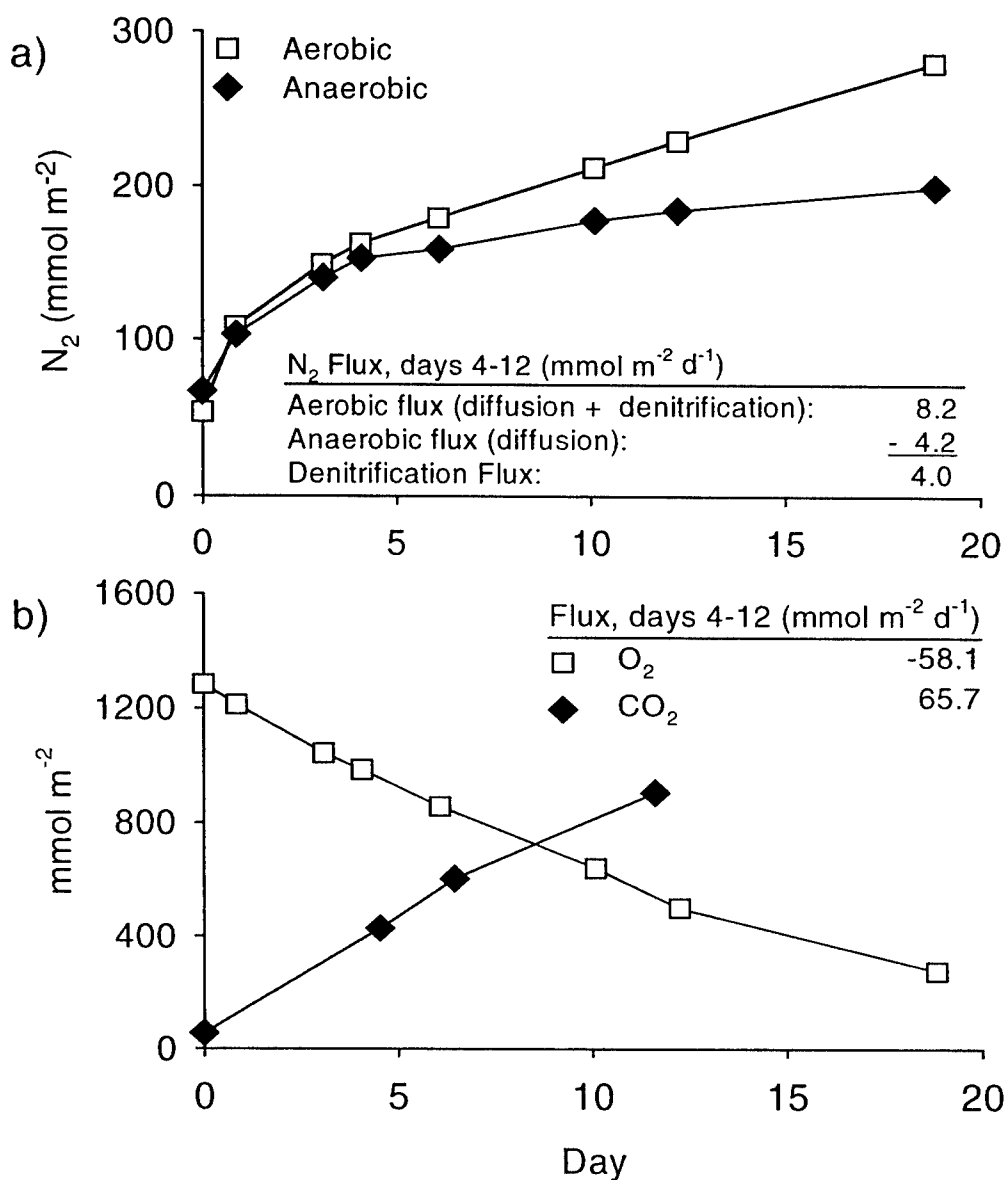


Figure 3.2 **a)** Nitrogen gas efflux from saltmarsh creek sediment cores to N_2 -free gas headspace in aerobic and anaerobic microcosms. Anaerobic N_2 efflux results from atmospheric leakage into the microcosm + diffusion of dissolved sediment porewater N_2 present at microcosm closure. Aerobic N_2 flux results from leakage + diffusion + autochthonous denitrification. Subtracting the slopes of the linear portions of the curves yields the coupled nitrification-denitrification rate. **b)** O_2 consumption and CO_2 production (dissolved inorganic + gas) in sediment microcosms measured simultaneously with N_2 flux. CO_2 value at day 0 is mean of 8 determinations made on initial headspace water on other dates (standard error is smaller than width of point).

after 4 days were greater than anaerobic N_2 fluxes due to additional N_2 generated by autochthonous denitrification of NO_3^- produced *in situ* through nitrification. NH_4^+ fluxes were always out of the sediments (Table 3.1), while NO_x^- fluxes were inconsiderable, < 2 % of N mineralization rates.

Denitrification and O_2 fluxes were determined on sediments collected on 14 dates, from 9/17/97 to 11/9/00 (Table 3.1). CO_2 , NH_4^+ , and NO_x^- fluxes (in microcosms with no added headspace NO_3^-) were determined on only some of these dates as shown in Table 3.1. Headspace O_2 concentrations decreased due to aerobic heterotrophy and the oxidation of reduced metabolic products such as NH_4^+ and S^{-2} . O_2 consumption rates remained constant as long as O_2 concentrations remained above 10% vol, and O_2 consumption was determined from measurements taken while O_2 concentrations were above 30%. Concomitantly, CO_2 concentrations in the headspace (~ 80% as dissolved CO_2) increased as a result of the heterotrophic degradation of organic matter. Although gas chromatographic measurements for S^{-2} and CH_4 were not calibrated, these metabolites were occasionally observed in the headspace above summer anaerobic cores. However, S^{-2} and CH_4 peaks were never observed above aerobic cores, indicating that these species were oxidized before escaping the sediments.

Sandy and muddy sediments were markedly different in porosity, density, and organic content (Table 3.2; $p < 0.001$). Sandy sediments were coarse-grained, with densities averaging $1.22 \pm 0.05 \text{ g cm}^{-3}$, while muddy sediments were fine-grained and only one third as dense as sandy sediments ($0.39 \pm 0.04 \text{ g cm}^{-3}$). Surficial sediment organic C in the sandy site averaged $0.55 \pm 0.05 \text{ mmol cm}^{-3}$, less than one half the

Table 3.1 Fluxes out of Mashapaquit Marsh sediments. Negative numbers indicate fluxes into sediments. Autochthonous denitrification determined by subtracting the N₂ flux in paired anaerobic cores from the mean N₂ flux in paired aerobic cores. Each number is the mean of fluxes determined in paired cores.

Date	Site	O ₂	CO ₂	Autochthonous Denitrification	NH ₄ ⁺	NO _x ⁻
9/17/97	S	-64.3		4.4		
	M	-80.8		11.4		
6/25/98	S	-74.3		5.9	9.6	
	M	-54.6		4.4	8.8	
8/11/98	S	-77.1		6.1	13.5	
	M	-115.8		12.6	10.5	
12/7/98	S	-67.1		6.3		0.1
	M	-39.5		2.2		0.0
3/16/99	S	-41.2	32.5	6.2		
	M	-25.4	50.8	3.3		
5/12/99	S	-44.3	51.3	4.4		
	M	-32.1	45.7	1.3		
7/1/99	S	-48.8	54.1	6.9	2.1	0.0
	M	-61.4	55.5	4.0	5.4	0.0
7/29/99	S	-59.5	69.1	8.7	1.1	0.2
	M	-102.7	105.7	9.0	7.6	0.0
11/11/99	S	-38.6	19.5	3.7		0.0
	M	-54.6	34.8	3.7		0.1
1/10/00	S	-9.9	13.5	0.2	0.4	0.0
	M	-13.9	14.6	1.3	1.2	0.0
4/24/00	S	-41.8	34.5	2.9	3.6	
6/22/00	S	-68.5	67.0	2.8	9.2	
	M	-103.8	103.5	10.1	5.7	
8/3/00	S	-57.1	54.5	6.1	4.8	
	M	-40.1	42.3	4.2	3.2	
11/9/00	M	-68.7		2.9	10.9	

Table 3.2. Characteristics of sandy (Site S) and muddy (Site M) sediments from Mashapaquit Marsh.

Parameter	units	Significance	Site S Mean	se	n	Site M Mean	se	n
Area of coverage	%		31			69		
Predominant benthic alga		Enteromorpha intestinata				Enteromorpha intestinata		
Density	g cm ⁻³		1.22	(0.05)	28	0.39	(0.04)	24
Porosity	mL cm ⁻³		53	(2)	28	81	(2)	24
Sediment C (top 2 cm)	mmol cm ⁻³		0.55	(0.05)	27	1.2	(0.1)	24
Sediment N (top 2 cm)	mmol cm ⁻³		0.052	(0.009)	28	0.113	(0.013)	24
C/N molar ratio			10.1	(0.4)	24	10.7	(0.2)	24
¹³ C	δ ¹³ C		-20.8	(0.8)	6	-18.5	(0.2)	6
¹⁵ N	g at % ¹⁵ N		0.3692	(0.0003)	6	0.3686	(0.0003)	6
Total pigment ^a (top 2 cm)	μg cm ⁻³		1010	(330)	4	590	(100)	4
Pigment / sediment C	μg mg ⁻¹		8.8	(3.1)	4	1.8	(0.7)	4
O ₂ consumption	mmol O ₂ m ⁻² d ⁻¹		58	(6)	13	62	(9)	13
CO ₂ production	mmol C m ⁻² d ⁻¹		46	(7)	8	58	(10)	8
Autochthonous denitrification	mmol N m ⁻² d ⁻¹		4.9	(0.6)	13	5.4	(1.1)	13
O ₂ consumption / sediment C	mmol O ₂ mol C ⁻¹ d ⁻¹		5.3	(0.6)	12	2.6	(0.3)	12
NO _x ⁻ uptake rate constant ^b	L m ⁻² d ⁻¹		53	(7)	7	67	(8)	7
Mean surface water NO _x ⁻	μM		47		^c	43		^c
Allochthonous denitrification	mmol N m ⁻² d ⁻¹		2.5	(0.4)	7	2.9	(0.3)	7

^a Chlorophyll α + pheophytin

^b 1st order rate constant

^c Weighted averaged of 8 samples collected over a tidal cycle in January and August.

organic C content of the muddy site ($1.2 \pm 0.1 \text{ mmol cm}^{-3}$). Stable isotope ratios of C and N also differed between the sites. The $\delta^{13}\text{C}$ of sediment carbon in the two sites was -20.8 ± 0.8 (sandy), and -18.5 ± 0.2 (muddy) in contrast to the $\delta^{13}\text{C}$ of *Spartina alterniflora* vegetation (-12.6) and peats (-15.0). Total pigment content (chlorophyll α + pheophytin) in sandy sediments ($1010 \pm 330 \text{ } \mu\text{g cm}^{-3}$) was twice that of muddy sediments ($590 \pm 100 \text{ } \mu\text{g cm}^{-3}$). Normalizing the pigment content to sediment organic C gave a measure of the relative amount of sediment organic C associated with labile algal biomass. Sandy sediments contained $8.8 \pm 3.1 \text{ } \mu\text{g pigment mg}^{-1} \text{ C}$, while muddy sediments contained $1.8 \pm 0.7 \text{ } \mu\text{g pigment mg}^{-1} \text{ C}$.

Although significant differences in composition were found between the sediment types, metabolic rates were not significantly different ($p > 0.25$). The mean sediment O_2 consumption of sandy sediments was $58 \pm 6 \text{ mmol O}_2 \text{ m}^{-2} \text{ d}^{-1}$, the same as the rate measured in muddy sediments ($62 \pm 9 \text{ mmol m}^{-2} \text{ d}^{-1}$). No significant differences were found in CO_2 production rates (46 ± 7 vs. $58 \pm 10 \text{ mmol m}^{-2} \text{ d}^{-1}$), or denitrification (4.9 ± 0.6 vs. $5.4 \pm 1.1 \text{ mmol N m}^{-2} \text{ d}^{-1}$). However, when these metabolic rates were normalized to the organic C content of the sediments, the difference in the metabolic activity of the constituent organic matter becomes apparent. Sandy sediments were twice as reactive ($5.3 \pm 0.6 \text{ mmol O}_2 \text{ mol}^{-1} \text{ C d}^{-1}$) as muddy sediments ($2.6 \pm 0.3 \text{ mmol O}_2 \text{ mol}^{-1} \text{ C d}^{-1}$).

Analysis of sediments collected along 8 transects was combined with field mapping to classify Mashapaquit Marsh creekbottom sediments into muddy and sandy based on their density (Figure 3.1). Sandy sediments were coarse and light in

appearance, with densities > 0.8 . Muddy sediments were fine and dark in appearance, with densities < 0.8 . Although some sediments appeared intermediate in composition, the frequency distribution was bimodal, with one peak in the range $0 - 0.2 \text{ g cm}^{-3}$, and the other at $1.4 - 1.6 \text{ g cm}^{-3}$. 31% of the marsh creekbottom was classified as sandy, and the remainder (69%) as muddy.

O_2 consumption, CO_2 production, and autochthonous denitrification within the salt marsh creek sediments all followed a seasonal cycle of activity with lows in the winter and highs in late summer (Figure 3.3). O_2 consumption by sandy sediments ranged from $9.9 - 106 \text{ mmol m}^{-2} \text{ d}^{-1}$, while that of muddy sediments ranged from $13.9 - 116 \text{ mmol m}^{-2} \text{ d}^{-1}$, an approximately 10-fold range at each site. CO_2 consumption by sandy sediments ranged from $13.5 - 69.1 \text{ mmol m}^{-2} \text{ d}^{-1}$, while that of muddy sediments ranged from $14.6 - 105.7 \text{ mmol m}^{-2} \text{ d}^{-1}$, a 5 - 7 fold range at each site. The range of autochthonous denitrification rates was larger, from $0.2 - 8.7 \text{ mmol m}^{-2} \text{ d}^{-1}$ in sandy sediments, and $1.3 - 12.6 \text{ mmol m}^{-2} \text{ d}^{-1}$ in the muddy sediments. Variation between years was high, although lower than within-year variation. June and August measurements (for O_2 consumption and autochthonous denitrification) were made in three separate years. In these months, O_2 consumption within a single site varied by < 3 fold, while denitrification varied by < 5 fold. Measurements were made in November in two years; between-year variation in this month was lower than that observed during the summer months

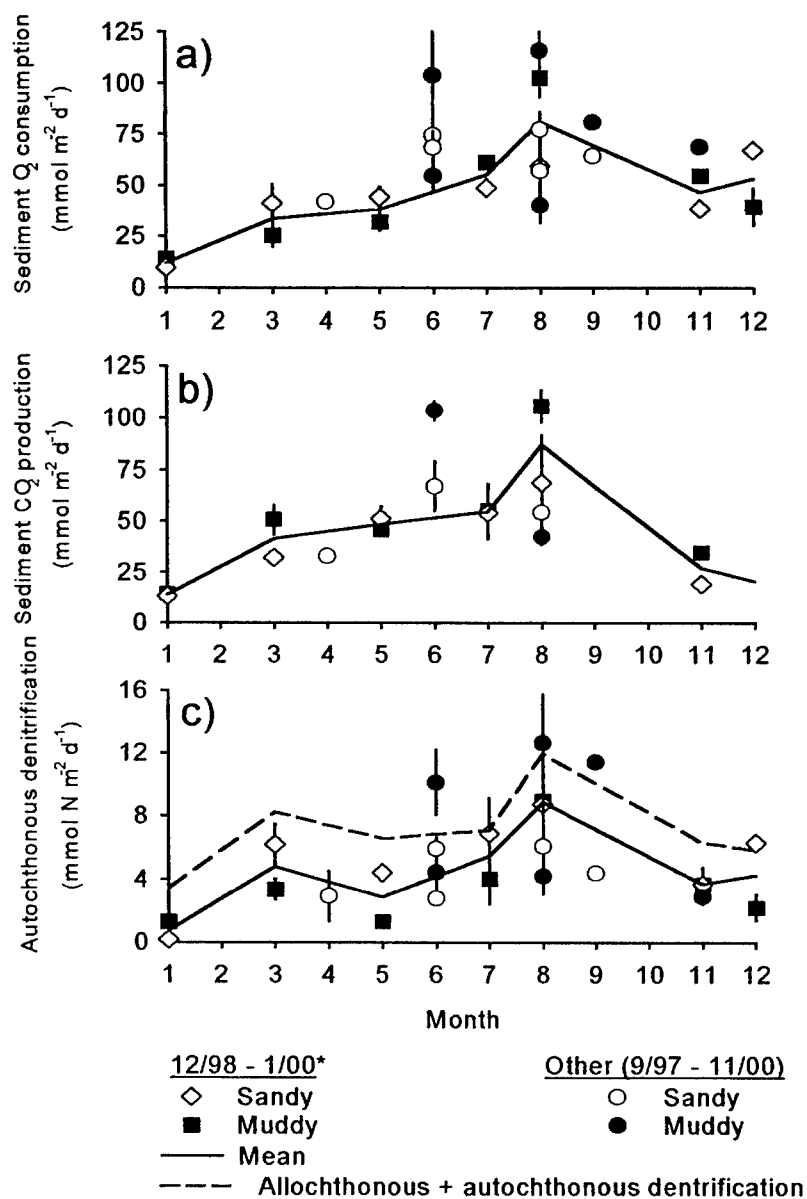


Figure 3.3 Seasonal cycles of sediment-watercolumn fluxes measured over 4 years from 1997 - 2001 in sandy and muddy saltmarsh creek sediments. Bimonthly measurements were made in 1999 (12/98 - 01/00 - the average flux across both sites is indicated by the solid line), with less frequent measurements (concentrated during the summer) made during the other years. Points are means (\pm standard error) of paired microcosms. **a)** Sediment O_2 consumption. **b)** Sediment CO_2 production (dissolved inorganic + gas). CO_2 fluxes were measured less frequently than O_2 and denitrification fluxes. **c)** Autochthonous denitrification with total denitrification (autochthonous + allochthonous) indicated by dotted line.

Sediment fluxes of O₂ and CO₂ were both correlated with temperature (Figures 3.4a and 3.4b), although the correlations were strongest for CO₂. Autochthonous denitrification rates showed no strong relationship to temperature ($r^2 \leq 0.37$), although the highest rates in the muddy sediments occurred at the upper end of the temperature range (Figure 3.4c).

Metabolic rates were highly correlated with sediment C concentrations (Figure 3.5). Sediment O₂ demand rose with increasing sediment C for both sandy and muddy sediments, but the sediment C of muddy sediments was less metabolically active than that of sandy sediments, requiring a higher sediment C concentration to achieve the same Sediment O₂ uptake rate. The same pattern was repeated for CO₂ production, autochthonous denitrification, and sediment NO₃⁻ uptake. Sediment C was most highly correlated with autochthonous denitrification (Pearson product moment correlation coefficient $r = 0.87$), in sandy sediments, whereas in muddy sediments, it was most highly correlated with CO₂ production ($r = 0.85$). Sandy sediments had highly variable sediment C contents, as demonstrated by the size of the standard error bars. Each point is the mean of two cores collected within 1 m of each other. Muddy sediments, on the other hand, were more homogenous in sediment C content.

Summer denitrification rates were determined on two occasions at four sites along the marsh creek (Figure 3.1). Sites 3 and 4 consisted of muddy sediments with similar characteristics to site M, and had similar sediment C-specific O₂ and CO₂ flux rates (Figure 3.6a). However, N fluxes differed between the sites (Figure 3.6b). As discussed

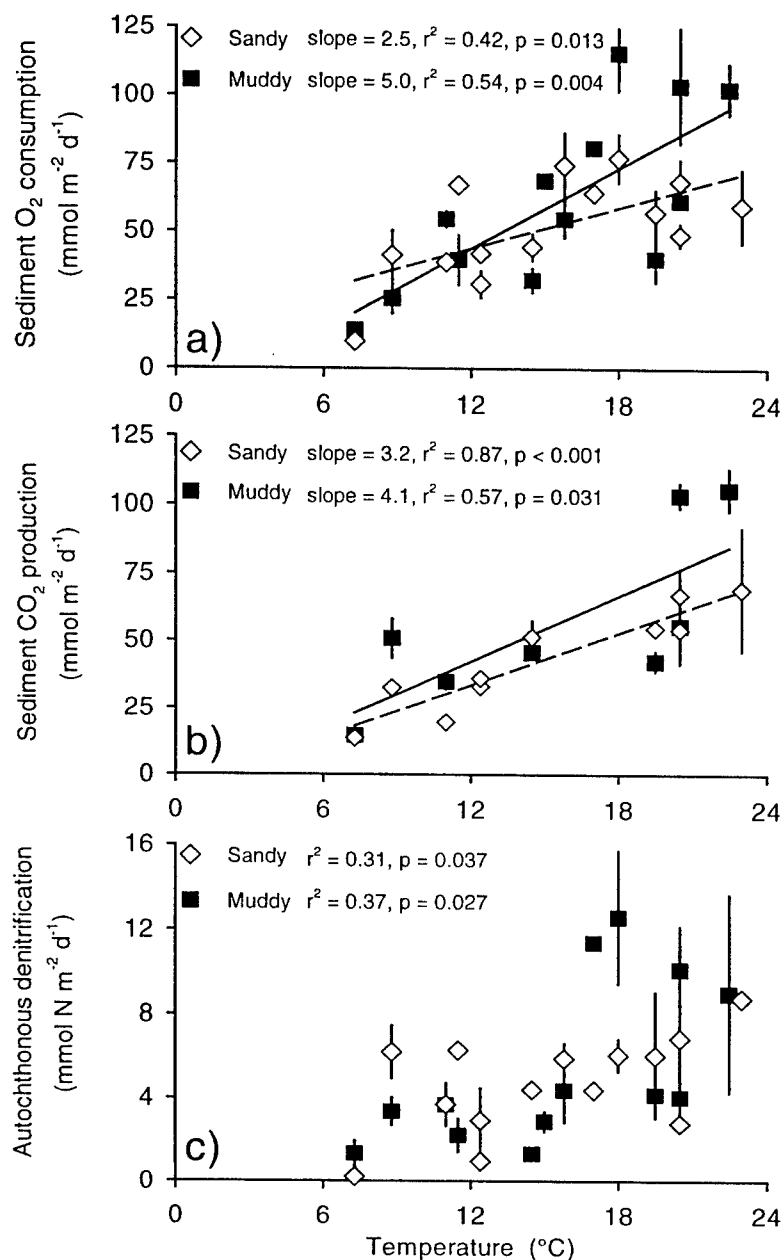


Figure 3.4 Relationship between field temperature and sediment metabolic rates. **a)** O₂ consumption. **b)** CO₂ production. **c)** Autochthonous denitrification. Data are from seasonally sampled sediment cores incubated at *in situ* field temperatures, rather than temperature manipulations. Points are means (± standard error) of paired microcosms. Lines are linear regressions, and the slope, coefficient of determination (r^2), and significance of the regression (p) is indicated on each figure. No regression line was drawn for denitrification because of low correlation with temperature.

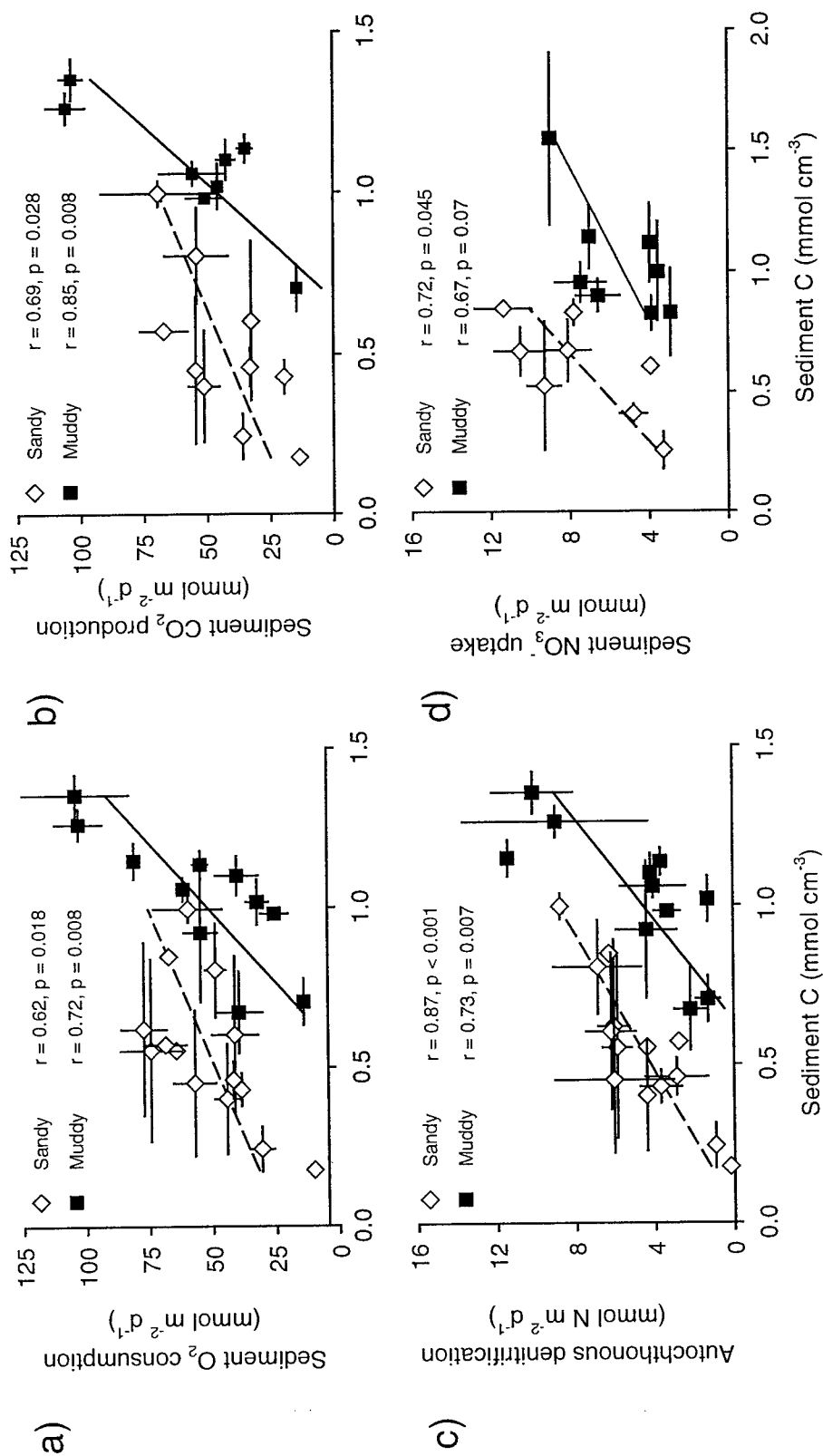


Figure 3.5 Relationship between sediment organic carbon content and metabolic rates. **a)** O_2 consumption. **b)** CO_2 production. **c)** Autochthonous denitrification. **d)** NO_3^- uptake (at high NO_3^- concentration). Data is from seasonal sampling and variations in carbon content within the sediment types are due to spatial heterogeneity within a single sampling site. Points are means (\pm standard error) of paired microcosms. The Pearson product moment correlation coefficient (r) and its significance (p) are indicated on the figures.

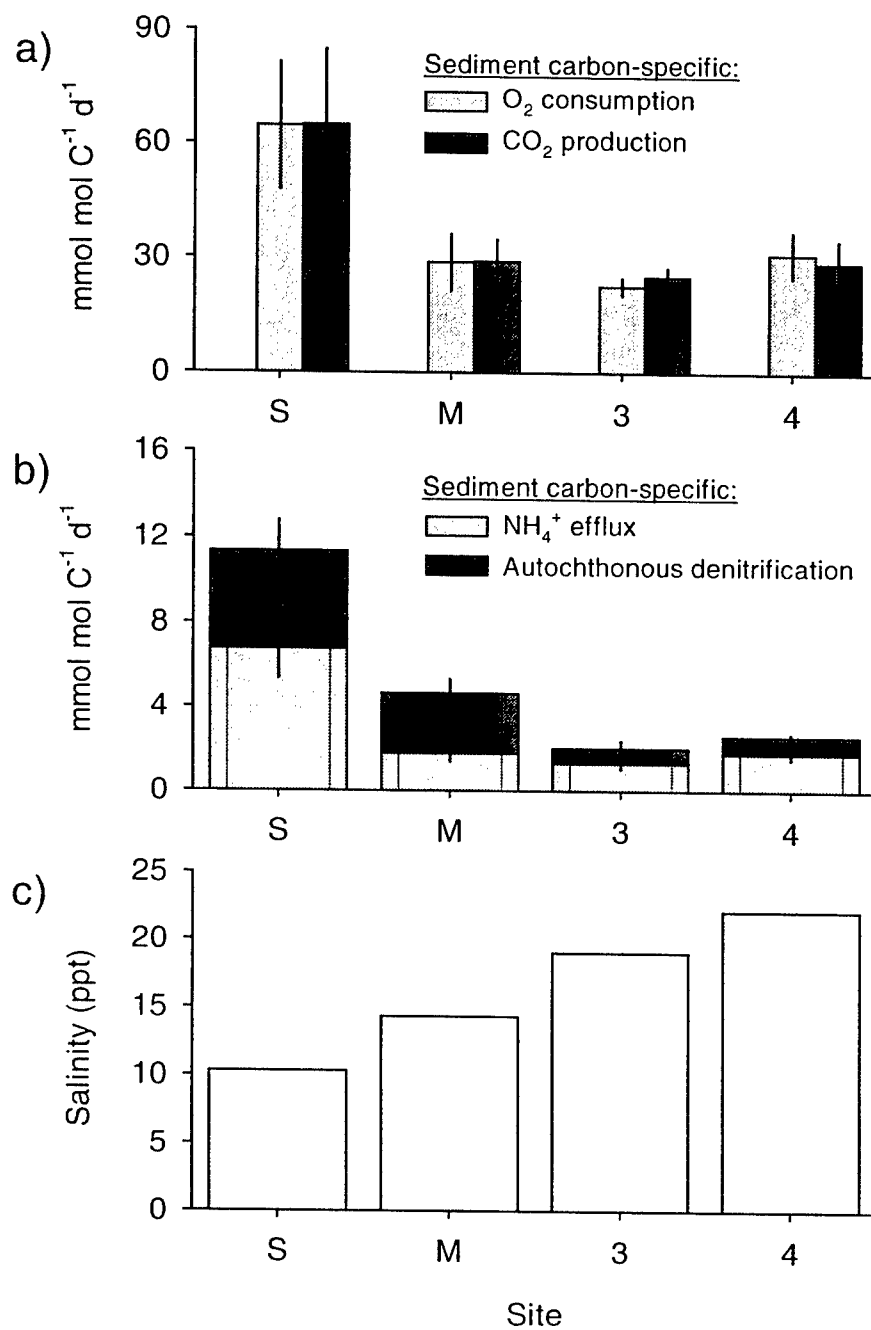


Figure 3.6 Carbon-specific fluxes at 4 sites along a salinity gradient (see Figure 3.1). **a)** Carbon specific O_2 consumption and CO_2 production. **b)** Carbon-specific NH_4^+ efflux + autochthonous denitrification = N mineralization. **c)** Salinity.

above, sediment organic material at site S was more labile than material at site M, and therefore sediment C-specific mineralization (NH_4^+ efflux + denitrification, Figure 3.6a) was higher than at all the other sites. C-specific mineralization and denitrification rates were lower at sites 3 and 4 than at site M. The sites were located along a salinity gradient, with mean bottom water salinity rising from the head to the mouth of the salt marsh creek.

In aerobic microcosms receiving NO_3^- -enriched headspace water, NO_x^- concentrations declined as a result of denitrification within the sediment (Figure 3.7a). Algal NO_x^- uptake was inhibited in the dark incubations. A significant contribution of dissimilatory NO_3^- reduction to NH_4^+ to NO_3^- uptake was ruled out because average allochthonous N_2 production equaled average NO_3^- uptake (Figure 3.7b; t test, $p = 0.21$). Mean mineralization ($\text{NH}_4^+ + \text{NO}_3^- + \text{N}_2$) fluxes in NO_3^- -free microcosms were not greater than mineralization fluxes in NO_3^- -amended microcosms ($p = 0.9$), further support for the minor role of dissimilatory NO_3^- reduction to NH_4^+ in these sediments. Since NO_3^- uptake was due to denitrification alone and because of the high uncertainty associated with the measurement of allochthonous N_2 production (depending on N_2 flux rates from 3 microcosms [2 NO_3^- -free and 1 NO_3^- -amended]), NO_3^- uptake was used as a measure of allochthonous denitrification. The decrease in NO_x^- concentration was substrate-limited, and could be modeled using the Monod equation (Figure 3.7a inset). In some microcosms however, sediment NO_x^- uptake appeared to follow first-order kinetics. First-order NO_x^- uptake rate coefficients were calculated for all microcosms using the

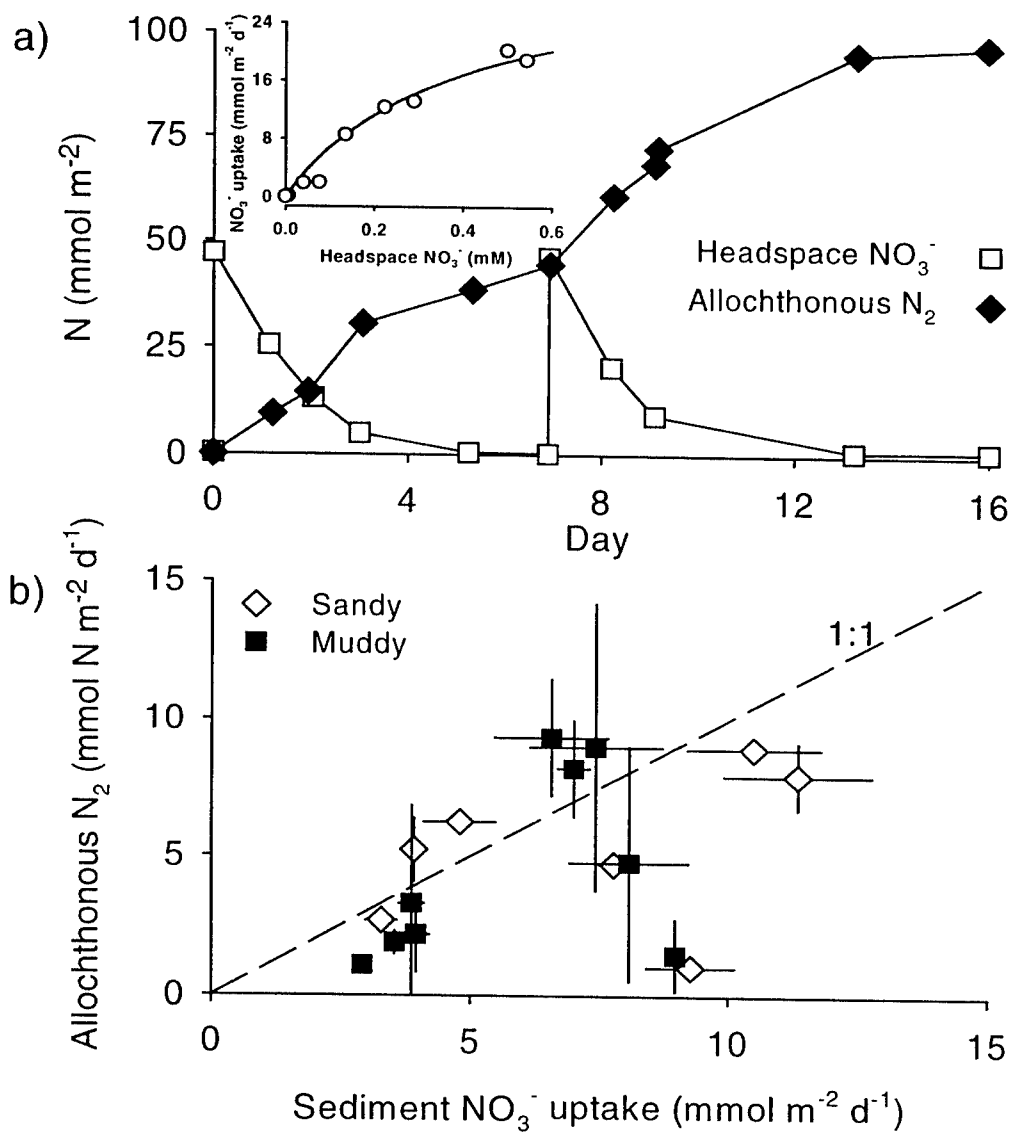


Figure 3.7 a) Example of watercolumn NO_x^- -driven denitrification in an aerobic saltmarsh creek sediment microcosm (5/12/99). Open diamonds show loss of NO_x^- after spikes at 0 and 7 d. Closed squares show concomitant evolution of N_2 from denitrification of watercolumn NO_x^- (determined by subtracting N_2 flux in NO_x^- -free from NO_x^- -containing microcosms.). 92 mmol m^{-2} of nitrate were consumed while 97 mmol m^{-2} N_2 were generated (in excess of that generated by coupled nitrification-denitrification). Inset shows kinetics of NO_x^- uptake for both NO_x^- spikes. Curve is based on least-squares fit after inversion transform of both axes (Lineweaver-Burke plot). **b)** Relationship of watercolumn NO_x^- -driven N_2 production to loss of headspace NO_3^- for all cores incubated in study. Points are means of paired cores \pm standard error.

initial linear part of the uptake curve, since field NO_3^- levels were within this range (Table 3.2).

Allochthonous denitrification rates were determined from 12/98 to 1/01 (Figure 3.3c). Allochthonous denitrification rates ranged from $0.9 - 3.9 \text{ mmol m}^{-2} \text{ d}^{-1}$ in sandy sediments, and from $1.5 - 3.7 \text{ mmol m}^{-2} \text{ d}^{-1}$ in muddy sediments. No clear seasonality was observed for allochthonous denitrification. However, because of the seasonality of autochthonous denitrification, the contribution of allochthonous denitrification to total denitrification peaked in January (78%), while the lowest proportion was found in July (23%). The average annual integrated autochthonous denitrification rate was $1.6 \text{ mol N m}^{-2} \text{ y}^{-1}$, while that of allochthonous denitrification was $1.0 \text{ mol N m}^{-2} \text{ y}^{-1}$, or 39% of the total denitrification ($2.7 \text{ mol N m}^{-2} \text{ y}^{-1}$) in these salt marsh creekbottom sediments.

The first order rate constant (k) of NO_3^- uptake were lower in aerobic vs. anaerobic microcosms (Figure 3.8). The difference in k between aerobic and anaerobic sediments gives a measure of the degree of inhibition of allochthonous denitrification resulting from more oxic sediment conditions. In muddy sediments, the inhibition of the denitrification of water column NO_3^- under aerobic conditions decreased at higher levels of sediment oxygen demand, so that above $50 \text{ mmol O}_2 \text{ m}^{-2} \text{ d}^{-1}$, no difference was found in NO_3^- uptake between aerobic and anaerobic microcosms.

The elemental ratios of C, O_2 and N fluxes across the sediment-water interface were highly consistent across all seasons and sediment types (Figure 3.9). Correlation coefficients (r) ranged from $r = 0.94$ for the CO_2/O_2 ratio, to 0.97 for the C/N ratio. The

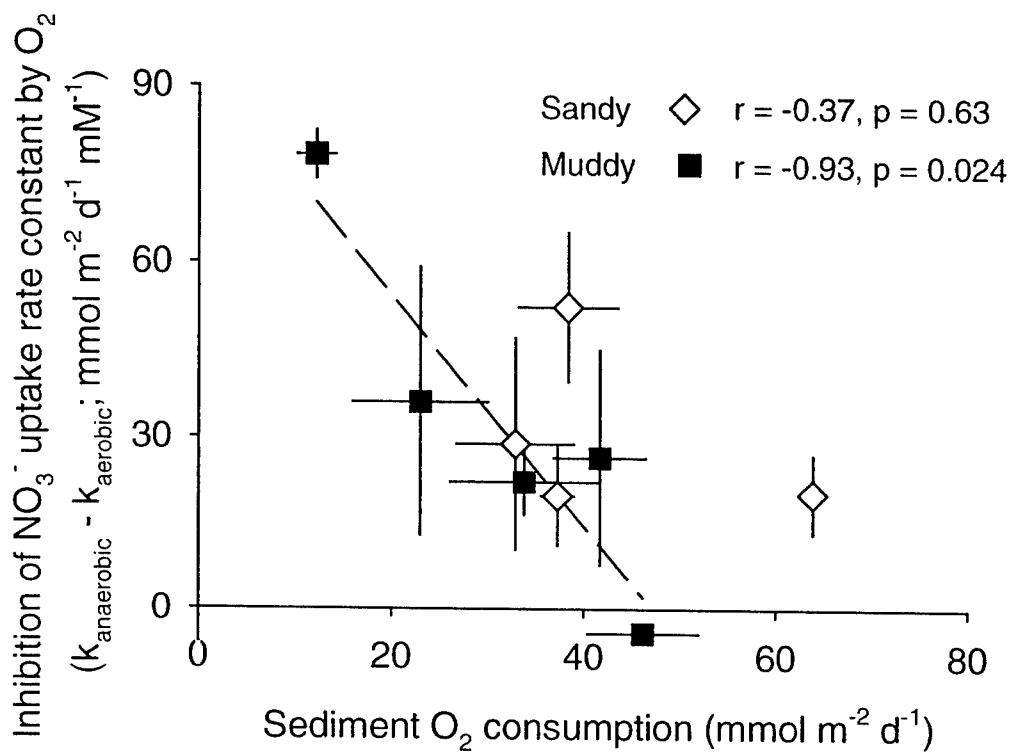


Figure 3.8 Inhibition of sediment NO_x^- uptake by presence of O_2 decreases with increasing sediment O_2 consumption. Inhibition of sediment NO_x^- calculated by subtracting the first-order rate constant of aerobic NO_x^- uptake from that in anaerobic uptake. Points are means of paired cores \pm standard error. Line represents a least squares fit to muddy points alone. Pearson product moment correlation coefficients (r), and significance (p) are indicated for both sediment types.

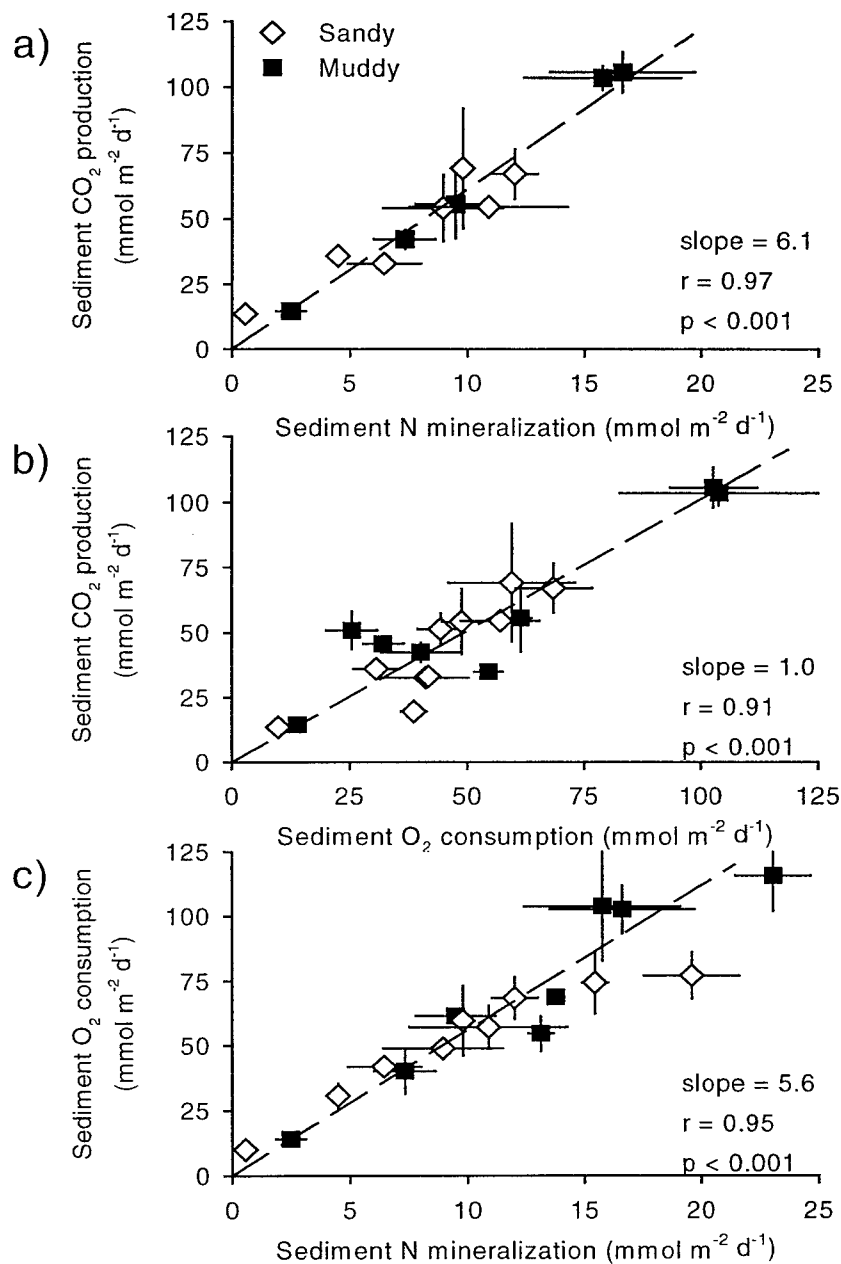


Figure 3.9 Elemental ratios of C, N, and O₂ fluxes across the sediment-water interface in saltmarsh creek sediment microcosms. Points are means of paired cores \pm standard error. Lines are the least squares line (constant = 0) through all points (slope of the line, Pearson product moment correlation coefficient (r), and significance (p) indicated on the figure). CO₂ production is dissolved + gas, N mineralization is the sum of NH_4^+ + NO_x^- + N_2 fluxes.

slope of the least squares line (constant = 0) for the C/N ratio was 6.1, less than the C/N ratio of sediment organic material (range 7.5 - 14.7), at the lower end of the range for suspended particulate matter in the surface waters of the salt marsh creek (5.9-10.4), but near to the Redfield ratio for algal biomass (6.6). The respiratory quotient (r_q , or CO_2 consumed / O_2 produced) at both sites S and M averaged 1.0, indicating complete oxidation of S^{-2} and other reduced end-products of anaerobic metabolism. The absence of S^{-2} and CH_4 in the headspaces of aerobic microcosms and supports the contention that both of these anaerobic metabolites are oxidized before escaping from the sediments.

Nitrification accounted for an average of 18% (range 6 – 30%) of the total sediment O_2 consumption of the sediments (O_2 [nitrification] / O_2 [total]) (Figure 3.10). The sediment CO_2 flux attributable to coupled nitrification-denitrification reactions (CO_2 [nitrification-denitrification] / CO_2 [total]) was the sum of chemoautotrophic CO_2 consumption by nitrifiers and heterotrophic CO_2 production by denitrifiers, but the direction of this summed flux was always out of the sediments. This CO_2 flux on average accounted for 10% (2 – 22%) of the total CO_2 production of the sediments. The role of coupled nitrification-denitrification in the total sedimentary N cycle (N [denitrified] / N [mineralized]) was larger, accounting for 46% (21 – 89%) of the total NH_4^+ regenerated in the sediments. The contributions of nitrification and denitrification fluxes to total sediment metabolism (O_2 , CO_2 , and N) averaged a constant proportion over the entire range of metabolic rates and across sediment types.

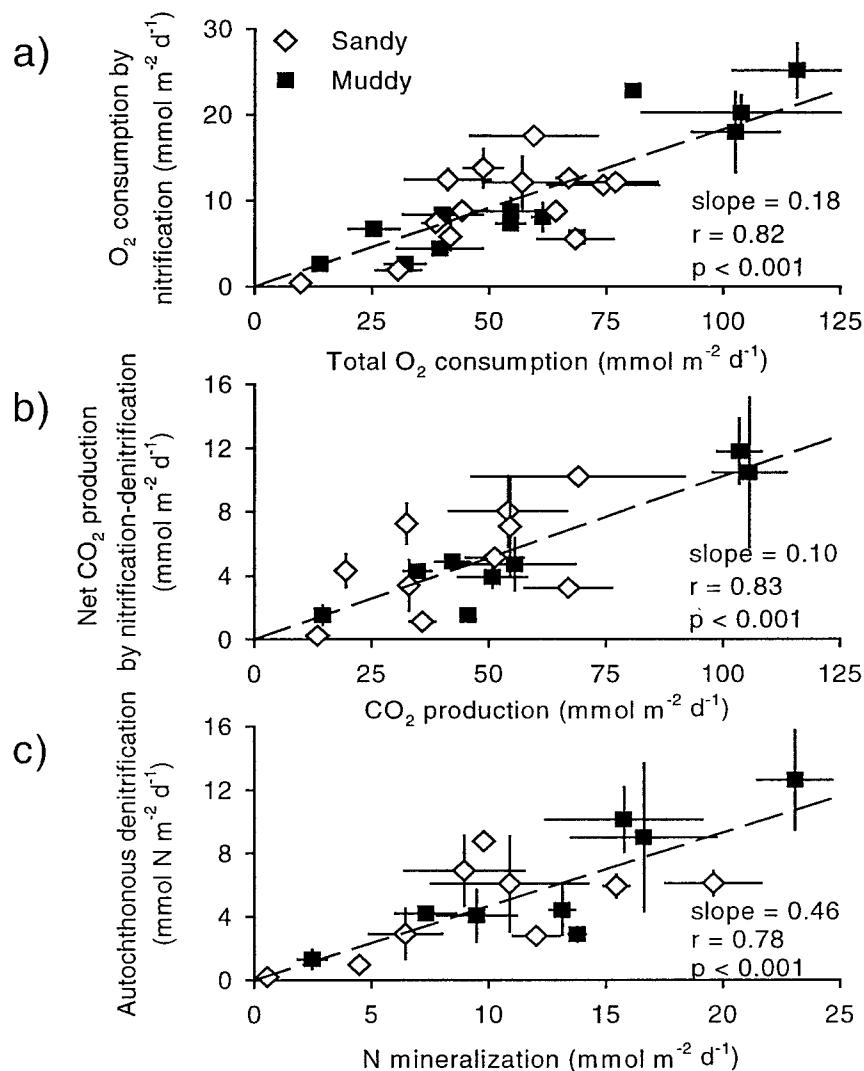


Figure 3.10 Elemental fluxes resulting from autochthonous denitrification (determined stoichiometrically from N₂ flux) in saltmarsh creek sediments. Slope of least-squares fits indicate the proportion of the elemental flux due to nitrification-denitrification. **a)** O₂ consumption of nitrification in relation to overall sediment O₂ consumption. O₂ consumption of nitrification calculated according to the stoichiometry $\text{NH}_3 + 2\text{O}_2 \rightarrow \text{HNO}_3 + \text{H}_2\text{O}$. **b)** CO₂ production resulting from coupled nitrification-denitrification (autotrophic CO₂ consumption of nitrification + heterotrophic CO₂ production from denitrification [$106 \text{CH}_2\text{O} + 84.8 \text{HNO}_3 \rightarrow 106\text{CO}_2 + 42.4\text{N}_2 + 148.4 \text{H}_2\text{O}$]) in relation to total CO₂ production. **c)** Autochthonous denitrification N flux in relation to total N mineralization. The Pearson product moment correlation coefficient (r) and its significance (p) are indicated on the figures. Points are means of paired cores \pm standard error.

Discussion

Metabolic cycling of O_2 , CO_2 , and N in creekbottom sediments of Mashapaquit Marsh appeared to be controlled primarily by sediment organic C content and quality, along with seasonal effects, including temperature. Autochthonous denitrification was a significant contributor to the overall cycling of N, C, and O_2 in these saltmarsh sediments.

O_2 consumption by nitrification in these sediments averaged 18%. Other studies of inner estuaries found contributions (recalculated from published data) of 17% (Seitzinger *et al.*, 1984), 26% (Yoon and Brenner, 1992), 35% (Zimmerman and Brenner, 1994), and 38% (Seitzinger, 1987). Similarly, in deep-sea sediments from the North Atlantic, O_2 consumption by nitrification was calculated to be 35% (Christensen and Rowe, 1985). However, the stoichiometries of organic matter degradation and nitrification constrain the contribution of autochthonous denitrification to total sediment O_2 fluxes. Even if 100% of the NH_4^+ generated by the degradation of Redfield organic matter (C:N = 6.6) were nitrified and denitrified, nitrification could only account for a maximum 30% of the total O_2 flux. The higher contributions reported in the literature might result from net import of allochthonous NH_4^+ into the sediments, changes in sediment NH_4^+ storage, incomplete oxidation of reduced metabolites (S^{2-} , CH_4), or alternate metabolic pathways whose contribution to N metabolism in natural environments is still not known. A number of the newly described metabolic pathways would have the effect of reducing the O_2 demand of coupled nitrification-denitrification (Jetten, *et al.*, 1997). N_2 gas can be produced anaerobically from NH_4^+ and nitrite, a

process known as nitrifier denitrification. In anaerobic NH_4^+ oxidation, NH_4^+ is used chemolithotrophically by denitrifying organisms, resulting in the anaerobic conversion of NO_3^- and NH_4^+ to N_2 gas.

Carbon cycling by autochthonous denitrification in the present study was 10% of the total dark cycling of sediment C (CO_2 production by denitrification = 11%; autotrophic CO_2 fixation by nitrification = 1%). Adding the CO_2 production resulting from allochthonous denitrification increases the average denitrification C cycling from 10% to 17%, similar to the effect of autochthonous nitrification on O_2 consumption. An early study of a Danish estuary found that denitrification accounted for only 3 - 4% of sediment C cycling (Jørgensen and Sørensen, 1985), but denitrification was determined using the acetylene block assay, which is known to underestimate denitrification rates (Seitzinger *et al.*, 1993). Other studies using either N_2 flux or ^{15}N isotope pairing methods for measuring denitrification found contributions of from 1 - 5% in coastal marine sediments (Trimmer *et al.*, 2000) to values of 9.3% - 18.5% for estuarine sediments (Yoon and Brenner, 1992; Zimmerman and Brenner, 1994; Trimmer *et al.*, 2000).

Of the NH_4^+ remineralized in the sediments, 46% was nitrified and denitrified, within the range reported for estuaries and coastal marine sediments (15% - 75%) (reviewed in Seitzinger, 1987). In Mashapaquit Marsh sediments, autochthonous denitrification was limited by nitrification, rather than denitrification, since there was a NO_x^- flux into the sediments, while in most estuaries, NO_x^- is effluxed from the sediment,

indicating that denitrification, rather than nitrification limits autochthonous denitrification (Seitzinger, 1987).

Although groundwater NO_x^- is removed directly by denitrification, groundwater NO_x^- is the probable source of remineralized sediment N as well. The sediment organic material that drives creekbottom respiration and autochthonous denitrification in this study was found to be primarily algal in origin. Export of macrophytic plant material from the vegetated marsh to creekbottom sediments is known to be small (Wolaver *et al.*, 1983; White and Howes, 1994b). Further, in the present study, the molar C/N ratio of CO_2 and N fluxes from the sediments (6.1; Figure 3.9a), and the $\delta^{13}\text{C}$ of sediment organic C point to an algal source for mineralized N, consistent with recent findings in other salt marshes based on stable isotope analysis (Page, 1997; Boschker *et al.*, 1999). Exchanges between creekbottom sediments and tidal water are small, though significant; but the overall balance is toward export from the marsh (Valiela and Teal, 1979; Smith, 1999). The only significant input of N to the marsh is groundwater NO_x^- , and it must be this N which supports creekbottom production of benthic algae, the primary source for labile sediment organic material. Smith (1999) found that allochthonous denitrification of groundwater NO_x^- was enough to account for only a maximum of 70% of N missing from a tidal exchange budget of Mashapaquit Marsh. Although comparisons of day/night N budgets and light/dark sediment flux incubations did not support significant photosynthetic uptake of groundwater NO_x^- , it is probable that benthic algal N uptake, and subsequent N remineralization and autochthonous denitrification accounted for the remaining missing N.

Since no NO_3^- efflux from the sediments was observed, autochthonous denitrification must have been limited by the supply of NO_3^- through nitrification. Autochthonous denitrification rates measured in this study (mean 5.2, range 0.2 – 12.6 $\text{mmol N m}^{-2} \text{ d}^{-1}$; Table 3.1) were at the high end of the range reported for estuarine sediments (Jørgensen and Sørensen, 1985; Jenkins and Kemp, 1984; Seitzinger, 1987; Jensen *et al.*, 1996), although rates of up to 5.0 $\text{mmol N m}^{-2} \text{ d}^{-1}$ have also been reported from an unpolluted Florida estuary (Seitzinger, 1987). However, high denitrification rates are most often found in systems receiving high N loads and in sediments with high organic C contents (Jørgensen and Sørensen, 1985). Denitrification rates as high as 197 $\text{mmol N m}^{-2} \text{ d}^{-1}$ have been measured in sediments near a sewage outfall (Trimmer *et al.*, 2000).

The Mashapaquit Marsh creekbottom sediments of this study receive 32 $\text{mmol N m}^{-2} \text{ d}^{-1}$ from the surrounding watershed (Smith, 1999). Two other studies report denitrification N_2 flux rates for embayments in Cape Cod, Mass. Nowicki (1999) found very low rates ranging from 0.05 – 0.58 $\text{mmol N m}^{-2} \text{ d}^{-1}$ in an estuary (Towns Cove) receiving 2.1 $\text{mmol N m}^{-2} \text{ d}^{-1}$ from the surrounding watershed (Giblin and Gaines, 1990), while Lamontagne and Valiela (1995) measured rates up to 17 (mean ~3.3) $\text{mmol N m}^{-2} \text{ d}^{-1}$ in another marsh estuarine system (Childs River) receiving 35 $\text{mmol N m}^{-2} \text{ d}^{-1}$ (Valiela *et al.*, 1992), similar to denitrification rates in the Mashapaquit Marsh.

In sediments with high labile organic C content, such as in this study, the reducing potential of the sediments is high, and all NO_x^- produced *in situ* is denitrified, while watercolumn NO_x^- diffuses into the sediments and is denitrified as well. Nitrate uptake

rates in this study were limited by sediment C at high NO_x^- concentrations ($> 300 \mu\text{M}$; Figure 3.5d). However, there is sufficient labile organic carbon to denitrify *in situ* levels of NO_x^- ($43 \mu\text{M}$), and so allochthonous denitrification is primarily controlled by water column NO_x^- concentration (Figure 3.7a inset) (Smith, 1999).

NO_x^- uptake and denitrification by sediments only takes place in sediments with higher O_2 consumption rates ($> 15 \text{ mmol O}_2 \text{ M}^{-2} \text{ d}^{-1}$) (Jensen *et al.*, 1996; Trimmer *et al.*, 2000; this study). The NO_x^- diffusion rate to anaerobic sediment zones in the sediment is limited by the degree of sediment oxygenation. In muddy sediments, where diffusion predominates over advection, O_2 penetration is inversely related to the O_2 uptake rate of the sediments (Figure 3.8). In sediments with high O_2 uptake rates, oxygen diffusing into the sediments is depleted quickly, and anaerobic zones are readily accessible to diffusing NO_x^- .

Within each site (S and M), metabolic rates were related to sediment C concentrations, but sediment C quality differed between sites (Figure 3.5, Table 3.2). The organic material at site S was about twice as reactive as that of site M (C-specific O_2 consumption 5.3 vs. $2.6 \text{ mmol O}_2 \text{ mol}^{-1} \text{ C d}^{-1}$), though half as concentrated (0.55 vs. $1.19 \text{ mmol C cm}^{-3}$), with the result that metabolic fluxes of O_2 , CO_2 and autochthonous denitrification were not significantly different between the sites ($p > 0.07$). Organic C in the sandy sediments contained higher proportions of algal C, as indicated by the higher photosynthetic pigment content of sediment C (8.8 vs. $1.8 \mu\text{g mg}^{-1} \text{ C}$). Fresh algal C likely accounted for more than four times as much of the sediment C in sandy sediments as in muddy sediments. However, molar C/N flux ratios (6.1) from both sediments were

similar to the Redfield algal ratio (6.6). Likewise the $\delta^{13}\text{C}$ value of both sediments were similar and suggestive of algal biomass (Table 3.2). In addition, the slopes of the responses of metabolic rates to sediment C were similar in both sediments, though the intercepts were different (Figure 3.5), indicating a similar relationship between the labile fraction of muddy sediment C and sandy C. Although the mean C/N ratio of sediment organic materials at both sites was the same (10.1 – 10.7; Table 3.2), a plot of sediment C/N ratio against sediment C content showed that the C/N ratio declined as sediment C content declined (unpublished data). Extrapolating the trend back to 0 mmol C cm⁻³ for sandy sediments gives a C/N ratio of 6.9, further confirmation of the elemental composition of the labile fraction of organic material in these sediments. This pattern suggests that although the source of the organic material in both sediments was likely algal, muddy sediments contained a fraction of refractory material not subject to degradation. Sandy sediments are sites of groundwater intrusion, and this flow likely prevents the accumulation of refractory material.

Studies comparing “sandy” and “muddy” sediments have generally found lower metabolic rates in sandy sediments (Jørgensen and Sørensen, 1985; Jensen *et al.*, 1996; Trimmer *et al.*, 2000). These sediments are usually classified by porosity (mL H₂O cm⁻³ sediment) and organic C content (% C.), however, these characteristics may be poor indicators of sediment metabolic activity. Although the % C content of Mashapaquit Marsh sandy sediments was ~ 10% of that of muddy sediments, the C content of sandy sediments (mmol C cm⁻³) was 50% of the C content of muddy sediments (Table 3.2). Even C content expressed on a volume basis does not adequately describe sediment C

characteristics, since as in the present study, the lability of organic C differed between the sediment types (Table 3.2). My finding of similar rates in both sediment types illustrates the inadequacy of rough descriptions of sediment characteristics. Two sediments with the same C content by weight might have very different C contents by volume, especially when comparing mineral with organic sediments. In this study, I calculated organic C content as mmol C cm^{-3} ($\% \text{ C} \times \text{sediment density}$). Sediment C lability expressed in units of O_2 or CO_2 flux per unit of sediment C content facilitates intersystem comparisons of sediment metabolic potentials.

Temperature appeared to account for a significant proportion of the variability in O_2 and CO_2 fluxes and in denitrification rates (Figure 3.4, $r^2 = 0.31 - 0.87$), though it was not possible to separate temperature from other seasonal effects. Although the absolute concentration of sediment organic C did not vary seasonally (unpublished data), it is likely that seasonal cycles of algal production had an effect on the lability of sediment C pools. Other seasonal effects which could be confounded with temperature include benthic irrigation and sediment redox state. Nonetheless, assuming that the temperature effect was a direct one, it would correspond to a Q_{10} for each reaction of from 1.6-2.0, similar to those reported in the literature for estuarine sediments (Q_{10} for O_2 consumption = 2.7, Jørgensen and Sørensen, 1985; Q_{10} for denitrification = 2.1, Zimmerman and Benner, 1994). Other studies have found spring maxima for denitrification, in contrast to my late summer maximum (Jørgensen and Sørensen 1985; Nowicki 1999). A spring maximum indicates the predominance of non-temperature seasonal factors in controlling metabolism (i.e. spring algal blooms), whereas my findings may support the

predominance of temperature-driven seasonal effects in this salt marsh creekbottom.

Nonetheless, the temperature effect for denitrification was weak ($r < 0.37$), indicating a greater potential role for seasonal or other effects.

High groundwater NO_x^- loads to the creekbottom sediments of Mashapaquit Marsh likely lead to high algal production rates and high concentrations of labile organic matter in the sediments. Degradation of this organic material supports high rates of O_2 , CO_2 , and N cycling, including denitrification of water column NO_x^- and half of the regenerated N. Allochthonous denitrification contributes significantly to total denitrification (39%). Denitrification is also a significant contributor to the total metabolism of these salt marsh sediments, contributing nearly 20% to the cycling of C and O.

CHAPTER 4

Competition Between Plant Uptake and Coupled Nitrification-Denitrification for NH_4^+ Measured *in situ* in Salt Marsh Sediments

Abstract

Spartina alterniflora is the dominant plant of Atlantic coastal salt marshes of the USA. The N cycle of the vegetated marsh tends to retain N through a close coupling of remineralization and plant uptake, with denitrification a major pathway for N loss. I studied the competition between plant uptake and nitrification-denitrification as it relates to patterns of short-term nitrogen retention and loss in a New England *S. alterniflora* marsh, Great Sippewissett Marsh, Massachusetts. An *in situ* ^{15}N -ammonium ($^{15}\text{NH}_4^+$) tracer approach was used in natural marsh, in plots receiving long-term nitrogen loading (>27 yr), and in hydrologically-controlled greenhouse lysimeters. In natural marsh areas during the growing season, the short-term fate of NH_4^+ was dominated by plant uptake, which accounted for 66%, while denitrification accounted for 34% of remineralized N. However, in the winter the situation was reversed, with denitrification dominating. Although N addition stimulated plant growth (3-fold), consequent sediment oxidation and increased availability of NH_4^+ resulted in a competitive shift toward the bacterial nitrifying-denitrifying community. Under high N addition rates ($15.5 \text{ mol m}^{-2} \text{ yr}^{-1}$), denitrification accounted for 72% of the short-term fate of NH_4^+ and 95% over the long-term. Based upon seasonal measurements of $^{15}\text{NH}_4^+$ loss, an approximate annual rate of denitrification was calculated of $0.73 \text{ mol N m}^{-2} \text{ yr}^{-1}$ ($0.7 - 12.2 \text{ mmol N m}^{-2} \text{ d}^{-1}$) and $12.6 \text{ mol N m}^{-2} \text{ yr}^{-1}$ ($11.1 - 136 \text{ mmol m}^{-2} \text{ d}^{-1}$). Deeper water table excursions in hydrologically-controlled laboratory lysimeters oxidized the sediment, increasing plant growth rates by 2 – 3-fold. Plant growth was suppressed in flooded treatments by high porewater S^{2-} ($\sim 5 \text{ mM}$), making the excess NH_4^+ available for coupled nitrification-

denitrification. The importance of plant growth and tidal inundation in controlling the N cycle in regularly flooded salt marsh sediments emphasizes the need for *in situ* techniques to measure denitrification and N cycling.

Introduction

High primary production and position at the interface between land and sea make salt marshes important transformers of N (Nixon, 1980). Regularly flooded peats of the rhizomatous grass *Spartina alterniflora* make up nearly 50% of the area of a New England salt marsh, and plant-mediated transformations of N dominate the N cycle of these areas (Valiela and Teal, 1979; White and Howes, 1994a). Nearly monospecific stands of *S. alterniflora* colonize the tidal low marsh because *S. alterniflora* is particularly well adapted to the stresses of salinity fluctuations and sediment anoxia (McGovern *et al.*, 1979; Howes and Teal, 1994). Although the marsh sediments are high in NH_4^+ , productivity is limited by N availability (Sullivan and Daiber, 1974; Valiela and Teal, 1974). This apparent paradox stems from the inhibition of plant N uptake by S^{-2} , a by-product of microbial SO_4^{-2} reduction in the sediments (Howes *et al.*, 1981; Mendelssohn *et al.*, 1981). This inhibition can be overcome by N fertilization, but within the salt marsh, *S. alterniflora* productivity is naturally higher along the creek banks, where porewater drainage promotes air entry leading sediment S^{-2} oxidation (Howes and Goehring, 1994). High productivity causes a shift in the growth form of the plant, from the 10 cm high short form to the >1m high tall form. In long-term N fertilization experiments, short-form *S. alterniflora* stands grew to resemble the tall form of the plant

(Valiela *et al.*, 1978). Overcoming the N limitation of plant growth played a role in this transformation, but growth was further stimulated by a positive feedback between plant growth and sediment aeration (Howes *et al.*, 1986). In the short *S. alterniflora* marsh, away from the creek banks, drainage of the peat sediments in between tidal inundations is negligible. The main route for water loss from the sediments is evapotranspiration, which allows air to enter and oxidize the sediment (Dacey and Howes, 1984). When plant growth is stimulated by N addition, evapotranspiration increases sediment oxidation, further stimulating plant growth (Howes *et al.* 1986).

A recent N budget for the short *S. alterniflora* areas of Great Sippewissett Marsh, Massachusetts, USA shows an N cycle dominated by N remineralization and plant uptake with annual plant N demand twice the rate of N fixation, the dominant source of new N to this marsh (White and Howes, 1994a). Remineralization of NH_4^+ from decaying plant biomass in the sediments is the major source of substrate to support coupled nitrification-denitrification, the largest N loss term (White and Howes, 1994a). Nitrification competes with plant uptake for remineralized NH_4^+ , accounting for as much as 25% of the $\sim 1.1 \text{ mol N m}^{-2} \text{ yr}^{-1}$ total remineralized in plant biomass, and removing it from the pool available for plant uptake.

Denitrification is acknowledged as an important flux in salt marsh N cycling, but measuring its contribution has proved difficult. Autochthonous denitrification in vegetated marsh sediments involves the remineralization of NH_4^+ within the sediments, diffusion to aerobic zones where nitrification can take place, followed by subsequent diffusion of nitrification-produced NO_3^- to anaerobic zones for denitrification (Patrick

and Reddy, 1976). Since denitrification represents a gaseous loss of N, it has often been measured as the difference between inputs and outputs in a mass balance approach, but the compounding of errors when many terms are summed makes this approach subject to uncertainty (White and Howes, 1994a). Direct measurements of denitrification have been made using a variety of *in vitro* techniques. The acetylene block technique was sufficient to demonstrate denitrification potential in sediments, but because acetylene blocks nitrification as well as denitrification, it is inadequate for measuring coupled nitrification-denitrification rates (Van Raalte and Patriquin, 1979; Koch *et al.* 1992). In addition, inhibition by acetylene is sometimes incomplete in the presence of S^{2-} (Sørensen *et al.*, 1987). More recently, ^{15}N isotopic tracer methods have been developed which allow the measurement of nitrification and denitrification through isotope dilution and recovery of reaction products. These techniques have been used on plant-free sediment cores, but such studies leave out the important structuring effects of plant metabolism on N cycling (Abd. Aziz and Nedwell, 1986; DeLaune *et al.*, 1998). Oxygen transport to the roots of aquatic macrophytes can create aerobic rhizospheres of high surface area which promote coupled nitrification-denitrification (1989).

In order for measurements of coupled nitrification-denitrification rates to accurately reflect rates in natural vegetated marsh sediments, the sensitivity of nitrification-denitrification to plant N uptake rates, tidal inundation frequency and sediment oxidation state must be considered. This requires *in situ* measures of denitrification under normal conditions of tidal inundation, light, redox conditions, and sub-surface hydrology. Kaplan *et al.* (1979) measured N_2 evolution into He headspaces

in sediments enclosed in bell jars (8 cm dia.), but their method involved the removal of aboveground biomass, alteration of sediment hydrology, and short incubations in dark enclosures. White and Howes (1994a), in their study of long-term N retention in salt marsh sediments, used injected $^{15}\text{NH}_4^+$ as a tracer in undisturbed sediments. Comparing losses in field and laboratory lysimeters, they found that losses to tidal waters and through subsurface drainage were insignificant, and that losses were attributable to denitrification. By the third day after labeling, the original label had been either denitrified or taken up into biomass, and subsequent losses were slow and due to remineralization of biomass-incorporated label. The picture that emerged supported the contention that plants were able to out-compete the bacterial nitrifying-denitrifying community for inorganic N, but that the bacterial pathway was significant in N removal from vegetated sediments. However, the processes which controlled this competition remained unclear.

In the present study, I use an *in situ* $^{15}\text{NH}_4^+$ tracer approach to determine the seasonal pattern of the short-term (days) fate of inorganic nitrogen within *S. alterniflora* sediments, primarily with regard to the partitioning of regenerated N between plant uptake and nitrification-denitrification reactions. In addition, I assess the role of N availability and sediment oxidation on this plant-nitrifier competition both in marsh plots receiving long-term fertilization, and in lysimeters where sediment oxidation status was manipulated through hydrological regimes.

Methods

Site Description

The study was conducted at Great Sippewissett Marsh (Cape Cod, Massachusetts, USA). This marsh is dominated by short-form *S. alterniflora* growing in near monospecific stands on the marsh plain and tall-form *S. alterniflora* growing along creekbanks. The sediments consist of a highly organic peat (28.5% C) typical of New England salt marshes (Redfield, 1972). Measurements were made in stands of *S. alterniflora* similar to those previously investigated in this salt marsh (Valiela and Teal, 1979; White and Howes, 1994a). Field measurements of coupled nitrification-denitrification and plant N incorporation were made using an $^{15}\text{NH}_4^+$ tracer in undisturbed sediments of short-form *S. alterniflora* and in plots receiving N fertilization during the growing season for the past 27 - 31 years (Valiela *et al.*, 1976; Valiela *et al.* 1985). Fertilized plots were treated with 1.7 (LF), 5.2 (HF), or 15.5 (XF) mol N m⁻² yr⁻¹, 71% as pelletized sewage sludge (Milorganite; 10% N) and 29% as urea ten times each growing season (May-September).

Sediments of unfertilized and XF fertilized plots ("fertilized plots") differed in N availability and sediment oxidation (Table 4.1). Mean KCl-extractable NH_4^+ concentrations in fertilized sediments were 5 times, and total N content was twice that of unfertilized sediments. Water table excursions in fertilized sediments were > 3 times those of control sediments, due to increased plant growth and evapotranspiration, while porewater S^{2-} concentrations were reduced to more than one fifth the levels of unfertilized sediments as a result of the concomitant air entry and sediment oxidation.

Table 4.1. Characteristics of unfertilized and XF fertilized marsh plots during the growing season (June – September). Standard errors in parentheses.

	units	Unfertilized	XF fertilized
Nitrogen addition ^a	mol N m ⁻² yr ⁻¹	0	15.5
Sediments (top 10 cm)			
Porosity	mL cm ⁻³	0.85 (0.01)	0.80 (0.01)
Density	g cm ⁻³	0.16 (0.01)	0.21 (0.01)
N	mmol cm ⁻³	0.16	0.37
C	mmol cm ⁻³	3.9	4.1
KCl-extractable NH ₄ ⁺ ^b	μmol cm ⁻³	0.18 (0.06)	1.12 (0.44)
Mean water table excursion	cm	4.0 (0.7)	13.4 (2.2)
Salinity	ppt	25.4 (3.7)	28.2 (3.6)
Porewater S ⁻² ^b	mM	2.02 (0.68)	0.38 (0.12)
Plants			
Species		<i>Spartina alterniflora</i>	
Stem height ^c	cm	30	102
Peak biomass ^c	g m ⁻²	270 (66)	1100 (90)

^a As total N.

^b Average top 10 cm.

^c Howes *et al.* 1986.

In Situ Tracer Injection:

Field work: Denitrification was measured as coupled nitrification-denitrification ("denitrification") using $^{15}\text{NH}_4^+$ as a tracer, in a modification of the method of White and Howes (1994a). The tracer was injected into undisturbed marsh sediments, and its retention followed in sediment cores taken over a timecourse of 1 – 5 days, with measurements concentrated in the first 24 hours. All work was performed from boardwalks to avoid alteration of the marsh surface. Experiments were performed in unfertilized sites on 7 dates; on 5 of these, simultaneous measurements were made in fertilized plots. A solution of $^{15}\text{NH}_4\text{Cl}$ was line-injected (20 ga. needle), through the top 10 cm of sediment. Up to 14 such injections were made at each site ~0.5 m apart, and the injection point marked. At each time point, two injection sites were randomly chosen and a 20 cm dia area of aboveground biomass centered on the injection site was harvested. The sediment was collected using a piston corer (6.5 cm dia.) centered on the injection site. In the field the sediment cores were immediately sectioned into 3 layers of 5 cm thickness each, down to 15 cm depth. Each section was further cut into 4 pieces (to increase surface area for freezing), placed in labeled bags, and immediately packed in dry ice to stop biological activity. Two cores were taken immediately after tracer injection to calibrate T_0 tracer recovery. Another 2 uninjected cores were collected to measure the natural abundance of ^{15}N . Three replicate cores were collected for determination of KCl-extractable NH_4^+ . Porewater samples for salinity and S^{2-} determinations were collected using sippers (Howes *et al.*, 1985). The rate of water table drop due to evapotranspiration was determined in 1 cm dia. wells ($N = 3$ per site) (Dacey and Howes 1984). All holes

created by core removal were immediately filled with sediment cores from an adjacent area to prevent disturbance of the water table and air entry. However, since the specific yield of sediment porewater is only 1 – 3% of the total water content of the sediments (Dacey and Howes, 1984), and since injected $^{15}\text{NH}_4^+$ rapidly exchanges with “bound” porewater and sorbed NH_4^+ pools (White and Howes, 1994a), significant advection of the tracer due to disturbance of the water table is unlikely.

Method validation: The concentration and injection method of the ^{15}N tracer were chosen to minimize physical and biogeochemical disturbance of the sediment system. $^{15}\text{NH}_4^+$ solution (0.82 mL cm^{-1}) was injected into the sediments, adding < 3% to the water content of a 6.5 cm dia. sediment core. The solution contained $4.1 - 5.4 \mu\text{mol } ^{15}\text{NH}_4^+ \text{ cm}^{-1}$, or about 0.1% of the total sediment N mass, sufficient to bring the ^{15}N content of the recovered sediment from 0.36 atoms % to ~ 0.46 at. %. Since the KCl-extractable NH_4^+ content of the sediments ranged from $0.06 - 0.23 \mu\text{mol N cm}^{-3}$ in control sediments to $0.16 - 1.8 \mu\text{mol N cm}^{-3}$ in fertilized sediments, it was necessary to increase the KCl-extractable NH_4^+ pool by an average of $106 \pm 22\%$ in control and $36 \pm 16\%$ in fertilized sediments in order to significantly affect the ^{15}N ratio of the total sediment N pool.

Time 0 recovery of the tracer in 6.5 cm dia. cores harvested immediately after injection was $95.5 \pm 3.9\%$ in unfertilized and $95.6 \pm 1.3\%$ in fertilized sediments (Table 4.2). Since the injection was started at 10 cm depth, some of the tracer was recovered at the top of the lower 10 – 15 cm depth layer. The pattern of tracer recovery was

Table 4.2 T₀ recovery (%) of injected ¹⁵N tracer in 6.5 cm dia. sediment cores in control and XF fertilized saltmarsh plots. Standard errors in parentheses.

%	Control ^a		XF fertilized ^b	
0-5	35.4	(4.1)	39.5	(3.1)
5-10	42.0	(4.0)	51.5	(3.1)
10-15	18.5	(2.0)	5.8	(0.8)
Subtotal	95.5	(3.9)	95.6	(1.3)
Outer ^c	8.6	(3.8)	4.7	(1.3)
Total	104.1		100.3	

^a N = 12

^b 15.5 mol N m⁻² yr⁻¹. N = 10

^c 10 cm dia. outer core taken around 6.5 cm dia. inner core. N = 6.

consistent within sediment type (control or fertilized), with $18.5 \pm 5.5\%$ recovered in the 10 – 15 cm depth interval in control sediments, and $5.8 \pm 1.2\%$ recovered at that interval in fertilized sediments. The T_0 recovery of tracer indicates that most of the injected tracer is recovered within a 3.25 cm radius of the injection point and that no appreciable loss of tracer due to denitrification or material loss takes place during sediment core sampling and processing. This was confirmed by sampling a 10 cm dia. core with a 6.5 cm dia. inner core on 3 sampling dates. At T_0 , an average of $8.6 \pm 3.8\%$ and $4.7 \pm 1.3\%$ of the label was recovered outside of the 6.5 cm dia. sample core in control and fertilized sediments respectively. At the end of the timecourse, another such set of 10 cm dia. cores were taken, and the total amount of tracer which migrated out of the 6.5 cm dia. sampling area was determined by extrapolation using the experimentally-determined denitrification rate. Tracer migration averaged $3.9 \pm 2.0\% \text{ d}^{-1}$ ($N = 6$) in control sediments, and $2.3 \pm 1.6\% \text{ d}^{-1}$ ($N = 4$) in fertilized sediments over the 1 – 2 d timecourse of these experiments.

Another possible route for tracer loss is exchange across the sediment-water interface during tidal inundation. Earlier work showed that losses and vertical distribution of the tracer did not differ between field injections and laboratory lysimeters where tidal losses could not occur (White and Howes, 1994a). In order to further examine this possibility, tracer loss during periods of tidal inundation was compared with the loss during low tide exposure of the marsh sediments. Losses during inundation were only $0.6\% \text{ d}^{-1}$ higher than losses during exposure, and the difference was not significant (paired t-test, 1 tailed, $N = 7$, $p = 0.50$).

Hydrologically-Controlled Lysimeters

In the salt marsh, water table excursions result from evapotranspiration during periods of tidal exposure of the vegetated marsh sediments. In this experiment, water tables were allowed to drop to 5 predetermined levels, before distilled water was added to return the water table to the surface. Sediment cores (20.3 cm dia.) were collected, tightly fitted into lysimeters with side arms to monitor water-table level (White and Howes, 1994a), and maintained in a greenhouse. Five cores were randomly assigned to each of 5 hydrological treatments (0, 5, 10, 15, and 20 cm). These cycles of water table excursions were repeated throughout the experiment. *S. alterniflora* leaves were periodically rinsed with distilled water (and the water returned to the sediment) to remove accumulated salts. Sediments were collected in May, and held in the greenhouse under water table treatments for 55 days before addition of $^{15}\text{NH}_4^+$. On ten days during days 56 to 66, $^{15}\text{NH}_4^+$ ($5.7 \mu\text{mol cm}^{-1}$) was line-injected into the top 15 cm of sediment as in the field studies. Injections were made at three equally-spaced points within the lysimeter. On the following day, the injection sites were shifted by 60° so that the label was distributed evenly throughout the sediment. On day 67, the aboveground biomass was harvested and prepared for ^{15}N determination (see below). Porewater samples for S^{-2} analysis were withdrawn at 5 cm intervals using sippers, and fixed immediately. Each lysimeter was then sectioned at 5 cm intervals, and placed in a -20°C freezer. Any porewater or sediment that remained after core processing was retained for ^{15}N determination. The sediments were then prepared and assayed as in the field ^{15}N studies.

Sample preparation

For all of the ^{15}N experiments, frozen core sections were broken into $<15\text{ cm}^3$ pieces, and placed in plastic cups. The pieces were covered with $0.2\text{ N H}_2\text{SO}_4$ and extracted at $4\text{ }^\circ\text{C}$ for 24 hours, lowering the pH of the thawed pieces to <2 . The acid solution prevented volatilization of $^{15}\text{NH}_4^+$ during drying, and inhibited biological activity during sample processing. After acidification, the cups were placed in a convection oven at $60\text{ }^\circ\text{C}$ and dried to constant weight ($\sim 48\text{ h}$). Aboveground biomass samples were dried ($60\text{ }^\circ\text{C}$) and weighed. Acidified sediment and aboveground biomass was ground in a Cyclotec mill to $<0.5\text{ mm}$, and subsampled for total N and ^{15}N content determination on a mass spectrometer (Stable Isotope Facility, University of California, Davis). Subsamples of sediments were assayed for KCl-extractable NH_4^+ (see below).

Calculations

All sediment core sections were weighed before and after drying to determine porosity and dry density. The total mass of ^{15}N recovered in the samples was determined from the total N content and the abundance of ^{15}N . The natural abundance of ^{15}N , determined from parallel unlabelled cores, was subtracted in order to determine the amount of recovered tracer ^{15}N . Uptake of tracer into aboveground biomass averaged 2.5%. For purposes of calculating the denitrification tracer loss, this translocated ^{15}N was assigned to each of three sediment depth horizons (0 – 5 cm, 5 – 10 cm, 10 – 15 cm) according to the relative abundance of live biomass (80, 15, and 5%, decreasing with depth), calculated from the data of White and Howes (1994a). Corrections were also made for the migration of tracer outside of the 6.5 cm dia. sampling area (see above). As

$^{15}\text{NH}_4^+$ is removed from the total NH_4^+ pool, the rate of tracer loss would be expected to decline, since over time, the tracer makes up a decreasing proportion of the total NH_4^+ pool. For this reason, on theoretical grounds, tracer loss should follow an exponential decay curve:

$$N_t = N_0 e^{(-kt)} \quad (1)$$

where N_t is the amount of tracer remaining after time t , N_0 is the initial amount, and k is the rate constant. The linear transform of this equation:

$$N_t = -kt + \ln(N_0) \quad (2)$$

allows for a least squares fit to the data. The initial rate of tracer loss (R_0) can then be determined by taking the first derivative of (1) and solving for $t = 0$.

$$R_0 = -k N_0 \quad (3)$$

However, in practice, a linear model was sometimes found to be a better fit to the initial 24 hr of data. Accordingly, the best fit model was used. Tracer loss ($\% \text{ d}^{-1}$) was then multiplied by the KCl-extractable NH_4^+ pool (in unamended sediments) to arrive at the total coupled nitrification-denitrification rate.

Nitrogen Retention in Fertilized Marsh Plots

Just prior to the beginning of the yearly fertilization, two 30 cm long cores (6.5 cm dia.) were removed with a piston corer from pairs of experimental plots (control, and 3 levels of fertilization). The cores were sectioned (2 cm down to 10 cm depth, 5 cm thereafter), dried (60°C) to constant weight, and a subsample ground and analyzed for

particulate N (see *Analytical*, below). N retention was determined by subtracting the N content of control sediments from fertilized sediments.

Analytical

Particulate carbon and N were determined on a Perkin-Elmer 2400 elemental analyzer. Salinity was measured using a calibrated YSI conductivity meter. KCl-extractable NH_4^+ was determined by extraction with 2N KCl (adjusted to $\text{pH} < 2$) for 24 hr, followed by sterile filtration and analysis of NH_4^+ by a colorimetric indophenol method (Scheiner, 1976). Porewater S^{2-} was analyzed colorimetrically (Cline 1969).

Results

In Situ $^{15}\text{NH}_4^+$ Tracer Studies

Short-term timecourses of $^{15}\text{NH}_4^+$ tracer yielded a temporal pattern consistent with coupled nitrification-denitrification losses, and were used to calculate *in situ* denitrification rates (Figure 4.1, Table 4.3). Incorporation of $^{15}\text{NH}_4^+$ tracer into plant biomass eventually removed all the ^{15}N from the NH_4^+ pool, preventing further short-term loss through nitrification-denitrification. Although tracer was injected (~6 – 19% of total, Table 4.2) into the bottom (10 – 15 cm) sediment layer, mean tracer loss at this depth was not significantly different from 0 (control sediments mean = $-1.9 \pm 2.0 \text{ \% d}^{-1}$, z test, $p = 0.16$, fertilized sediments mean = $4.6 \pm 9.8 \text{ \% d}^{-1}$, z test, $p = 0.08$).

Partitioning of the label between the upper two depth layers was sometimes highly variable (Figure 4.1a); however, when recoveries in the two layers were pooled, a good

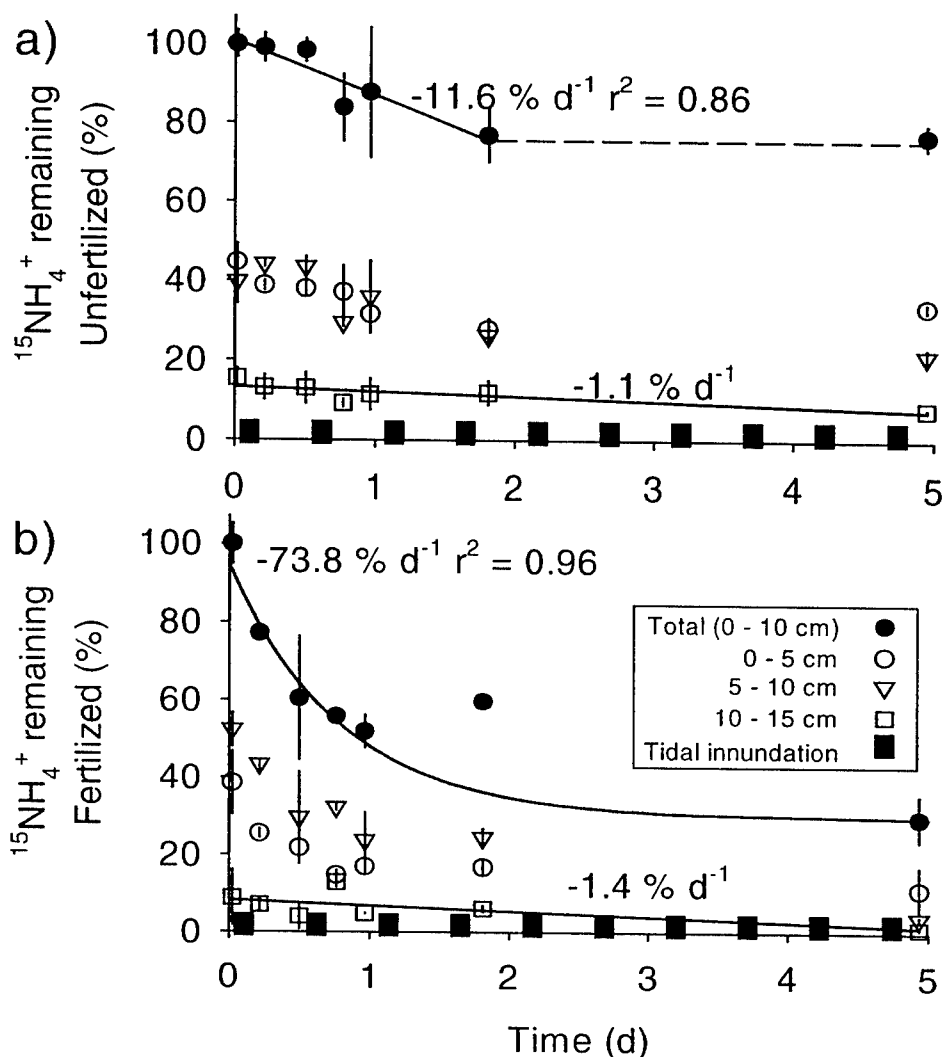


Figure 4.1 Short-term $^{15}\text{NH}_4^+$ tracer recovery from undisturbed vegetated salt marsh sediments (7/10/99) **a)** Unfertilized control marsh. **b)** Fertilized marsh plot receiving $15.5 \text{ mol N m}^{-2} \text{ yr}^{-1}$ as organic N. Recovery for 3 sediment layers (open symbols) calculated as % of total injected tracer. Partitioning of recovered label between the top two layers (open circles, 0 --5 and open triangles, 5 -- 10 cm) was variable, and combining the two layers gave the best fit (closed circles; recovery reported as % of tracer injected into top two layers, includes corrections for translocation and migration of label out of the sampling area [see Methods]). Tracer loss by coupled nitrification-denitrification was modeled using either a linear or an exponential fit to calculate tracer loss at time 0 (slope and coefficient of determination shown). Short-term loss of tracer ceases when all tracer has either been denitrified or incorporated into biomass. Tidal innundations (duration 3 - 4 hr) are indicated by black blocks on x axis. Error bars are standard errors ($N = 2$).

Table 4.3 Loss and retention of $^{15}\text{NH}_4^+$ tracer from unfertilized and XF fertilized ($15.5 \text{ mol N m}^{-2} \text{ yr}^{-1}$) vegetated salt marsh plots. Standard errors in parentheses.

Date	Denitrification ^a mmol N m ⁻² d ⁻¹	N	r ²	—Tracer incorporation into biomass ^b —	
				Time required hr ^c	% ^d
Unfertilized					
8/19/97	5.4 (1.5)	7	0.95 ^h	25	67
10/2/97	2.2 (3.4)	3	0.54 ^h	— ^e	— ^e
4/13/98	2.9	2		— ^e	— ^e
6/9/99	1.8 (0.6)	3	0.98 ⁱ	27	69
9/1/99	12.2 (0.5)	3	1.00 ⁱ	22	55
12/13/99	1.1 (0.3)	4	0.97 ^h	— ^f	— ^f
7/10/00	0.7 (0.2)	6	0.86 ^h	37	71
Mean				28 (3)	66 (3)
Annual ^g	0.73 (0.29) mol N m ⁻² yr ⁻¹				
Fertilized (XF)					
10/2/97	11.1 (8.5)	3	1.00 ^h	— ^e	— ^e
6/9/99	30 (4.2)	4	0.96 ⁱ	31	21
9/1/99	136 (115)	4	0.96 ^h	19	33
12/13/99	20.2 (7.9)	3	1.00 ⁱ	71	13
7/10/00	112 (41)	5	0.96 ⁱ	28	30
Mean				26 ^j (4)	28 (4) ^j
Annual ^g	12.6 (5.7) mol N m ⁻² yr ⁻¹				

^a Denitrification determined separately for each 5 cm depth interval, then summed over 15 cm (see Table 4.3).

^b Aboveground + belowground biomass.

^c Time required for complete tracer uptake. Determined by extrapolation when necessary.

^d % of injected tracer recovered in sediments + aboveground biomass after complete uptake.

^e Not determinable after 1 day.

^f Not determinable after 4 days.

^g Annually integrated rate. Assumptions: no denitrification from 12/15 – 2/28, when sediments are typically frozen; denitrification on 9/15 equal to that measured on 10/2 since regional temperatures fall rapidly in mid-September.

^h Linear model

ⁱ Exponential model

^j For comparison to control, does not include December date.

fit was obtained, either with a linear or exponential model. Since mean rates of tracer loss ($\% \text{ d}^{-1}$) were the same for both layers, ^{15}N recovery over the top 10 cm was summed for calculation of the denitrification rate. Mid-summer measurements were made in each year 1997-2000, with the seasonal data collected over two years. I have constructed a “composite” year of denitrification measurements, since long term monitoring of ecological and biogeochemical rates in this salt marsh has shown that measurements made in any single year can be applied to other years (Teal and Howes, 1996). In unfertilized sediments, total tracer loss rates ranged from 9.7 to 28.8 $\% \text{ d}^{-1}$, with the exception of one early September date, when the rate was 150 $\% \text{ d}^{-1}$ (Figure 4.2a). In fertilized sediments, tracer loss rates ranged between 69 and 79 $\% \text{ d}^{-1}$, with the exception of June, when the rate was 131 $\% \text{ d}^{-1}$.

In unfertilized natural sediments, KCl-extractable NH_4^+ exhibited no clear seasonality, with concentrations ranging from 0.064 to 0.23 $\mu\text{mol cm}^{-3}$ throughout the year. In contrast, in the fertilized sediments, KCl-extractable NH_4^+ concentrations were 5 – 10 times the control concentration (0.16 – 1.8 $\mu\text{mol cm}^{-3}$), with a summer maximum (Figure 4.2b). Denitrification rates in both fertilized and unfertilized sites showed clear seasonality. Control *Spartina* sites had low rates (0.7 – 2.9 $\text{mmol m}^{-2} \text{ d}^{-1}$) from October to July with a peak in late summer up to 12.2 $\text{mmol m}^{-2} \text{ d}^{-1}$ (Figure 4.2c, Table 4.3). Early summer and fall rates in fertilized sediments ranged from 11 – 30 $\text{mmol m}^{-2} \text{ d}^{-1}$, with mid and late summer rates ranging from 112 – 136 $\text{mmol m}^{-2} \text{ d}^{-1}$. These composite seasonal measurements yield an approximate annually-integrated denitrification rate in control sediments of 0.73 $\text{mol N m}^{-2} \text{ yr}^{-1}$, primarily a result of the high early September

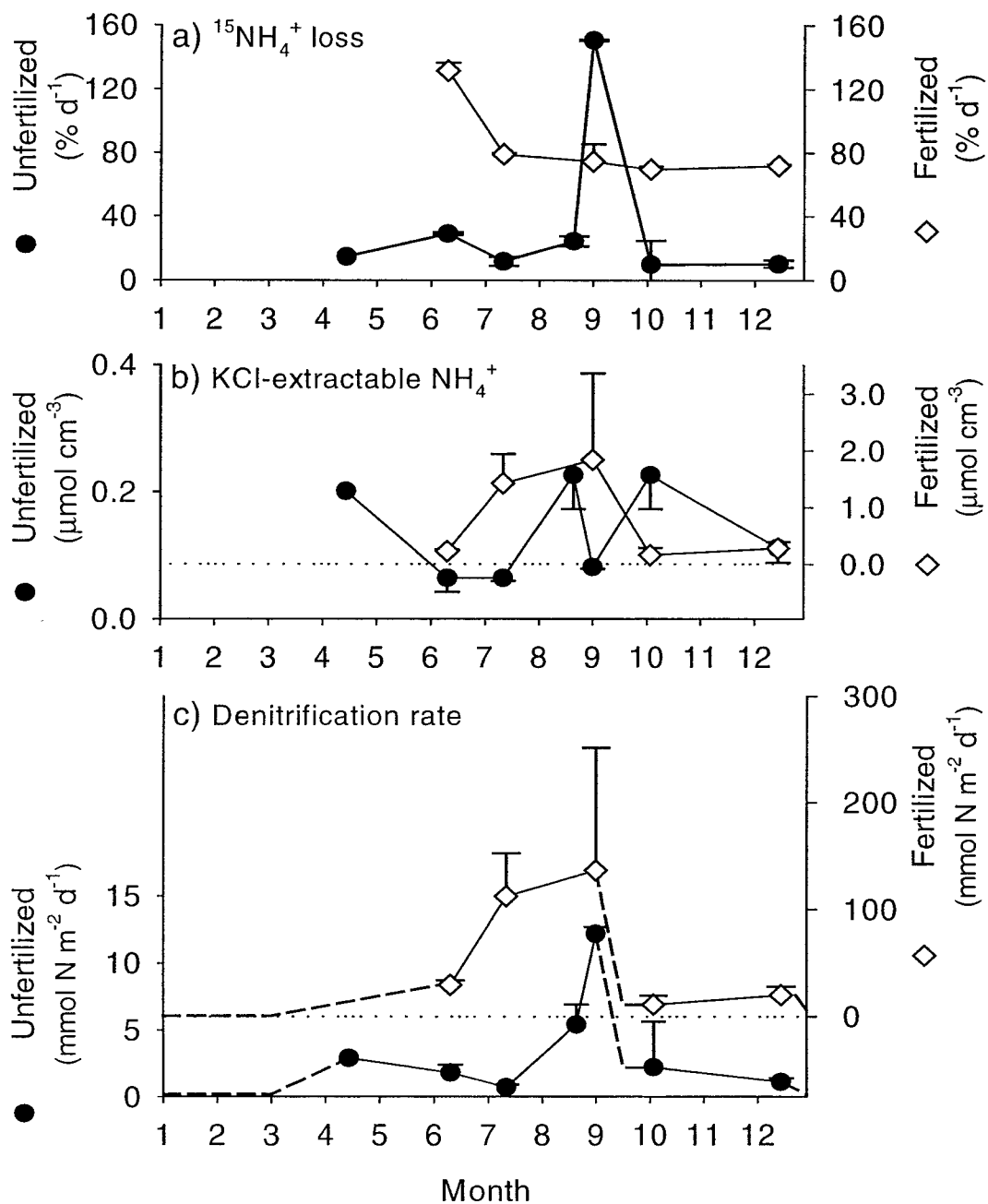


Figure 4.2 Seasonal denitrification rates in salt marsh sediments (0 – 10 cm). **a)** Initial loss rate of $^{15}\text{NH}_4^+$ tracer in unfertilized and XF fertilized marsh plots during growing season. **b)** Concentration of KCl-extractable NH_4^+ in sediments of unfertilized and XF fertilized marsh plots. **c)** Denitrification rate calculated by multiplying the $^{15}\text{NH}_4^+$ loss (% d⁻¹) by the KCl-extractable NH_4^+ pool size (mmol N m^{-2}). Error bars are standard errors (N = 2 for tracer loss and N = 2 – 3 for KCl-extractable NH_4^+).

rate, and $12.6 \text{ mol N m}^{-2} \text{ yr}^{-1}$ in the fertilized grass stands (receiving $15.5 \text{ mol N m}^{-2} \text{ yr}^{-1}$) (see Table 4.3 for calculation of annual rate).

The time required for complete tracer uptake during the growing season averaged slightly over 24 hr in both sediments (Table 4.3). Only incubations of sufficient duration to "fix" the $^{15}\text{NH}_4^+$ (until recovery plateaued - Figure 4.1)) could be used in this analysis (April and October incubations were excluded). Total short-term retention of tracer in biomass (aboveground + belowground) was 66% in unfertilized plots during the growing season, with the balance, 34%, being denitrified (Table 4.3). However, in the fertilized plots, denitrification losses accounted for 72% of the available N, while only 28% was retained in biomass. In unfertilized grass stands, summer short-term biomass N retention was predominately (92%) in the below ground pool (Figures 4.3a and 4.3b). However, in fertilized stands, translocation of N into aboveground biomass in late summer was high, accounting for 34% of the total biomass retention. Short term belowground retention of $^{15}\text{NH}_4^+$ during the growing season in fertilized plots averaged 21%, significantly lower than the 61% retained in unfertilized plots (Figure 4.3a). There was no belowground biomass ^{15}N uptake in unfertilized marsh plots during the winter, but 17% of the tracer was retained in fertilized sediments. Translocation of ^{15}N into aboveground biomass was higher in fertilized sediments than in unfertilized, but showed the same seasonality, with low translocation early in the summer peaking in July, and declining to 0 by December (Figure 4.3b).

In the ^{15}N tracer injections in the field plots, the size of the KCl-extractable NH_4^+ pool was increased by 106% in unfertilized plots and by 36% in the fertilized plots by the

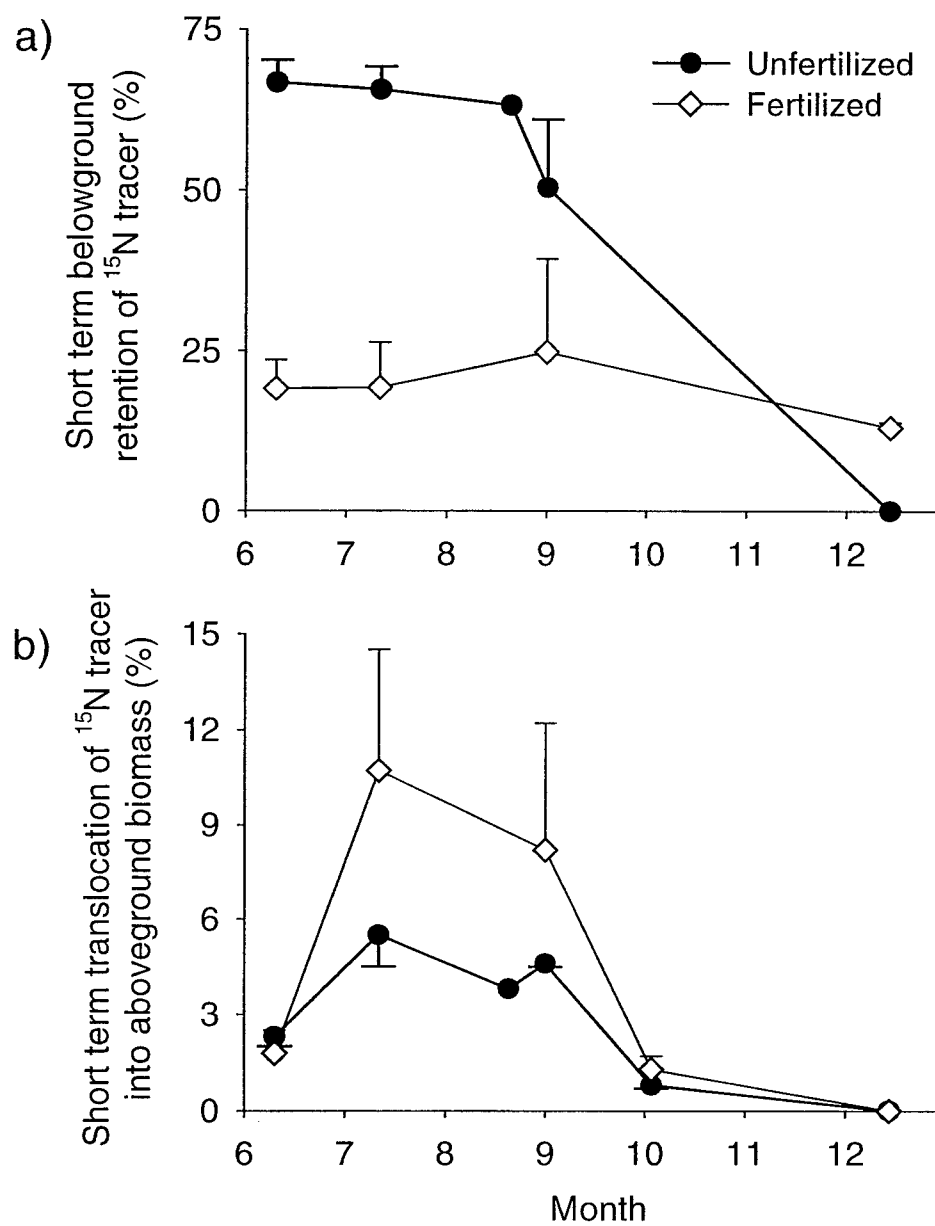


Figure 4.3 Short term retention of $^{15}\text{NH}_4^+$ tracer in biomass. **a)** Belowground biomass. **b)** Aboveground biomass.

addition of the $^{15}\text{NH}_4^+$ tracer. This was necessary in order to have a sufficiently large isotope signal against the large N background of the sediments. While this short-term increase in N availability likely stimulated denitrification rates, neither the calculated rates nor the partitioning of tracer measured in this study were affected by the increase in the size of the NH_4^+ pool. The results of measurements in the fertilized plots show that both plant N uptake and denitrification increase with increased N availability. However, as shown above, the proportion of added N that is denitrified increases from 34% to 72% as N loading increases from control levels to XF fertilized levels. In the unfertilized sediments, the daily loading rate of remineralized N was $6 \text{ mmol m}^{-2} \text{ d}^{-1}$ (calculated from the annual remineralization rate of White and Howes [1994a] adjusted for the growing season based on the annual respiration curve of Howes *et al.* [1984]). The annual fertilizer N loading to the XF plots was $15.5 \text{ mol N m}^{-2} \text{ yr}^{-1}$. This represents a daily N load during the 100 d period of N fertilizer application of $155 \text{ mmol m}^{-2} \text{ d}^{-1}$, for a total of $161 \text{ mmol m}^{-2} \text{ d}^{-1}$ (fertilizer + remineralization N loading). This is a conservative assumption, since sediment N remineralization in the fertilized plots is likely higher than in the unfertilized plots). Therefore the increase in the partitioning of available N into denitrification can be expressed as 0.25% per $\text{mmol m}^{-2} \text{ d}^{-1}$ increase in N loading. Although the $^{15}\text{NH}_4^+$ injection increased the KCl-extractable NH_4^+ pool by 36%, and may have temporarily increased denitrification rates by a similar amount, this addition of tracer represents an N load to the sediments of only $14 \text{ mmol m}^{-2} \text{ d}^{-1}$, or a < 4% increase in the partitioning of N to denitrification. Similarly, although the tracer injection increased the KCl-extractable NH_4^+ pool in the unfertilized sediments by an average of

106%, the error introduced into measurements of N partitioning was, as for the fertilized plots, < 4%.

In the short-term, increases in N availability result in increases in plant N uptake and denitrification. As shown above, the partitioning of N between plants and nitrifiers is not significantly altered by the tracer injection levels used in this study. Therefore, under the conservative assumption that denitrification increases proportionally to the increase in the KCl-extractable NH_4^+ pool caused by the tracer addition, the proportional loss of the tracer ($\% \text{ d}^{-1}$) will be the same as the loss in an unlabeled sediment. The proportional tracer loss ($\% \text{ d}^{-1}$) also remains constant despite probable heterogeneity in the distribution of the injected $^{15}\text{NH}_4^+$ tracer because the same proportion of the label is lost regardless of the ratio of labeled $^{15}\text{NH}_4^+$ to background $^{15}\text{NH}_4^+$. Since the proportional loss of tracer is a conservative property, the correct denitrification rate can be calculated simply by multiplying the proportion of the tracer lost to denitrification by the original size of the KCl-extractable NH_4^+ pool, the approach used in this study.

Hydrologically-Controlled Lysimeters

In hydrologically-controlled laboratory lysimeters, manipulation of water table excursion levels affected sediment oxidation state which in turn affected aboveground biomass growth rates (Figure 4.4). Sulfide concentrations in the top 5 cm of sediment were highest in the continually flooded lysimeters (0 cm), but there was no clear effect of the other treatments (5 – 20 cm) (Figure 4.4a). Although only the flooded hydrological treatment had a clear effect on porewater S^{-2} in the upper 5 cm of sediment, S^{-2} concentrations deeper in the sediment were affected by water table excursions greater

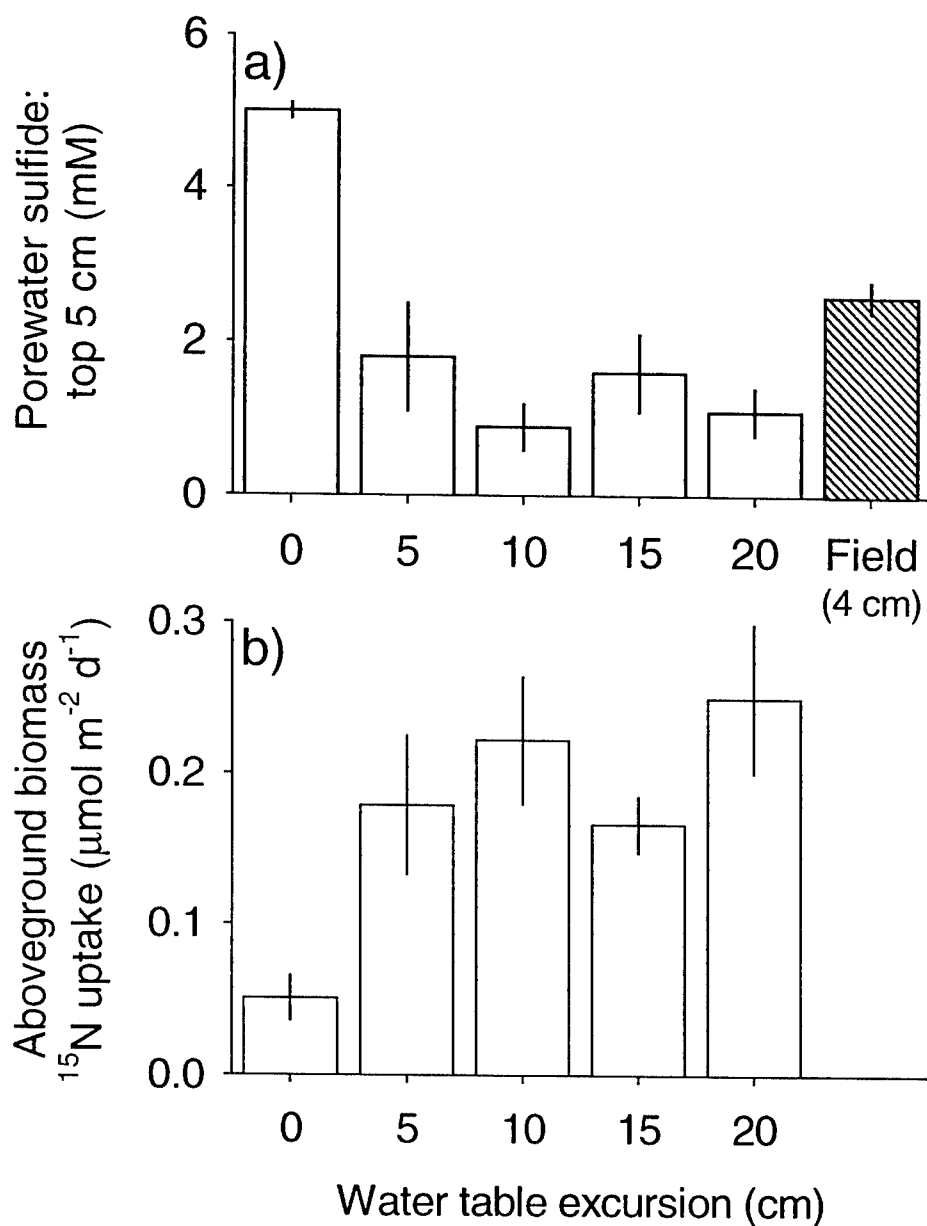


Figure 4.4 Sulfide and biomass in hydrologically-controlled laboratory lysimeters and reference site (measurements made at same time lysimeter cores were harvested). **a)** Concentration of porewater S^{2-} (top 5 cm). **b)** ^{15}N incorporation into aboveground biomass during 12 day course of $^{15}NH_4^+$ injection. Error bars are standard errors ($N = 5$ for lysimeters, $N = 3$ for field).

than 5 cm (data not shown). Field S^{-2} concentrations in sediments with a water table excursion of ~4 cm fell between the 5 cm and the flooded lysimeter treatments. Conversely, ^{15}N uptake into aboveground biomass was lowest in the flooded lysimeters, but rose to its highest level in lysimeters with 20 cm water table excursions (Figure 4.4b). Although a hydrological treatment effect on S^{-2} concentration was only found in the flooded treatment, peak aboveground biomass in individual lysimeters was found to be inversely related to the porewater S^{-2} concentration in the top 5 cm of the sediment, where 80% of the live root matter is found (White and Howes 1994a), similar to the relationship found in the field (Figure 4.5). ^{15}N uptake into aboveground biomass followed the same trend, with uptake decreasing at higher S^{-2} concentrations (Figure 4.5 inset).

The 0 – 15 cm depth distribution of KCl-extractable NH_4^+ shows that > 50% of the NH_4^+ was found in the top 5 cm of the sediment (Figure 4.6a). Most of the effect of flooding on the NH_4^+ pools was at this depth. Field concentrations were within the range measured for 5 – 20 cm water table excursions, though concentrations were lower in the upper layer of field sediments relative to the lysimeters. Aboveground biomass accumulation over the 67 days of hydrological treatment (Figure 4.6b) was lowest in the flooded treatment, with similar levels found among the other treatments. Aboveground biomass collected at the field site was slightly lower than that of the 5 cm water table excursion treatment. While growth over the 67 days of the experiment in the flooded treatment was ~50% of that in the 5 – 20 cm treatments, the difference in ^{15}N uptake during the final 12 days of the experiment was only 25% (Figure 4.4b). This difference

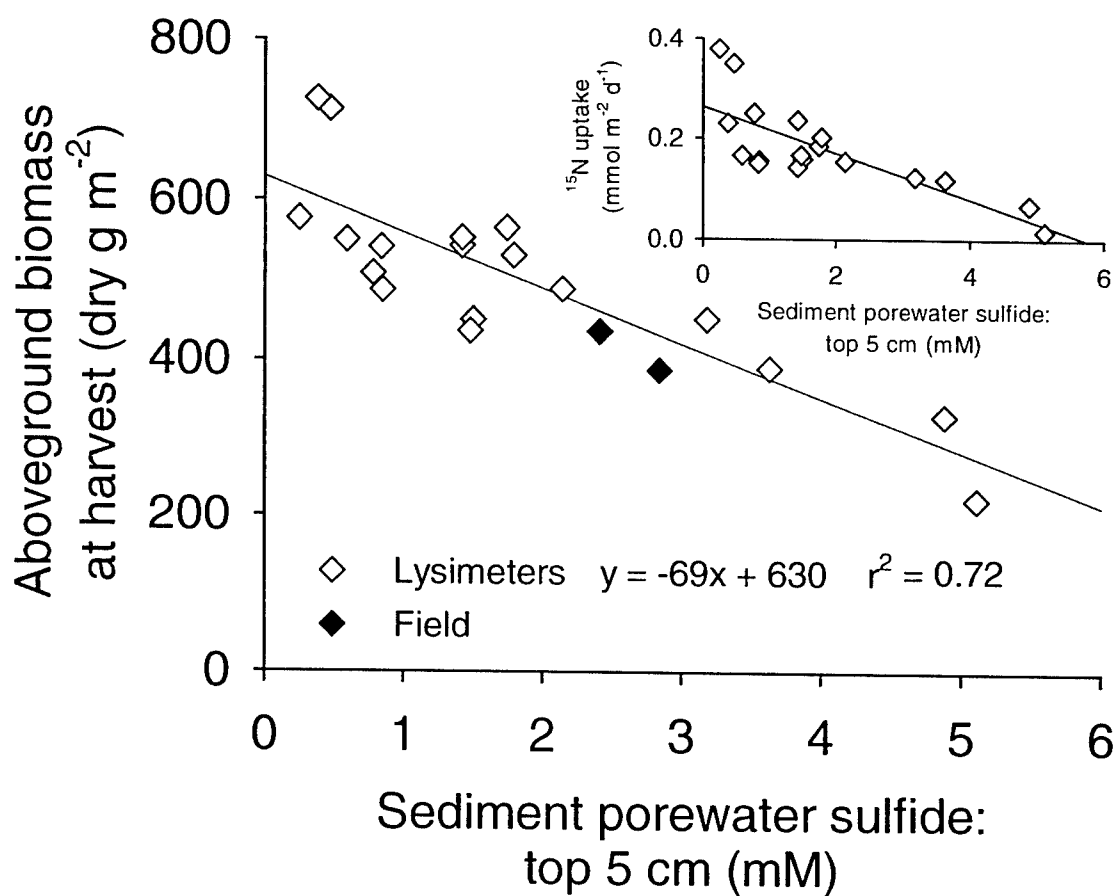


Figure 4.5 Relationship of sediment porewater S⁻² to aboveground biomass in hydrologically-controlled lysimeters and reference field site. Inset shows S⁻² relationship to ¹⁵N incorporation into aboveground biomass.

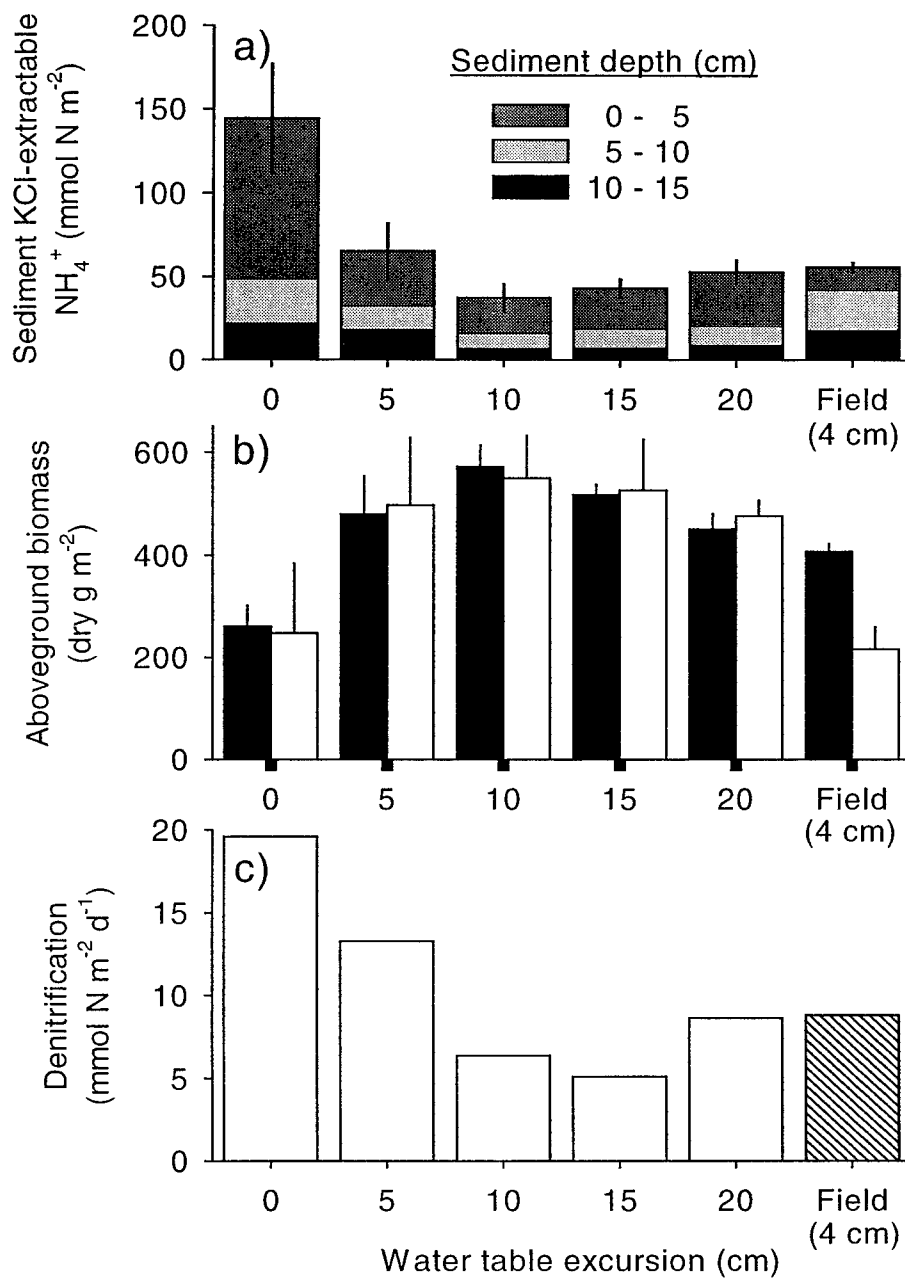


Figure 4.6 Sediment N availability and biomass N uptake in hydrologically-controlled lysimeters. **a)** Depth-specific concentration of KCl-extractable NH_4^+ . **b)** Aboveground dry biomass growth and total N translocation into aboveground biomass during 67 days of treatment. Error bars are standard errors ($N = 5$ for lysimeters, $N = 3$ for field). **c)** Denitrification rate (see text for calculations).

likely resulted from both a temporal lag from the onset of flooding to the buildup of S^{-2} and a late-season slowing of growth in the flooded lysimeters.

In lysimeters with 5 – 20 cm water table excursions, KCl – extractable NH_4^+ pools and S^{-2} levels were similar to those found in the field (Figures 4.4a and 4.6a), where > 90% of the injected tracer was denitrified or taken up into biomass by 1 day (Table 4.3). In the lysimeters, tracer was injected on ten consecutive days, and the sediments processed 24 hours after the last injection. Thus a maximum of only 1% of the total ^{15}N tracer injected could have remained in the NH_4^+ pool of the 5 – 20 cm lysimeters, and so all of the tracer recovered in the sediments must have been incorporated into biomass. The denitrification rate in these lysimeters can then be calculated in the same way as in the field injections, assuming that an equal proportion of the injected tracer was lost on each of the ten days (Figure 4.6c). The lysimeter rates calculated by this method, averaged $8.6 \text{ mmol N m}^{-2} \text{ d}^{-1}$, compared with $8.8 \text{ mmol N m}^{-2} \text{ d}^{-1}$ in the field (average of two field measurements made during the same season [8/19 and 9/1]. Table 4.3).

However, the calculation method used for the 5 – 20 cm lysimeters cannot be used to calculate denitrification rates in the flooded lysimeters. In the flooded lysimeters, NH_4^+ accumulates because denitrification and plant uptake are not sufficient to balance N remineralization (Figure 4.6a). Therefore, during the 10 days of injection, $^{15}NH_4^+$ also likely accumulated, making the total recoverable ^{15}N a composite of the decay curves of 10 injections. The total proportion of tracer lost over 10 days is then an overestimate of the amount lost on any 1 day. The difference in denitrification rates between the 5 cm

excursion treatment and the flooded treatment can, however be calculated by an N mass balance. N uptake into aboveground biomass in the flooded lysimeters was 250 mmol m⁻² less than that of the 5 cm treatment (Figure 4.6b). If we make the very conservative assumption that the ratio of belowground to aboveground N uptake is 1:1 (the ratio of peak biomass in the field is 2.4 [Valiela *et al.*, 1985; White and Howes, 1994a]), and that mineralization rates are the same in all treatments (likely since sufficient SO₄⁻² to drive sulfate reduction was present [porewater salinity = ~20 ppt]), then a total of 500 mmol m⁻² extra N was available in the flooded lysimeters. However, only 79 mmol m⁻² extra KCl-extractable NH₄⁺ was present in the flooded lysimeters (Figure 4.6a). Therefore, the 421 mmol m⁻² unaccounted for must have been denitrified. Distributed over the 67 days of the experiment, this conservative estimate represents 6.3 mmol m⁻² d⁻¹ of denitrification in excess of the 5 cm excursion, for a total of 19.6 mmol m⁻² d⁻¹ (Figure 4.6c).

Another approach to calculating the denitrification rate of the flooded lysimeters is to estimate the proportion of tracer recovered in the sediments that was incorporated into biomass. If we assume that the ratio of belowground N uptake to aboveground N uptake was the same across all treatments, then based on the measured N uptake into aboveground biomass, the proportion of the ¹⁵N recovered in the sediments of the flooded lysimeters that was incorporated into belowground biomass was 25%. The short term fate of the ¹⁵NH₄⁺ tracer can then be compared across all treatments in a mass balance. The fate of added ¹⁵NH₄⁺ was the same among the treatments with 5 – 20 cm water table excursions (Figure 4.7). However, in the flooded treatment of the lysimeters, short-term retention of ¹⁵N in total biomass was only about one half of the retention in the other

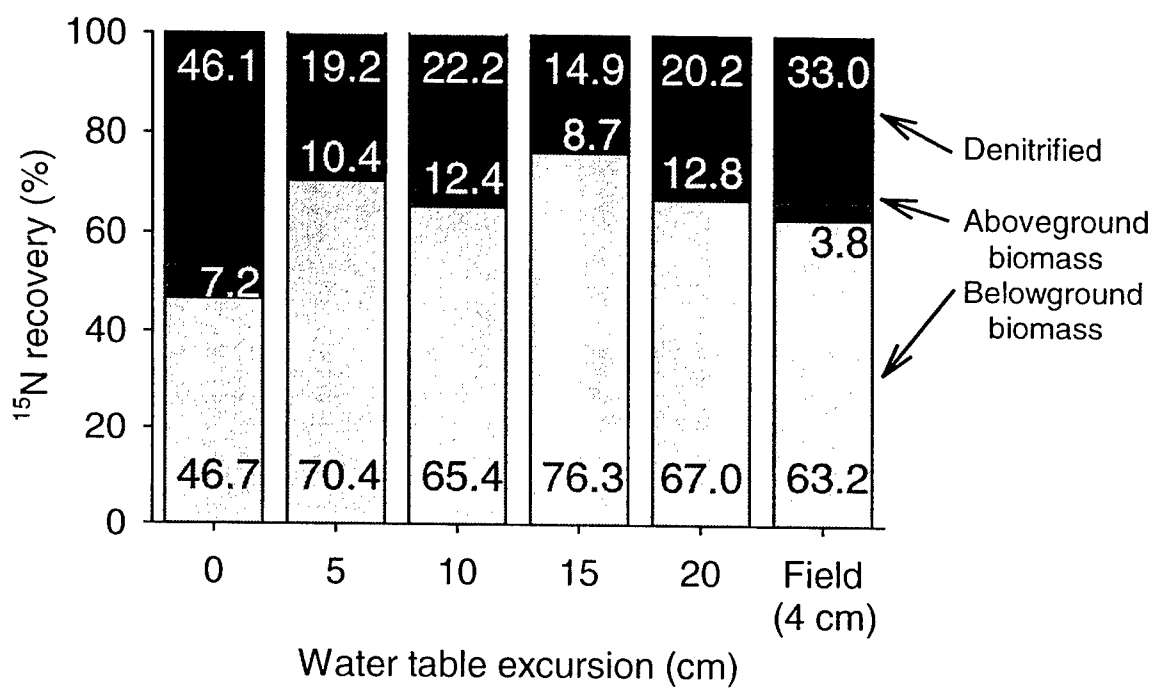


Figure 4.7 Short-term fate of $^{15}\text{NH}_4^+$ for top 15 cm of sediment in hydrologically-controlled lysimeters ($N = 4$). 0 cm excursion belowground pool corrected for unreacted $^{15}\text{NH}_4^+$ pool. Field results from 8/19/97.

treatments (Figure 4.7). Denitrification losses were correspondingly greater, at 2.5 times the losses in the 5 – 20 cm treatments, and the denitrification rate estimated by the ^{15}N mass balance is $21.5 \text{ mmol m}^{-2} \text{ d}^{-1}$, equal to the rate calculated above from the N mass balance. The short term fate of $^{15}\text{NH}_4^+$ added to lysimeters with 5 – 20 cm water table excursions showed a similar pattern to field $^{15}\text{NH}_4^+$ injections. On a corresponding date in mid-August, 67% of the injected tracer was recovered in biomass, while denitrification losses accounted for the remaining 33% (Figure 4.3). Although the proportion of the tracer recovered in the aboveground biomass was lower in the field than in the lysimeters, this aboveground recovery was for a 25 hr experiment, while field experiments showed that although incorporation of the tracer into biomass is complete after 28 hr, ^{15}N translocation continues for 4 – 5 days. Denitrification in the field did account for a greater proportion of the tracer, though since the field site had a water table excursion of only 4 cm, the short-term fate of added tracer would be expected to be intermediate between the 0 and 5 cm treatments. Further support for greater denitrification losses in the flooded treatments comes from the apparent inverse relationship between ^{15}N incorporation into aboveground biomass and tracer loss by denitrification from the top 5 cm (Figure 4.8).

Discussion

Plant uptake was found to dominate short-term ^{15}N retention during the growing season in *S. alterniflora* marsh sediments. In contrast, during the winter, with no plant growth or uptake, denitrification dominated the short-term fate N. Additions of N

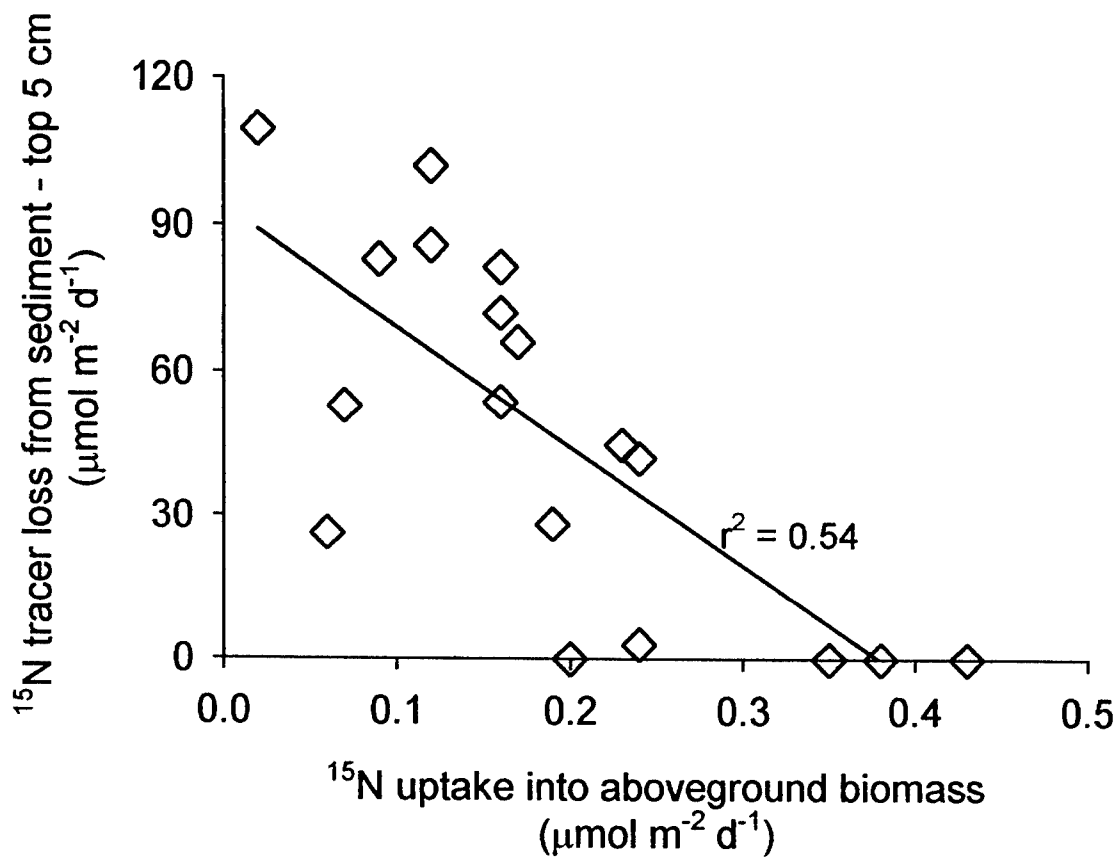


Figure 4.8 Loss of ^{15}N tracer by coupled nitrification-denitrification versus plant ^{15}N uptake in hydrologically-controlled lysimeters. Line is least squares fit to data with equation: $^{15}\text{N loss} = -247 (^{15}\text{N biomass uptake}) + 94$.

fertilizer increased both plant uptake and coupled nitrification-denitrification, but shifted the dominance to denitrification. The pattern of loss and retention of N in lysimeters with water table excursions was similar to that in field injections. However, in lysimeters where plant N uptake was inhibited by flooding, denitrification was stimulated and the competitive balance shifted toward denitrification.

In stands of short *S. alterniflora* during the growing season, plant N uptake consumes 66% of regenerated NH_4^+ , while the remainder, 34% is available for coupled nitrification-denitrification. This partitioning of remineralized N was also found in earlier work in the same marsh (White and Howes, 1994a). While the annual availability of N increased 15 times from control levels to the highest fertilization level, peak aboveground biomass increased by only 4 times (Figure 4.9). The excess N not fixed into plant biomass was then available for coupled nitrification-denitrification, which was 17 times greater annually in fertilized than in unfertilized plots. The differential effect of N loading on plant uptake and denitrification is further supported by the long-term retention of added N in the sediments of fertilized marsh plots. As total N loading increased 6 times from the LF to the XF level of fertilization, plant biomass increased by just over 2 fold, while denitrification losses increased by nearly 10 fold (Figure 4.9). The increased nitrification in fertilized plots was a result of the increased availability of substrate and the increased oxidation of the sediments via evapotranspiration stimulated by plant growth (Table 4.1; Howes *et al.*, 1986).

From June to August, during the seasonal fertilization of the experimental plots, KCl-extractable NH_4^+ in the XF fertilized sediments was 13 times as high as in the

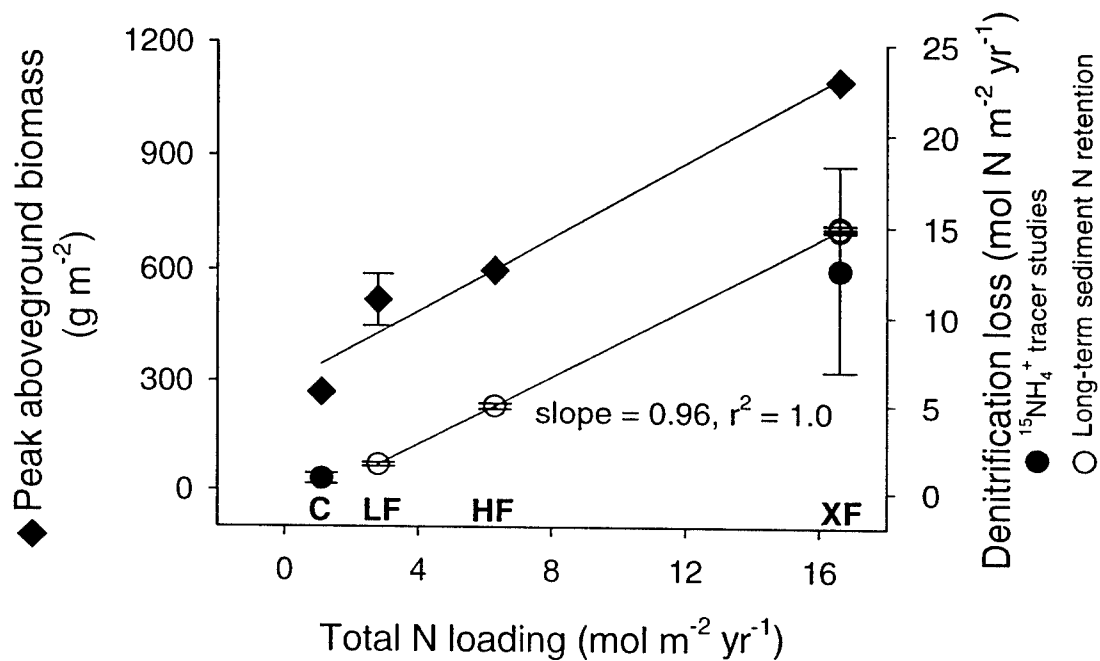


Figure 4.9 a) Peak aboveground biomass (Howes *et al.*, 1986; Valiela *et al.*, 1976) and denitrification over a range of N loading to the sediment. Total N loading is N remineralization + fertilizer N loading. N remineralization from annualized data of White and Howes, 1994a. Levels of fertilizer N are (LF: 1.7, HF: 5.2, and XF: 15.5 mol N m⁻² d⁻¹). Error bars are standard errors.

unfertilized plots (Figure 4.2b). However, during the remainder of the year, when the plots were not being fertilized, KCl-extractable NH_4^+ in the XF fertilized sediments was only 1.2 times as high as in unfertilized sediment (Figure 4.2b), indicating that between periods of fertilization, the increase in plant uptake and denitrification was sufficient to remove most of the added N fertilizer. In December, when plant N incorporation was low or 0, denitrification was also low in both unfertilized and fertilized plots. Under winter conditions, denitrification dominated the N cycle of the sediments, and only in fertilized sediments was there found a small (17%) partitioning of tracer into belowground biomass (Figure 4.3a).

Similarly, in the hydrologically-controlled lysimeters, the suppression of plant N uptake made enough N available to stimulate coupled nitrification-denitrification by at least 50%, although the stimulation of denitrification was not enough to remove all of the extra N made available by the inhibited plant uptake (Figure 4.6a). Although flooding the sediment reduces sediment oxidation (Figure 4.4a), the diffusion of remineralized NH_4^+ to O_2 -containing zones in the upper sediment was rapid enough to support an increased coupled nitrification-denitrification rate. However, the increase in denitrification rates in the flooded lysimeters was not enough to shift the balance of competition in favor of denitrification; plant N uptake accounted for 54% of the total uptake, with the balance (46%) accounted for by denitrification.

Throughout most of the season (October to July) denitrification rates in unfertilized sediments of the Great Sippewissett Marsh measured by the $^{15}\text{NH}_4^+$ tracer method were $< 3.0 \text{ mmol N m}^{-2} \text{ d}^{-1}$, while the annually integrated rate was $0.73 \text{ mol N m}^{-2}$

yr⁻¹ (Table 4.3), or an average daily rate of 2.0 mmol N m⁻² d⁻¹. The pattern of ¹⁵N retention in sediments observed in this study is similar to that observed by White and Howes (1994a) in the Great Sippewissett Marsh during the initial days of their long-term retention study. In their study, 25% of the tracer was denitrified and 75% incorporated into plant biomass by their first timepoint, 3 days after injection. Further loss of the incorporated label was low, with remineralization controlling its availability for coupled nitrification-denitrification. By averaging the initial loss over 3 days, they derived a denitrification rate of 1.8 mmol N m⁻² d⁻¹ for a date in late May. Both their rate and most of the rates measured in this study are at the upper end of the range cited in the literature (reviewed in White and Howes, 1994a); however, the two late summer measurements in the present study are the highest reported for these sediments (Figure 4.2).

Verification of denitrification rates calculated by the ¹⁵N tracer method can be had from the long-term mass balance N in the fertilized plots. Annual denitrification losses in the fertilized plots can be assessed relative to the known retention of fertilizer N within the sediments. Long-term N retention in the XF plots was 4.4% of the fertilizer N loading of 15.5 mol m⁻² yr⁻¹, or a loss of 14.8 mol m⁻² yr⁻¹, slightly higher than the annual denitrification loss of 12.6 mol m⁻² yr⁻¹ calculated from the ¹⁵NH₄⁺ tracer measurements (Figure 4.9; Table 4.3). High *S. alterniflora* growth rates in fertilized sediments lead to increased evapotranspiration, more rapid water table drops, and subsequent oxidation of the sediment, as demonstrated by porewater S⁻² concentrations (Howes *et al.*, 1986; Table 4.1). These conditions of high NH₄⁺ availability and increased sediment oxidation support the high denitrification rates in the fertilized sediments.

Experimental manipulations with hydrologically-controlled lysimeters support the hypothesis that aboveground biomass growth in *S. alterniflora* is controlled by sediment oxidation state (Mendelssohn *et al.*, 1981; Howes *et al.*, 1986). In zones of short-form *S. alterniflora*, sediment oxidation status is a function of the degree of air entry, which results from evapotranspiration of sediment porewater (Dacey and Howes, 1984). Sediment oxidation state is therefore controlled by both the plant production rate and by the length of time between tidal inundations. The hydrological manipulations of lysimeters imitated this process by varying the length of time between additions of water to the lysimeters, resulting in a variety of sediment oxidation states (Figure 4.4a). Both aboveground biomass at harvest and translocation of ^{15}N to aboveground biomass were inversely and linearly related to S^{-2} concentration in the top 5 cm of the sediment (where 80% of the live roots are located; White and Howes, 1994a) (Figure 4.5). The same relationship between porewater S^{-2} and plant growth was found both in the field and in the laboratory lysimeters. Similarly, plant growth along the creekbanks is stimulated because porewater drainage aerates the sediments, reducing S^{-2} levels (Howes and Goehring, 1994).

By injecting a $^{15}\text{NH}_4^+$ tracer into undisturbed vegetated salt marsh sediments, short term *in situ* coupled nitrification-denitrification rates were obtained in sediments undergoing natural fluctuations in sediment oxidation status as a result of tidal inundation and evapotranspiration. Coupled denitrification in unfertilized salt marsh sediments was controlled by plant N uptake rates. Results showed that during the growing season, biomass uptake out-competed coupled denitrification for NH_4^+ in control sediments,

whereas at high fertilizer N loading, biomass N uptake of N did not increase proportionally to N loading, but with increasing plant-mediated oxidation of the sediment, excess N became available for coupled nitrification-denitrification. In experiments with hydrologically-controlled laboratory lysimeters, suppression of plant N uptake by flooding the sediment made more N available for coupled nitrification-denitrification. Increasing water table excursions aerated the sediments, reducing porewater S^{2-} concentrations and stimulating plant growth, removing N from pools available for coupled denitrification.

CHAPTER 5

Conclusions

The research reported in this dissertation emphasizes the importance of salt marshes in the nitrogen cycle of the coastal environment. The understanding of the nitrogen cycle within salt marshes, their response to increased nitrogen loads, and the ability of denitrification to remove potentially harmful nitrogen have significant practical applications. Increased development along the Atlantic coast of the USA during the past century has dramatically increased the nitrogen loads to coastal waters, leading to eutrophication, with its attendant problems of water column anoxia, fish kills, loss of shell fish habitat, odors, and potential contributions to harmful algal blooms such as red tide. In order to control the harmful effects of excess nitrogen, state and municipal governments are implementing regulations designed to reduce nitrogen effects on sensitive environments. However, because of the expense of lowering nitrogen fluxes from wastewater treatment plants, agriculture and on-site wastewater treatment, careful planning and design, whether of new wastewater treatment facilities or of regulatory frameworks is essential to managing nitrogen economically. An understanding of the role of salt marshes in coastal watersheds and their abilities to remove nitrogen is a valuable tool in regional nitrogen management.

Knowledge of salt marsh nitrogen cycling processes also plays an important role in the development of artificial wetlands for nitrogen removal from contaminated water and wastewater. Denitrification in these artificial systems is an important route of nitrogen loss (Hamersley *et al.*, 2001). The processes controlling denitrification in natural and artificial wetlands are the same, and experiments in naturally or experimentally enriched natural wetlands, such as this study, when combined with studies

of artificially wetlands receiving very high loads of nitrogen, enable the formation of a complete picture of the interactions of high nitrogen loadings with the complex chemical and biological environment of a salt marsh (Hamersley *et al.*, in submission a & b).

The contribution of salt marshes to the denitrification of terrestrial N during its passage into marine environments is a function of the exposure of surface and groundwater flows to salt marsh sediments. This contact takes place primarily within the salt marsh tidal creek bottoms, whereas the vegetated marsh sediments are largely uncoupled from terrestrial N sources. In this regard, salt marsh creek bottoms function in the same manner as the better-studied estuaries. This similarity is supported by the similarity of creek bottom metabolic and denitrification rates to rates reported from estuaries receiving similar N loads (Chapter 3). Likewise, the removal of influent N via denitrification (40 – 50%) in sediments of Mashapaquit Marsh was within the narrow range (40 – 50%) reported from other estuaries (reviewed in: Seitzinger, 1988; Smith, 1999). Along the Atlantic coast of the United States, salt marshes border estuaries, salt ponds, and other areas of surface or ground water influx to the marine environment. The area covered by salt marshes increases from Maine to South Carolina and Georgia, along with their contribution to coastal N cycling. However, the predominance of salt marsh environments along sites of freshwater efflux into marine environments likely indicates an important role in the glacial tills of the north Atlantic states. Salt marshes and estuaries both play an important role in controlling the flux of N from terrestrial to marine environments, and therefore the productivity of coastal embayments.

The creek bottom sediments of Mashapaquit Marsh, which received 32 mmol of terrestrial N m⁻² d⁻¹, are at the upper end of the N loading range reported for estuarine sediments. In the nearby Nauset Marsh Estuary, which receives only 2.1 mmol N m⁻² d⁻¹ (Nowicki, 1999), and denitrification rates in creek bottom and estuarine sediments, averaged about 20 times lower than in Mashapaquit Marsh. Direct losses of groundwater NO₃⁻ by denitrification were also found to be low in this marsh. High fluxes of N into salt marsh creek bottom sediments affect both primary production and denitrification. Studies in nearby environments demonstrate increased primary productivity in coastal salt ponds receiving high N inputs (Howes and Goehring, 1996). Nearly half of the N taken up by algal growth in Mashapaquit Marsh (Chapter 3), was subsequently denitrified and denitrification was also driven directly by water column NO₃⁻. However, experiments in sediment mesocosms (Seitzinger and Nixon, 1985) and comparisons among estuaries receiving different N loading (Seitzinger, 1988) indicate that as N loading increases, denitrification can only account for a constant or diminishing fraction of the influent N. The ability of denitrification to remove N is probably limited by the residence time of N over the sediments, which limits both the direct denitrification of NO₃⁻ and the incorporation of N into benthic algal biomass.

Thus while salt marshes play an important role in mitigating the effects of anthropogenic N on coastal environments, and while in quantitative terms, this mitigation increases with increased N loading, the ability of salt marshes to remove terrestrial N has limits. As states and municipalities seek to regulate the impact of development and its associated N impacts on coastal resources, it is important to understand the role of salt

marshes in the N cycle of the coastal zone. Existing salt marshes provide important benefits, ameliorating the need for expensive treatment solutions to wastewater NO_3^- . Salt marshes can also be constructed to fulfill this need where they have been destroyed or are lacking. For each of these options, extensive knowledge of the dynamics of the interaction of groundwater N with salt marsh environments is required for planning and prediction of the effects of increased N loads on coastal environments (Howes *et al.* 1996).

In contrast, vegetated salt marsh sediments are largely uncoupled from external N fluxes, being supported primarily by N fixation (Valiela and Teal, 1979). Although denitrification losses are significant, up to 50% of inputs, contributions to the coastal N cycle are small (~15%), mostly as NH_4^+ and recalcitrant dissolved organic N (White and Howes, 1994). This export may support some primary production in tidal creeks and estuaries, though its importance as an N source is diminished in systems receiving high terrestrial N inputs. However, the accretion of organic matter is supported and limited by N inputs, and this accretion (as vegetated peats) plays an important role in the physical structure of coastal environments, protecting upland areas from storm surges and erosion.

In this study, denitrification, N cycling, and sediment metabolism in the tidal creeks and vegetated sediments of a New England salt marsh were studied with a number of techniques. An experimental and model study was undertaken to optimize the accuracy of N_2 flux measurements of sediment denitrification made in closed chambers. Denitrification and O_2 consumption in salt marsh sediments were dependent on labile C pools, which were depleted during long incubations, causing measured rates to decline.

The incubation time required for reduction of diffusive fluxes of sediment porewater N_2 pools into a low- N_2 headspace was highly dependent on sediment thickness. In these salt marsh sediments, denitrification took place predominately in the top 2 cm, allowing rate determinations to be made on thin sediment sections, shortening incubation times.

Inhibition of measured N_2 fluxes due to accumulation of headspace N_2 and the collapse of the sediment-water diffusion gradient was as much as 13% in gas headspaces and 80% in water headspaces, but could be eliminated by the use of headspace thicknesses of > 10 cm gas. Flushing of the headspace to remove accumulated NH_4^+ did not affect denitrification rates, but did temporarily disturb N_2 fluxes. Controlling for diffusive N_2 fluxes with incubations of parallel anaerobic flux chambers where nitrification-denitrification was inhibited shortened incubation times by 50% or more, but any significant macrofaunal irrigation made anaerobic sediments poor controls, and introduced significant errors into the calculation of denitrification fluxes.

N_2 flux incubations should be made as short as possible by reducing sediment thickness, and/or employing parallel anaerobic cores when macrofaunal irrigation is minimal. Gas headspaces should be at least 10 cm in thickness, and incubations with water headspaces should be very short (hours). Headspace flushing increases the effort expended in the experiments, and may not have any effect on measured denitrification rates. Limitations of the N_2 flux method largely arise because conditions in closed chambers are not at equilibrium. Improvements to the approach can be made by shortening incubations or by maintaining headspace equilibrium by a continuous flow of water over the headspace. However, accurate measurement of changes in N_2 under these

conditions requires expensive equipment such as a mass spectrometer. The advantages must be weighed against the retention of a method, which can be applied widely to environmental decision-making.

Denitrification in tidal salt marsh creeks was found to be driven by the availability of labile algal biomass as much as by seasonal factors such as temperature. Sandy sediments had half the sediment C content of muddy sediments, but rates of O_2 consumption, CO_2 production, and denitrification were the same in both sites. Sediment metabolism in both sites was based on respiration of an organic source with a C/N molar ratio of 6.1. Sandy sediments had a higher abundance of photosynthetic pigment-associated C, while muddy sediments had in addition a pool of non-reactive C. The respiration quotient at both sites was 1.0, indicating that the products of anaerobic metabolism were oxidized before escaping the sediments. Coupled nitrification-denitrification was a significant contributor to the cycling of C, O, and N. O_2 consumption by nitrification was responsible for 18% of the total O_2 flux into the sediments. CO_2 production by denitrification predominated over CO_2 fixation by nitrification, and the net CO_2 flux was 10% of the total heterotrophic CO_2 flux from the sediments. 46% of remineralized N was subject to coupled nitrification-denitrification. Allochthonous denitrification of groundwater NO_3^- accounted for 39% of the combined total denitrification rate, which averaged $2.7 \text{ mol m}^{-2} \text{ yr}^{-1}$.

Since denitrification in the tidal creek sediments is driven by algal biomass, its N source must be groundwater NO_3^- , the dominant N source to the creek bottom. Since autochthonous denitrification represents 61% of the total denitrification, NO_3^- uptake by

benthic algae must exceed allochthonous denitrification. However, no difference in NO_3^- uptake was seen either in field chamber incubations or in artificially-lit laboratory flux chambers (Smith, 1999). Additionally, comparisons of tidal NO_3^- fluxes during the day and night revealed no differences (Smith, 1999). Visual observation suggests that much of the benthic algal production takes place in mats of *Enteromorpha intestinata*, which may not have been included in either the field or laboratory flux chambers. In addition, photon flux densities at the sediment surface in either of the chamber incubations may not have been as high as field levels, due to the obscuring effects of the chamber walls, or the limitations of artificial lighting. Nitrate uptake by benthic algae could be measured in large field enclosures of algal mats designed to minimize interference with solar radiation. These measurements could be compared with measures of algal cover and biomass production as a second measure of N incorporation into biomass. In the present study, isotope ratios of ^{15}N and ^{13}C were consistent with an algal source for sediment organic matter. Continued studies including ^{35}S and separate analysis of the contributors to sediment organic matter (benthic fauna, algal matter, humic matter, and *Spartina* biomass) could serve to further elucidate the source of sediment C.

In undisturbed sediments of the vegetated marsh, plant N uptake out-competes coupled nitrification-denitrification for remineralized NH_4^+ during the growing season. Plant uptake accounts for 66% of remineralized N, while denitrification accounts for the remainder. In the winter, however, plant uptake is 0, and denitrification predominates. Both plant uptake and denitrification increase with increased N availability, but plant N uptake does not increase as fast as denitrification, and at an N fertilization level of 15.5

$\text{mol m}^{-2} \text{ yr}^{-1}$, denitrification dominates the N cycle, accounting for 72% of the available N, while plant uptake only accounts for 28%. Sediment hydrological conditions affect plant growth via their effect on sediment oxidation. In flooded sediments, S^{2-} concentrations are elevated, inhibiting plant growth. Coupled nitrification-denitrification responds to substrate availability, even under conditions of low sediment oxidation, for when plant N uptake was suppressed by flooding, denitrification consumed at least 84% of the excess N made available. Under conditions of sediment flooding, the competition for remineralized NH_4^+ shifts in favor of denitrification, but plant uptake still accounts for > 50% of remineralized N. Denitrification rates calculated with the $^{15}\text{NH}_4^+$ tracer ranged from $0.7 - 12.2 \text{ mmol m}^{-2} \text{ d}^{-1}$ in unfertilized marsh, or $0.73 \text{ mol m}^{-2} \text{ yr}^{-1}$ annually. In fertilized sediments, denitrification rates were much higher, averaging $12.6 \text{ mol m}^{-2} \text{ yr}^{-1}$ (range $11.1 - 136 \text{ mmol m}^{-2} \text{ d}^{-1}$).

With the understanding of the sediment N cycle gained in this study and with understanding of the utility of ^{15}N tracer methods for determining the partitioning of remineralized N, a number of easy experiments can be envisioned. Although denitrification rate measurements require an extremely laborious, and generate large numbers of samples, measurements of plant/nitrifier partitioning can be made much more simply. Since after the initial denitrification loss and incorporation of the tracer into biomass, little further change takes place over 28 d (White and Howes, 1994a), only one set of injected sediment cores need be harvested, 3 or more days after the initial injection. The partitioning of N between plants and nitrifiers could then be easily determined in a number of environments. Of interest would be differences in partitioning between stands

of different marsh grass species. Changes in the partitioning of N between plants and nitrifiers in swards of different species could result from differences in sediment oxidation (high marsh vs. low marsh) or from differences in the growth rate of the plant species. Determining plant/nitrifier N partitioning at all of the different fertilizer levels of the long-term fertilization plots would fill in a scheme that at present has only two end members. Also of interest is the differential effect of long-term vs. short term N additions. Long-term N additions change plant growth form and sediment oxidation, whereas short-term N additions would have little effect, allowing separation of the effects of sediment oxidation from N availability. Measurements in the present study were concentrated during the summer, but the dynamics of the seasonal crossover from denitrification to plant dominance of uptake during spring and summer would answer questions about the relative seasonal cycles of plant N uptake and denitrification as affected by seasonally-varying sediment oxidation states.

Denitrification in the varying environments of the salt marsh is best studied with a combination of techniques. Closed flux chambers are useful for simultaneous determinations of a variety of biogeochemical fluxes, however, sediments incubated *in vitro* are not subject to the diurnal tidal, solar, and temperature cycles found *in situ*. Stable isotope studies can be done *in situ*, but are best combined with other measures of biogeochemical fluxes for a complete understanding of elemental fluxes of the salt marsh.

REFERENCES

- Abd. Aziz, S. A. and D.B. Nedwell. 1986. The nitrogen cycle of an East Coast, U.K. saltmarsh: II. Nitrogen fixation, nitrification, denitrification, tidal exchange. *Estuar. Coast. Shelf Sci.* 22:689-704.
- Berner, R.A. 1980. Early Diagenesis. Princeton University Press, Princeton, NJ. 241 pp.
- Blackburn, H.T. 1979. Method for measuring rates of NH_4^+ turnover in anoxic marine sediments, using a $^{15}\text{N}\text{-NH}_4^+$ dilution technique. *Appl. Environ. Microbiol.* 37:760-765.
- Braker, G., Alaya-del-Rio, H.L., Devol, A.J., Fesefeldt, A., and J.M. Tiedje. 2001. Community structure of denitrifiers, *Bacteria*, and *Archaea* along redox gradients in Pacific Northwest Marine Sediments by Terminal Restriction Fragment Length Polymorphism analysis of amplified nitrite reductase (*nirS*) and 16S rRNA genes. *Appl. Env. Microbiol.* 67:1893-1901.
- Bonin, P., Barbotin, J.N., Dhulster, P., and J.-C. Bertrand. 1986. Nitrate reduction in simulated microniches by a denitrifying marine bacterium. *Can. J. Microbiol.* 33:276-279.
- Boschker, H.T.S., de Brouwer, J.F.C., and T.E. Cappenberg. 1999. The contribution of macrophyte-derived organic matter to microbial biomass in salt-marsh sediments: Stable carbon isotope analysis of microbial biomarkers. *Limnol. Oceanogr.* 44:309-319.
- Bowden, W.D. 1986. Gaseous nitrogen emissions from undisturbed terrestrial ecosystems: An assessment of their impacts on local and global nitrogen budgets. *Biogeochemistry* 2:249-279.
- Bowden, W.D. 1987. The biogeochemistry of nitrogen in freshwater wetlands. *Biogeochemistry* 4:313-348.
- Boynton, W.R., Kemp, W.M., Osborne, C.G., Kaumeyer, K.R., and M.C. Jenkins. 1981. Influence of water circulation rate on *in situ* measurements of benthic community respiration. *Mar. Biol.* 65:185-190.
- Broecker, W. and T.-H. Peng. 1982. Tracers in the Sea. Lamont-Doherty Geological Observatory, New York. 690 pp.
- Capone, D.G. and M.F. Bautista. 1985. A groundwater source of nitrate in nearshore marine sediments. *Nature* 313:214-216.
- Cavigelli, M.A. and G. P. Robertson. 2000. The functional significance of denitrifier community composition in a terrestrial ecosystem. *Ecology.* 81:1402-1414.
- Chapman, H.D., Liebig, G.F. and D.S. Rayner. 1949. A lysimeter investigation of nitrogen gains and losses under various systems of covercropping and fertilization, and a discussion of error sources. *Hilgardia* 19:3.

- Chèneby, D., Philippot, L., Hartmann, A., Hénault, C., and J.-C. Germon. 2000. 16S rDNA analysis for characterization of denitrifying bacteria isolated from three agricultural soils. *FEMS Microbiol. Ecol.* 34:121-128.
- Christensen, J.P. and G.T. Rowe. 1984. Nitrification and oxygen consumption in northwest Atlantic deep-sea sediments. *J. Mar. Res.* 42:1099-1116.
- Christensen, J.P., Murray, J.W., Devol, A.H., and L.A. Codispoti. 1987. Denitrification in continental shelf sediments has major impact on the oceanic nitrogen budget. *Global Biogeochem. Cycles.* 1:97-116.
- Cline, J.D. 1969. Spectrophotometric determination of hydrogen sulfide in natural waters. *Limnol. Oceanogr.* 14:454-458.
- Cornwell, J.C., Kemp, W.M., and T.M. Kana. 1999. Denitrification in coastal ecosystems: methods, environmental controls, and ecosystem level controls, a review. *Aquatic Ecol.* 33:41-54.
- Dacey, J.W. and B.L. Howes. 1984. Water uptake by roots controls water table movement and sediment oxidation in short *Spartina* marsh. *Science.* 224:487-489.
- DeLaune, R.D., Lindau, C.W., Sulaeman, E., and A. Jugsujinda. 1998. Nitrification and denitrification estimates in a Louisiana forest soil as assessed by ^{15}N isotope dilution and direct gaseous measurements. *Water Air Soil Pollut.* 106:149-161.
- D'Elia, C.F., Steudler, P.A. and N. Corwin. 1977. Determination of total N in aqueous samples using persulfate digestion. *Limnol. Oceanogr.* 22:760-764.
- Devol, A.H. 1987. Verification of flux measurements made with *in situ* benthic chambers. *Deep-Sea Res.* 34:1007-1026.
- Devol, A.H. 1991. Direct measurement of nitrogen gas fluxes from continental shelf sediments. *Nature.* 349:319-321.
- Devol, A.H. and J.P. Christensen. 1993. Benthic fluxes and nitrogen cycling in sediments of the continental margin of the eastern North Pacific. *J. Mar. Res.* 51:345-372.
- Ferguson, S.J. 1994. Denitrification and its control. *Antonie van Leeuwenhoek* 66:89-110.
- Fujita, R.M., Wheeler, P.A., and R.L. Edwards. 1980. Assessment of macroalgal nitrogen limitation in a seasonal upwelling region. *Mar. Ecol. Prog. Ser.* 53:293-303.
- Gardner, W.S., T.F. Nalepa and J.M. Malczyk. 1987. Nitrogen mineralization and denitrification in Lake Michigan sediments. *Limnol. Oceanogr.* 32:1226-1238.
- Giblin, A.E. and A.G. Gaines. 1990. Nitrogen inputs to a marine embayment: The importance of groundwater. *Biogeochemistry* 10:309-328.
- Goering, J.J. and M.M. Pamatmat. 1971. Denitrification in sediments of the sea off Peru. *Invest. Pesq.* 35:233-242.

- Güss, S. 1998. Oxygen uptake at the sediment-water interface simultaneously measured using a flux chamber method and microelectrodes: Must a diffusive boundary layer exist? *Est. Coast. Shelf Sci.* 46:143-156.
- Hamersley, M.R., Howes, B.L., White, D.S., Johnke, S., Young, D., Peterson, S.B., and J.M. Teal. 2001. Nitrogen balance and cycling in an ecologically engineered septage treatment system. *Ecological Engineering*. 18:61-75.
- Hamersley, M.R., Howes, B.L., and D.S. White. Particulate organic carbon availability controls denitrification in a septage-treating artificial wetland. *Water Research* (in submission a).
- Hamersley, M.R., Howes, B.L., and D.S. White. The contribution of floating plants to ammonium and nitrogen removal via nitrification/denitrification in a septage-treating artificial wetland. *Journal of Environmental Quality* (in submission b).
- Harvey, J.W. and W.E. Odum. 1990. The influence of tidal marshes on upland groundwater discharge to estuaries. *Biogeochemistry* 10:217-236.
- Henriksen, K. and W.M. Kemp. 1988. Nitrification in estuarine and coastal marine sediments. pp. 207-249. In: T.H. Blackburn and J. Sørensen, eds. Nitrogen Cycling in Coastal Marine Environments. John Wiley & Sons. New York.
- Howes, B.L. and D.D. Goehringer. 1994. Porewater drainage and dissolved organic carbon and nutrient losses through the intertidal creekbanks of a New England salt marsh. *Mar. Ecol. Prog. Ser.* 114:289-301.
- Howes, B.L. and D.D. Goehringer. 1996. Ecology of Buzzards Bay: An estuarine profile. National Biological Service Biological Report 31. vi+141 pp.
- Howes, B.L. and J.M. Teal. 1994. Oxygen loss from *Spartina alterniflora* and its relationship to salt marsh oxygen balance. *Oecologia* 97:431-438.
- Howes, B.L., Howarth, R.W., Teal, J.M. and I. Valiela. 1981. Oxidation-reduction potentials in a salt marsh: Spatial patterns and interactions with primary production. *Limnol. Oceanogr.* 26:350-360.
- Howes, B.L., Dacey, J.W.H. and G.M. King. 1984. Carbon flow through oxygen and sulfate reduction pathways in salt marsh sediments. *Limnol. Oceanogr.* 29:1037-1051.
- Howes, B.L., Dacey, J.W.H. and J.M. Teal. 1985. Annual carbon mineralization and belowground production of *Spartina alterniflora* in a New England salt marsh. *Ecology* 66:595-605.
- Howes, B.L., Dacey, J.W.H. and D.D. Goehringer. 1986. Factors controlling the growth form of *Spartina alterniflora*: Feedbacks between above-ground production, sediment oxidation, nitrogen and salinity. *J. Ecol.* 74:881-898.
- Howes, B.L., Weiskel, P.K., Goehringer, D.D. and J.M. Teal. 1996. Interception of freshwater and nitrogen transport from uplands to coastal waters: The role of

- saltmarshes. pp. 287-310. In K.F. Nordstrom and C.T. Roman. *eds.*, Estuarine Shores: Evolution, Environments and Human Alterations. John Wiley and Sons Ltd.
- Jenkins, M.C. and W. M. Kemp. 1984. The coupling of nitrification and denitrification in two estuarine sediments. *Limnol. Oceanogr.* 29:609-619.
- Jensen, K.M., M.H. Jensen and E. Kristensen. 1996. Nitrification and denitrification in Wadden Sea sediments (Konigshafen, Island of Sylt, Germany) as measured by nitrogen isotope pairing and isotope dilution. *Aquat. Microb. Ecol.* 11:181-191.
- Jetten, M.S.M., Logemann, S., Muyzer, G., Robertson, L.A., de Vries, S., van Loosdrecht, M.C.M., and J.G.Kuenen. 1997. Novel principles in the microbial conversion of nitrogen compounds. *Antonie van Leeuwenhoek* 71:75-93.
- Jørgensen, B.B. 1977. Bacterial sulfate reduction within reduced microniches of oxidized marine sediments. *Mar. Biol.* 41:7-17.
- Jørgensen, B.B. 1978. A comparison of methods for the quantification of bacterial sulfate reduction in coastal marine sediments. 1. Measurements with radio-tracer techniques. *Geomicrobiol. J.* 1:11-27.
- Jørgensen, B.B. 1982. Mineralization of organic matter in the sea bed: The role of sulphate reduction. *Nature* 296:643-645.
- Jørgensen, B.B. and J. Sørensen. 1985. Seasonal cycles of O_2 , NO_3^- , and SO_4^{2-} reduction in estuarine sediments: the significance of an NO_3^- reduction maximum in spring. *Mar. Ecol. Prog. Ser.* 24:65-74.
- Joye, S.B., Smith, S.V., Holligaugh, J.T. and H.W. Paerl. 1996. Estimating denitrification rates in estuarine sediments: A comparison of stoichiometric and acetylene based methods. *Biogeochemistry* 33:197-215.
- Jury, W.A., Letey, J. and T. Collins. 1982. Analysis of chamber methods used for measuring nitrous oxide production in the field. *Soil Sci. Am. J.* 46:250-256.
- Kaplan, W., Valiela, I., and J.M. Teal. 1979. Denitrification in a salt marsh ecosystem. *Limnol. Oceanogr.* 24:726-734.
- Kautsky, N., H. Kautsky, U. Kautsky and M. Waern. 1986. Decreased depth penetration of *Fucus vesiculosus* (L.) since the 1940's indicates eutrophication of the Baltic Sea. *Mar. Ecol. Prog. Ser.* 28:1-8.
- Koch, M.S., Maltby, E., Oliver, G.A., and S.A. Bakker. 1992. Factors controlling denitrification rates of tidal mudflats and fringing salt marshes in South-west England. *Estuar. Coastal. Shelf Sci.* 34:471-485.
- Lamontagne, M.G. and I. Valiela. 1995. Denitrification measured by a direct N_2 flux method in sediments of Waquoit Bay, MA. *Biogeochemistry.* 31:63-83.
- Matthias, A.D., Yarger, D.N., and R.S. Weinbeck. 1978. A numerical evaluation of chamber methods for determining gas fluxes. *Geophys. Res. Let.* 5:765-768.

- Matulewich, V.A. and M.S. Finstein. 1978. Distribution of autotrophic nitrifying bacteria in a polluted river (the Passaic). *Appl. Environ. Microbiol.* 35:67-71.
- McCaig, A.E., Embley, T.M., and J.I. Prosser. 1994. Molecular analysis of enrichment cultures of marine ammonia oxidisers. *FEMS Microbiol. Lett.* 120:363-368.
- McGovern, T.A., Laber, L.J., and B.C. Gram. 1979. Characteristics of the salts secreted by *Spartina alterniflora* and their relation to estuarine production. *Estuarine Coastal Mar. Sci.* 9:351-356.
- Mendelssohn, I.A., McKee, K.L., and W.H. Patrick, Jr. 1981. Oxygen deficiency in *Spartina alterniflora* roots: Metabolic adaptation to anoxia. *Science* 214:439-441.
- Meyer-Reil, L.-A. 1994. Microbial life in sedimentary biofilms: The challenge to microbial ecologists. *Mar. Ecol. Prog. Ser.* 112:303-311.
- Middelburg, J.J., Soetaert, K., Herman, P.M.J. and C.H.R. Heip. 1996. Denitrification in marine sediments: A model study. *Global Biogeochem. Cycles.* 10:661-673.
- Morris, J.T. and J.W.J. Dacey. 1984. Effects of oxygen on ammonium uptake and root respiration by *Spartina alterniflora*. *Am. J. Bot.* 71:979-985.
- Nielsen, L.P. 1992. Denitrification in sediment determined from nitrogen isotope pairing. *FEMS Microbiol. Ecol.* 86:357-362.
- Nixon, S.W. 1980. Between coastal marshes and coastal waters: A review of twenty years of speculation and research on the role of salt marshes in estuarine productivity and water chemistry. pp. 437-525. *In*: P. Hamilton and K. MacDonald, eds. *Estuarine and Wetland Processes with and Emphasis on Modeling*. Plenum.
- Nixon, S.W., Oviatt, C.A., and S.S. Hale. 1975. Nitrogen regeneration and the metabolism of coastal marine bottom communities. *In*: J. Anderson and M. MacFayden, eds., *The Role of Terrestrial and Aquatic Organisms in Decomposition Processes*. Blackwell Scientific. Coleraine. pp. 269-283. xxx
- Nowicki, B.L. 1994. The effect of temperature, oxygen, salinity, and nutrient enrichment on estuarine denitrification rates measured with a modified nitrogen gas flux technique. *Estuar. Coast. Shelf Sci.* 38:137-156.
- Nowicki, B.L., Requentina, E. Van Keuren, D. and J. Portnoy. 1999. The role of sediment denitrification in reducing groundwater-derived nitrate inputs to Nauset Marsh Estuary, Cape Cod, Massachusetts. *Estuaries.* 22:245-259.
- Patrick, Jr., W.H. and K.R. Reddy. 1976. Nitrification-denitrification reactions in flooded soils and water bottoms: Dependence on oxygen supply and ammonium diffusion. *J. Environ. Qual.* 5:469-472.
- Paerl, H.W. and J.L. Pinckney. 1996. A mini-review of microbial consortia: Their roles in aquatic production and biogeochemical cycling. *Microb. Ecol.* 31:225-247.

- Page, H.M. 1997. Importance of vascular plant and algal production to macro-invertebrate consumers in a southern California salt marsh. *Estuar. Coast. Shelf Sci.* 45:823-834.
- Reddy, K.R., Patrick, Jr., W.H., and C.W. Lindau. 1989. Nitrification-denitrification at the plant root-sediment interface in wetlands. *Limnol Oceanogr.* 34:1004-1013.
- Redfield, A.C. 1972. Development of a New England salt marsh. *Ecological Monographs* 42:201-237.
- Ryther, J.H. and C.B. Officer. 1981. Impact of nutrient enrichment on water uses. In: B.J. Neilson and L.E. Cronin, eds. *Estuaries and Nutrients*. Humana. Clifton, NJ. pp. 247-262.
- Rysgaard, S., Thastum, P., Dalsgaard, T., Christensen, P.B. and N.P. Sloth. 1999. Effects of salinity on NH_4^+ adsorption capacity, nitrification, and denitrification in Danish estuarine sediments. *Estuaries*. 22:21-30.
- Scheiner, D. 1976. Determination of ammonia and Kjeldahl N by indophenol method. *Water Res.* 10:31-36.
- Schlesinger, W.H. 1991. *Biogeochemistry: An Analysis of Global Change*. Academic, London. 443 pp.
- Schmidt, E.L. and L.W. Belser. 1982. Nitrifying bacteria. In: A.L. Page, R.H. Miller, and D.R. Keeney, eds., *Methods of Soil Analysis, Part 2: Chemical and Microbiological Properties*. American Society of Agronomy. Madison, WI. pp. 1029-1031.
- Seitzinger, S.P. 1987. Nitrogen biogeochemistry in an unpolluted estuary: the importance of benthic denitrification. *Mar. Ecol. Prog. Ser.* 41:177-186.
- Seitzinger, S.P. 1988. Denitrification in freshwater and coastal marine ecosystems: Ecological and geochemical significance. *Limnol. Oceanogr.* 33:702-724.
- Seitzinger, S.P. 1994. Linkages between organic matter mineralization and denitrification in eight riparian wetlands. *Biogeochemistry*. 25:19-39.
- Seitzinger, S.P. and S.W. Nixon. 1985. Eutrophication and the rate of denitrification and N_2O production in coastal marine sediments. *Limnol. Oceanogr.* 30:1332-1339.
- Seitzinger, S.P., Nixon, S.W., Pilson, M.E.Q. and S. Burke. 1980. Denitrification and N_2O production in near-shore marine sediments. *Geochim. Cosmochim. Acta*. 44:1853-1860.
- Seitzinger, S.P., Nixon, S.W. and M.E.Q. Pilson. 1984. Denitrification and nitrous oxide production in a coastal marine ecosystem. *Limnol. Oceanogr.* 29:73-83.
- Seitzinger, S.P., Nielsen, L.P., Caffrey, J. and P.B. Christensen. 1993. Denitrification measurements in aquatic sediments: A comparison of three methods. *Biogeochemistry*. 23:147-167.

- Sewell, P.L. 1982. Urban groundwater as a possible nutrient source for an estuarine benthic algal bloom. *Estuarine Coastal Shelf Sci.* 15:569-576.
- Smith, K.N. 1999. Salt marsh uptake of watershed nitrate. Master's Thesis. Department of Geology, Graduate School of Arts and Sciences, Boston University, Boston, Massachusetts. 76 pp.
- Soetaert, K., Herman, P.M.J. and J.J. Middelburg. 1996. A model of early diagenetic processes from the shelf to abyssal depths. *Geochim. Cosmochim. Acta.* 60:1019-1040.
- Sørensen, J. 1978. Capacity for denitrification and reduction of nitrate to ammonia in a coastal marine sediment. *Appl. Env. Microb.* 35:301-305.
- Sørensen, J. Rasmussen, L.K. and I. Koike. 1987. Micromolar sulfide concentrations alleviate acetylene blockage of nitrous oxide reduction by denitrifying *Pseudomonas fluorescens*. *Can. J. Microbiol.* 33:1001-1005.
- Stephen, J.R., McCaig, A.E., Smith, Z., Prosser, J.I., and T.M. Embley. 1996. Molecular diversity of soil and marine 16S rRNA gene sequences related to β -subgroup ammonia-oxidising bacteria. *Appl. Environ. Microbiol.* 62:4147-4154.
- Sullivan, M.L., and F.C. Daiber. 1974. Response in production of cordgrass, *Spartina alterniflora*, to inorganic nitrogen and phosphorus fertilizer. *Chesapeake Sci.* 15:121-123.
- Teal, J.M. 1962. Energy flow in the salt marsh ecosystem of Georgia. *Ecology* 43:614-624.
- Teal, J.M. and B.L. Howes. 1996. Interannual variability of a salt-marsh ecosystem. *Limnol. Oceanogr.* 41:802-809.
- Teske, A., Alm, E., Regan, J.M., Toze, S., Rittman, B.E., and I. Stahl. 1994. Evolutionary relationships among ammonia- and nitrite-oxidizing bacteria. *J. Bacteriol.* 176:6623-6630.
- Trimmer, M., Nedwell, D.B., Sivy, D.B. and S.J. Malcolm. 2000. Seasonal benthic organic matter mineralization measured by oxygen uptake and denitrification along a transect of the inner and outer River Thames estuary, UK. *Mar. Ecol. Progr. Ser.* 197:103-119.
- Turner, R.E. 1976. Geographic variations in salt marsh macrophyte production: a review. *Contrib. Mar. Sci.* 20:47-68.
- Valiela, I. and J.M. Teal. 1974. Nutrient limitation in salt marsh vegetation. pp. 547-563. In: R.J. Reimold and W.H. Green, eds., *Ecology of Halophytes*. Academic. New York.
- Valiela, I. and J.M. Teal. 1979. The nitrogen budget of a salt marsh ecosystem. *Nature* 280:652-656.

- Valiela, I., Teal, J.M. and N.Y. Persson. 1976. Production and dynamics of experimentally enriched salt marsh vegetation: Belowground biomass. *Limnol. Oceanogr.* 21:245-252.
- Valiela, I., Teal, J.M., and W.G. Deuser. 1978. The nature of growth forms in the salt marsh grass *Spartina alterniflora*. *Amer. Natur.* 112:461-470.
- Valiela, I., Teal, J.M., Cogswell, C., Hartman, J., Allan, S., Van Etten, R. and D. Goehringer. 1985. Some long-term consequences of sewage contamination in salt marsh ecosystems. pp. 301-316. In: P.J. Godfrey, E.R. Kaynor, and J. Benforado, eds. *Ecological Considerations in Wetland Treatment of Municipal Wastewater*. Van Nostrand Reinhold, NY.
- Valiela, I., Costa, J., Foreman, K., Teal, J.M., Howes, B. and D. Aubrey. 1990. Transport of groundwater-borne nutrients from watersheds and their effects on coastal waters. *Biogeochemistry* 10:177-197.
- Valiela, I., Foreman, K., LaMontagne, M., Hersh, D., Costa, J., Peckol, P., DeMeo-Andreson, B., D'Avanzo, C., Babione, M., Sham, C.-H., Brawley, J., Lajtha, K. 1992. Couplings of watersheds and coastal waters: Sources and consequences of nutrient enrichment in Waquoit Bay, Massachusetts. *Estuaries* 15:443-457.
- van Kessel, J.F. 1977. Factors affecting the denitrification rate in two water-sediment systems. *Wat. Res.* 11:259-267.
- van Luijn, F., Boers, P.C.M. and L. Lijklema. 1996. Comparison of denitrification rates obtained by the N₂ flux method, the ¹⁵N isotope pairing technique and the mass balance approach. *Wat. Res.* 30:893-900.
- van Luijn, F., Boers, P.C.M., Lijklema, L. and J.-P.R.A. Sweerts. 1999. Nitrogen fluxes and processes in sandy and muddy sediments from a shallow eutrophic lake. *Wat. Res.* 33:33-42.
- Van Raalte, C.D. and D.G. Patriquin. 1979. Use of the "acetylene blockage" technique for assaying denitrification in a salt marsh. *Mar. Biol.* 52:315-320.
- Vanderborght, J.-P. and G. Billen. 1975. Vertical distribution of nitrate concentration in interstitial water of marine sediments with nitrification and denitrification. *Limnol. Oceanogr.* 20:953-961.
- Vince, S.W., Valiela, I., and J.M. Teal. 1981. An experimental study of the structure of herbivorous communities in a salt marsh. *Ecology* 62:1662-1678.
- Weiskel, P.K., DeSimone, L.A. and B.L. Howes. 1996. Transport of wastewater nitrogen and phosphorus through a coastal watershed. *Env. Sci. Tech.* 26:352-360.
- Weiss, R.F. 1970. The solubility of nitrogen, oxygen, and argon in water and seawater. *Deep-Sea Res.* 17:721-735.
- White, D.S. and B.L. Howes. 1994a. Long-term ¹⁵N-nitrogen retention in the vegetated sediments of a New England salt marsh. *Limnol. Oceanogr.* 39:1878-1892.

- White, D.S. and B.L. Howes. 1994b. Translocation, remineralization, and turnover of nitrogen in the roots and rhizomes of *Spartina alterniflora* (Gramineae). *Am. J. Bot.* 81:1225-1234.
- Wiljer, J and C.C. Delwiche. 1954. Investigations on the denitrifying process in soil. *Plant Soil.* 5:155-169.
- Wolaver, T.G., J.C. Zieman, R. Wetzel and K.L. Webb. 1983. Tidal exchange of nitrogen and phosphorus between a mesohaline vegetated marsh and the surrounding estuary in the Lower Chesapeake Bay. *Est. Coast. Shelf Sci.* 16:321-332.
- Wood, E., F. Armstrong, and F. Richards. 1967. Determination of nitrate in sea water by cadmium copper reduction to nitrite. *J. Mar. Bio. Ass. U.K.* 47:23-31.
- Yoon, W.B. and R. Benner. 1992. Denitrification and oxygen consumption in sediments of two south Texas estuaries. *Mar. Ecol. Prog. Ser.* 90:157-167.
- Yoshinari, T. and R. Knowles. 1976. Acetylene inhibition of nitrous oxide reduction by denitrifying bacteria. *Biochem. Biophys. Res. Commun.* 69:705-710.
- Zimmerman, A.R. and R. Benner. 1994. Denitrification, nutrient regeneration and carbon mineralization in sediments of Galveston Bay, Texas, USA. *Mar. Ecol. Prog. Ser.* 114:275-288.
- Zumft, W.G. 1992. The denitrifying prokaryotes. pp. 554-582. *In:* A. Balows, *ed.* The prokaryotes: A handbook on the Biology of Bacteria: Ecophysiology, Isolation, Identification, Applications. Springer-Verlag, New York, NY.

APPENDIX 1

Algorithm for numerical modeling of N₂ flux

(Chapter 2)

Table of variables used in algorithm (see Chapter 2 for details).

Name	Description	Units
Constants:		
bunsencoefN2	Bunsen coefficient for N ₂	mmol mL ⁻¹
diffdistance	thickness of sediment compartment	cm
diffuseN2	apparent diffusion coefficient	cm s ⁻¹
headgasthick	thickness of headspace gas layer	cm
porosity	sediment porosity	mL cm ⁻³
sedDeN2	denitrification rate	mmol cm ⁻³ min ⁻¹
sedslices	number of sediment compartments	
sedthick	sediment thickness	cm
time	total incubation time	min
Counters:		
currenttime	current time counter	min
currentslice	current sediment compartment, numbered from the bottom	
Arrays: (value assigned to each sediment layer)		
fluxanN2	N ₂ flux rate from anaerobic sediments	mmol cm ⁻² min ⁻¹
fluxoxN2	N ₂ flux rate from aerobic sediments	mmol cm ⁻² min ⁻¹
headanN2conc	partial pressure of headspace N ₂ in anaerobic chambers	mL mL ⁻¹
headoxN2conc	partial pressure of headspace N ₂ in aerobic chambers	mL mL ⁻¹
sedanN2conc	N ₂ concentration in anaerobic sediment porewater	mmol mL ⁻¹
sedoxN2conc	N ₂ concentration in aerobic sediment porewater	mmol mL ⁻¹
sedDeN2	denitrification rate	mmol cm ⁻³ min ⁻¹

Algorithm code: (comments are in italics preceded by "Rem")

Begin

diffdistance = sedthick / sedslices
currenttime = 0

Do While currenttime <= time

Rem N₂ flux rates between sediment compartments

currentslice = sedslices + 1
Do While currentslice > 2
 currentslice = currentslice - 1
 fluxoxN2(x) = porosity * diffuseN2 * (sedoxN2conc(currentslice) - sedoxN2conc(currentslice - 1) / diffdistance)
 fluxanN2(x) = porosity * diffuseN2 * (sedanN2conc(currentslice) - sedanN2conc(currentslice - 1) / diffdistance)
Loop
currentslice = currentslice - 1

Rem N₂ flux rates across sediment surface

fluxoxN2(x) = porosity * diffuseN2 * (sedoxN2conc(1) - headoxN2conc * bunsencoefN2) / (diffdistance / 2)
fluxanN2(x) = porosity * diffuseN2 * (sedanN2conc(1) - headanN2conc * bunsencoefN2) / (diffdistance / 2)

Rem Calculate new sediment N₂ concentrations

```
currentslice = sedslices + 1
Do While currentslice > 2
  currentslice = currentslice - 1
  sedoxN2conc(currentslice) = sedoxN2conc(currentslice) + sedDeN2(currentslice) - fluxoxN2(currentslice) /
  diffdistance
  sedoxN2conc(currentslice - 1) = sedoxN2conc(currentslice - 1) + fluxoxN2(currentslice) / diffdistance
  sedanN2conc(currentslice) = sedanN2conc(currentslice) - fluxanN2(currentslice) / diffdistance
  sedanN2conc(currentslice - 1) = sedanN2conc(currentslice - 1) + fluxanN2(currentslice) / diffdistance
Loop
currentslice = currentslice - 1
```

Rem Calculate new headspace N₂ concentration

```
sedoxN2conc(currentslice) = sedoxN2conc(currentslice) + sedDeN2(currentslice) - fluxoxN2(currentslice) /
diffdistance
headoxN2conc = headoxN2conc + fluxoxN2(currentslice) / headgasthickness
sedanN2conc(currentslice) = sedanN2conc(currentslice) - fluxanN2(currentslice) / diffdistance
headanN2conc = headanN2conc + fluxanN2(currentslice) / headgasthickness
currenttime = currenttime + 1
Loop
End
```

Document Library

Distribution List for Technical Report Exchange—November 1999

University of California, San Diego
SIO Library 0175C
9500 Gilman Drive
La Jolla, CA 92093-0175

Hancock Library of Biology & Oceanography
Alan Hancock Laboratory
University of Southern California
University Park
Los Angeles, CA 90089-0371

Gifts & Exchanges
Library
Bedford Institute of Oceanography
P.O. Box 1006
Dartmouth, NS B2Y 4 A2
CANADA

NOAA/EDIS Miami Library Center
4301 Rickenbacker Causeway
Miami, FL 33149

Research Library
U.S. Army Corps of Engineers
Waterways Experiment Station
3909 Halls Ferry Road
Vicksburg, MS 39180-6199

Institute of Geophysics
University of Hawaii
Library Room 252
2525 Correa Road
Honolulu, HI 96822

Marine Resources Information Center
Building E38-320
MIT
Cambridge, MA 02139

Library
Lamont-Doherty Geological Observatory
Columbia University
Palisades, NY 10964

Library
Serials Department
Oregon State University
Corvallis, OR 97331

Pell Marine Science Library
University of Rhode Island
Narragansett Bay Campus
Narragansett, RI 02882

Working Collection
Texas A&M University
Dept. of Oceanography
College Station, TX 77843

Fisheries-Oceanography Library
151 Oceanography Teaching Bldg.
University of Washington
Seattle, WA 98195

Library
R.S.M.A.S.
University of Miami
4600 Rickenbacker Causeway
Miami, FL 33149

Maury Oceanographic Library
Naval Oceanographic Office
Building 1003 South
1002 Balch Blvd.
Stennis Space Center, MS 39522-5001

Library
Institute of Ocean Sciences
P.O. Box 6000
Sidney, B.C. V8L 4B2
CANADA

National Oceanographic Library
Southampton Oceanography Centre
European Way
Southampton SO14 3ZH
UK

The Librarian
CSIRO Marine Laboratories
G.P.O. Box 1538
Hobart, Tasmania
AUSTRALIA 7001

Library
Proudman Oceanographic Laboratory
Bidston Observatory
Birkenhead
Merseyside L43 7 RA
UK

IFREMER
Centre de Brest
Service Documentation-Publications
BP 70 29280 PLOUZANE
FRANCE

REPORT DOCUMENTATION PAGE	1. REPORT NO. MIT/WHOI 2002-04	2.	3. Recipient's Accession No.
4. Title and Subtitle The Role of Denitrification in the Nitrogen Cycle of New England Salt Marshes			5. Report Date February 2002
			6.
7. Author(s) Michael Robert Hamersley			8. Performing Organization Rept. No.
9. Performing Organization Name and Address MIT/WHOI Joint Program in Oceanography/Applied Ocean Science & Engineering			10. Project/Task/Work Unit No. MIT/WHOI 2002-04
			11. Contract(C) or Grant(G) No. (C) (G)
12. Sponsoring Organization Name and Address Woods Hole Oceanographic Institution University of Massachusetts			13. Type of Report & Period Covered Ph.D. Thesis
			14.
15. Supplementary Notes This thesis should be cited as: Michael Robert Hamersley, 2002. The Role of Denitrification in the Nitrogen Cycle of New England Salt Marshes. Ph.D. Thesis. MIT/WHOI, 2002-04.			
16. Abstract (Limit: 200 words) Salt marshes play important roles within the coastal environment as wildlife and fish habitat, aesthetic resources, and storm buffers. Salt marshes also have the capability of mitigating terrestrial nitrogen fluxes to sensitive coastal waters. Excessive nitrogen from wastewater disposal or fertilizers can cause eutrophication, with accompanying water column anoxia, loss of shellfish habitat, fish kills, and odors. Denitrification, a microbial process active in the sediments of salt marshes, converts nitrate to nitrogen gas, making it unavailable to algal uptake. I used direct measurements of nitrogen gas (N ₂) fluxes and a ¹⁵ N stable isotope tracer to determine the contribution of denitrification to salt marsh sediment N cycling. I studied creekbottom denitrification by direct measurements of N ₂ fluxes in closed chambers against a low-N ₂ background. I undertook experiments and simulation modeling of sediment N ₂ fluxes in closed chambers to optimize the key experimental parameters of this approach. Direct measurements of O ₂ , CO ₂ , N ₂ , and inorganic N fluxes from the sediments of a salt marsh tidal creek were made in order to examine the interaction of denitrification with the carbon, oxygen, and N cycles. Finally, a ¹⁵ N-ammonium tracer was used to study competition between plants and nitrifying bacteria for remineralized ammonium			
17. Document Analysis			
a. Descriptors Denitrification Saltmarsh nitrification			
b. Identifiers/Open-Ended Terms			
c. COSATI Field/Group			
18. Availability Statement Approved for publication; distribution unlimited.	19. Security Class (This Report) UNCLASSIFIED	21. No. of Pages 165	
	20. Security Class (This Page)	22. Price	